RSC Advances

REVIEW

View Article Online
View Journal | View Issue

Cite this: *RSC Adv.*, 2026, **16**, 7863

Machine learning in next-generation AEM fuel cells: a systematic review†

Srikanth Ponnada ‡§*

Fuel cells have lately garnered interest as a potentially advantageous technology for clean and efficient energy conversion. One type that has caught people's attention is the anion exchange membrane fuel cell (AEMFC), which can run on a variety of fuels and operates at low and high temperatures. Exploring its basic working principles, important materials, obstacles, and recent breakthroughs, this perspective presents a comprehensive introduction to AEMFC technology. The anion exchange membrane (AEM) and the electrodes of the AEMFC work together to improve the cell performance and the efficiency of the system as a whole. Furthermore, this review emphasizes the ways in which AEMFC technology is being improved by ML and AI technologies. Through the identification of crucial parameters and the improvement of the membrane electrode assembly (MEA), these technologies have the potential to optimize the performance of AEMFCs while drastically cutting down on the time and effort needed for experimental testing. Finally, we take a look at the possibilities and threats for further study of fuel cell technology-based sustainable energy generation using AEMs in conjunction with new electrode materials. This article introduces a structured framework and categorizes the following key concepts: need for anion exchange membranes (AEM) > mechanisms of anion conductivities > ORR (oxygen reduction reaction) > interfacial phenomena at the electrode–AEM interface > water management > integration of artificial intelligence (AI)/machine learning > neural networks (NN) > schemes for learning > predictive modeling > optimization algorithms and optimizing algorithms > AI in fault detection > AI in maintenance of fuel cells and in materials discovery.

Received 5th November 2025
Accepted 18th December 2025

DOI: 10.1039/d5ra08517a

rsc.li/rsc-advances

Chemical and Biological Engineering Department, Colorado School of Mines, Golden 80401, CO, USA. E-mail: koolsreekanth@gmail.com; srikanth.ponnada@vsb.cz

‡ Currently at Nanotechnology Centre, Centre for Energy and Environmental Technologies (CEET), VSB Technical University Ostrava, 70800 Ostrava-Poruba, Czech Republic.

† Dedicated to Professor Andy M. Herring on his 60th birthday.

§ Electrochemical Society (ECS) Early Career Member.

Srikanth Ponnada

Dr Srikanth Ponnada MRSC is currently a Researcher & Lecturer at Centrum Nanotechnologii, CEET, VŠB-Technical University of Ostrava. He was a Post-doctoral Fellow at (Prof. Andy M. Herring's group) Chemical and Biological Engineering Department, Colorado School of Mines-U.S.A. Also, worked as a Postdoctoral Research Associate at the Indian Institute of Technology Jodhpur, India. He received his (B.S-M.S) Dual Degree in Applied Chemistry, Department of Engineering Chemistry from Andhra University College of Engineering (A), Andhra University-India and completed his PhD in the area of "Functional materials and their electrochemical applications in batteries and sensors". His current research interests includes functional materials synthesis, polymer electrolyte membranes, fuel cell assembly and engineering, conversion devices (AEM & PEM fuel cells), energy storage (Li–S, Li-ion, and all solid-state battery electrolytes), electrochemical sensors, electrocatalysis, electrochemical engineering for net zero emissions, carbon neutrality and AI-ML in electrochemistry. He previously worked at CSIR-Central Electrochemical Research Institute (CECRI)-India, as a Project Assistant (Level-III) in lead-free perovskites-based photovoltaics and electrocatalysis and at Indian Institute of Technology (ISM) Dhanbad-India as a project research fellow in gold nanoparticle assisted heterogeneous catalysis in alcohol and hydrocarbon oxidation reactions.

1. Introduction

Significant work has gone into developing green, renewable energy sources and energy-conversion technologies, like fuel cells and metal–air battery packs, in an attempt to alleviate the current severe environmental pollution and the global energy deficit.[1,2] Polymer electrolyte membrane fuel cells (PEFCs), also known as proton exchange membrane fuel cells, have been widely regarded as the most promising candidate for use as power sources in transportation systems and portable electronic gadgets because of their low impact on the surrounding ecosystem and high rate of effective energy conversion.[2,3] Hydrogen and oxygen electrochemically react in a PEM fuel cell for energy conversion. To separate the reactant gases and transfer ions, this system relies on a polymer electrolyte membrane (PEM). The anode, cathode, and polymer electrolyte membrane are the main parts of a polymer electrolyte membrane fuel cell (PEFC). The anode generally consists of a catalyst based on platinum that has been deposited onto a conductive support, such as carbon. Using this catalyst, hydrogen gas (H_2) may be broken down into its constituent ions (H^+) and electrons (e^-). An electric current is generated when electrons travel *via* an external circuit and protons pass across a polymer electrolyte membrane.[4,5] The polymer electrolyte membrane is an extremely thin proton-conducting substance that prevents electrons from passing through but enables protons to cross. Because of its strong proton conductivity and chemical stability, it is often made of a perfluoro sulfonic acid polymer, like Nafion. The membrane works as a barrier, stopping the reaction gases (hydrogen and oxygen) from mixing while allowing protons to pass through. The cathode, like the anode, features a catalyst, typically platinum, that accepts protons and electrons from the external circuit and catalyzes the reduction of oxygen gas (O_2). The principal reaction by-product in PEFCs is water (H_2O), formed when oxygen combines with the protons and electrons.[5–8] The operating temperatures of PEMFCs are as low as <100 °C; hence, they are suitable candidates for use in stationary power production and mobile electronics.[8] PEMFCs have several drawbacks: both their manufacturing and operating costs are high; in particular, they employ platinum-based catalysts and ion-conductive membranes, which are costly.[8–10,13] These components increase the cost of the fuel cell system, making it less affordable than alternative power-production systems. Durability and lifespan: PEMFCs degrade with time. Catalyst poisoning, membrane deterioration, and electrode corrosion diminish the cell efficiency and lifespan. PEMFC durability research is ongoing.[8–11,150] PEMFCs are susceptible to fuel and air pollution. Even modest levels of carbon monoxide (CO) may drastically degrade the platinum catalyst performance, reducing power production. This sensitivity demands careful fuel and air filtration, increasing the system complexity and expense. PEMFCs need effective water management. They need a balance of membrane water to conduct protons while avoiding flooding or drying. Startup, shutdown, and transient operating conditions make the management of the fuel cell water level difficult. PEMFCs function below 100 °C. These characteristics permit rapid startup times and increased power densities, but they restrict waste heat recovery and increase freezing risk at low temperatures. Some applications need extra heating or cooling to maintain operational conditions. Hydrogen infrastructure: pure hydrogen PEMFCs. Producing, storing, and distributing hydrogen is difficult. Without a robust hydrogen infrastructure, hydrogen fuel may be scarce, limiting PEMFC deployment.[9–12,14,149–156]

1.1 Need for anion exchange membranes (AEMs)

To overcome the above-discussed demerits of PEMFCs, researchers have focused on new dimensions of membranes in fuel cells that are capable of exchanging anions and demonstrate great versatility with fuels.[15] Anion exchange membrane fuel cells work based on electrochemical processes, with the anode and cathode receiving fuel and oxidant, respectively. The anion exchange membrane is critical in aiding the transit of hydroxide ions, allowing chemical energy to be converted into electrical energy. This distinguishes AEMFCs from other forms of fuel cells, such as proton exchange membrane fuel cells[16] Fig. 1. AEMFCs are conceptually similar to PEMFCs, with the key distinction being that the solid membrane is an alkaline AEM rather than an acidic PEM. In an AEMFC, the OH^- anion is carried from the cathode to the anode *via* an AEM, which is the inverse of the OH^- conduction direction in a PEMFC. Because the implementation of an AEM provides an alkaline pH cell environment, the AEMFC has numerous potential merits over the existing PEMFC technology. Some of the merits of AEMs are their superior ORR (oxygen reduction reaction) kinetics, non-platinum or platinum-free catalyst electrodes, and low costs, which make them key alternatives to PEMs.[17,18]

1.2 Case study of per- and poly-fluoroalkyl substance (PFAS) contamination

While PEMFCs are considered green, they use perfluoro sulphonic acid membranes, which have been proven to cause severe environmental imbalance. In recent years, a manufacturer known for producing adhesive tapes and safety materials (such as reflective signs and coatings) has been entangled with numerous lawsuits concerning contamination from per- and poly-fluoroalkyl substances (PFAS), which are components of the membranes. The key origin of this contamination is thought to be the fire-fighting foam, which includes either perfluorooctanoic acid (PFOA) or perfluorooctanesulfonic acid (PFOS).[19,20] Questions regarding PFAS pollution have prompted health evaluations among individuals residing near the manufacturing facilities, uncovering heightened levels of PFAS in their bloodstream, including PFOS. The US Environmental Protection Agency (EPA) has strengthened the recommended thresholds for PFOA and PFOS in drinking water; however, these thresholds are not legally binding.[21,22] In another instance, Asahi Kasei Plastics, North America, settled with the state of Michigan, committing to investigate and take corrective measures to address PFAS pollution at a former production facility.[23] PFAS chemicals, such as PFOS and PFOA, exhibit persistence, bioaccumulation, and toxicity, resulting in extensive environmental pollution.[20–24,201] Researchers are developing systems to remediate PFAS-contaminated water, to eliminate over 90% of PFAS on-site.[25] Sharma *et al.* studied the recycling and reuse of PFSA from the used membrane electrode

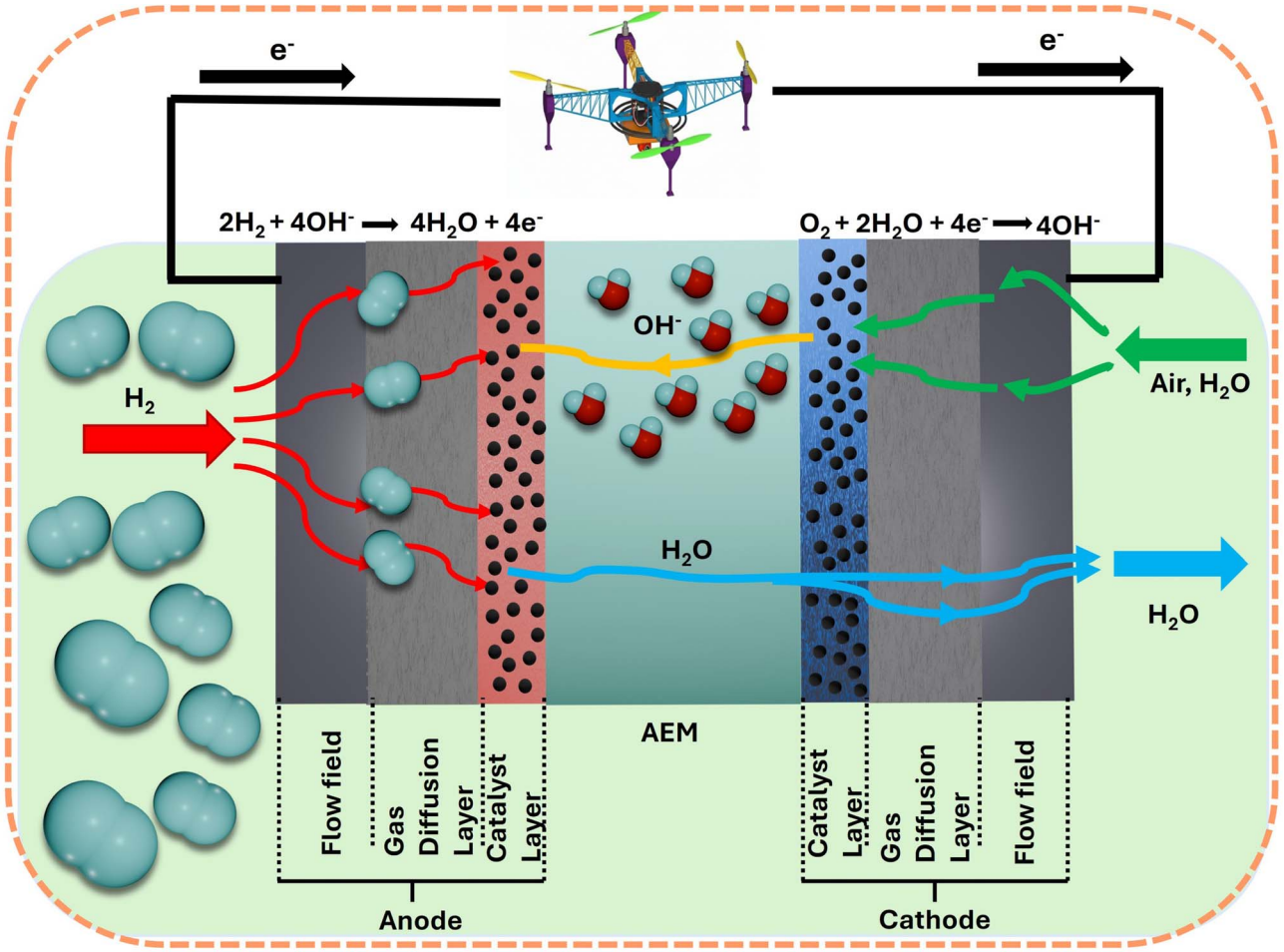

Fig. 1 Schematic of an anion exchange membrane fuel cell.

assembly (MEA) of PEMFCs. They adopted a method in which the Nafion from previous fuel cells is dissolved in ethanol and utilized in the production of new fuel cell components. The recycled Nafion is assessed using both the reintroduction and the absence of missing sulfonic groups. Both versions exhibited good performance; however, the one without extra sulfonation had the highest durability. This study demonstrates the practicality of reusing old Nafion in new fuel cells while maintaining excellent performance and durability, thus contributing towards the circular economy.[26]

1.3 Different anion exchange membranes

AEMs, *e.g.*, poly(terphenylene-methyl piperidine-biphenyl),[27] fluorinated poly(aryl piperidinium) membrane,[28] poly(styrene-*co*-4-vinylbenzyl chloride) (PSVBC)-based AEMs combined with polyquaternium-10,[29] hyperbranched poly(4-vinylbenzyl chloride) (HVBC),[30] Aemion+® membranes,[31] poly(fluorenyl aryl piperidinium),[32] quaternized PAES (Q-PAES), poly(arylene ether sulfone) (PAES) block copolymer membranes,[33] *etc.*, have been reported to show excellent stability, enhanced performance and high durability, making them excellent for fuel cell applications. In addition, AEMs expedite the process of oxygen reduction reaction (ORR) under alkaline conditions, hence improving the overall efficiency of the fuel cell.[31–34] The advancement of sophisticated AEMs has resulted in enhancements in ionic conductivity and mechanical durability, with certain membranes attaining high levels of conductivity (>150 mS cm^{-1} at 80 °C) and exceptional dimensional stability.[35] Zhegur-Khais *et al.* reported OH-conductivities exceeding 200 mS cm^{-1}, with a notable record of 300 mS cm^{-1}, evaluating the accurate hydroxide conductivity of anion exchange membranes.[170] Moreover, the utilization of cutting-edge substances and structural alterations, such as phase-separated morphologies and interpenetrating polymer networks, has led to the development of membranes that possess exceptional chemical and thermal durability, along with decreased swelling. The environmentally favorable characteristics of specific AEMs, such as those derived from chitosan, further enhance their attractiveness by positioning them as biodegradable alternatives. Additionally, their capacity to function in less corrosive settings, in contrast to the acidic PEMFCs, diminishes the deterioration of cell components, thus prolonging the lifespan of the fuel cell. Recent progress in comprehending hydration levels and their influence on ionic conductivity has enhanced the efficiency of AEMs, rendering them more suitable for extensive use. In summary, the combination of cost reductions, fuel adaptability, performance improvements, and environmental advantages

makes AEMs an extremely appealing choice for future fuel cell technologies.[34–37]

Advances in computer vision, voice recognition, language translation, and natural language comprehension have been achieved using artificial intelligence (AI) in the last 10 years. AI techniques have proven useful in addressing complicated issues in scientific and technical disciplines; the data-driven methodology has arisen as the fourth and latest paradigm. Complex jobs, like picture identification, disease diagnosis, and gaming, have been surpassed by AI (Artificial Intelligence)-driven systems. Machine Learning (ML), an expanding segment of artificial intelligence, concentrates on statistical algorithms that improve with experience. Support vector machines, kernel approaches, and neural networks are extensively utilized in this domain, with deep neural networks being the most significant area of inquiry, owing to their extensive applicability. These algorithms not only propel but also augment automation. As robots transform design, manufacturing, and transportation, signifying a new industrial revolution, achieving comparable breakthroughs in materials discovery necessitates AI, especially in emulating human scientific intuition, reasoning, and decision-making. Artificial Intelligence (AI) and Machine Learning (ML) techniques have demonstrated an ability to significantly improve the performance and efficiency of Anion Exchange Membrane Fuel Cells (AEMFCs). The need for lengthy experimental trials may be minimized with the use of these technologies, which may improve the membrane electrode assembly (MEA) by identifying critical parameters.[157–159] The advancement of chemical knowledge increasingly depends on the identification of novel electrocatalysts and reactions, a process now substantially facilitated by computational algorithms. These algorithms, which are organized collections of problem-solving protocols, may be designed to examine chemical structures and forecast new reactions. Machine learning augments this by allowing computers to learn from data and generate educated predictions. By delineating chemical issues inside an algorithmic framework, researchers may employ statistical methodologies to expedite the discovery of novel chemical insights. Researchers can effectively investigate chemical and electrochemical realms by concentrating on densely inhabited areas and using algorithms to assess features like molecule weight, reaction type, and/or reaction kinetics, thereby optimizing experimental settings for enhanced results. Although single-parameter optimization is commonly utilized in molecular synthesis, chemists exercise caution with completely automated searches because of the extensive complexity of potential molecular structures. The integration of machine learning with real-time electrochemistry presents considerable potential for revolutionizing the identification of materials, enhancing redox kinetics and reactions, reducing researcher bias, and markedly improving the efficiency and accuracy of scientific research.[157–160]

The efficacy of machine learning (ML) models is essentially contingent upon the quality, diversity, and accessibility of the foundational datasets. High-throughput synthesis (HTS), whether conducted manually or with complete automation, is essential for producing extensive, systematic datasets that document differences in reaction pathways, material compositions, and physicochemical attributes. Extensive datasets markedly increase the ML model's accuracy, boost generalizability, and provide more dependable predictions of optimal reaction conditions and material performance. When combined with automated experimental platforms, AI-driven high-throughput screening creates a closed-loop optimization framework, wherein machine learning models direct experimental design, and freshly generated data subsequently enhance model performance. This synergistic cycle expedites the discovery, optimization, and characterization of materials, resulting in the rapid identification of high-performance candidates and the more efficient adjustment of system parameters. Consequently, the systematic creation, meticulous curation, and public distribution of high-quality datasets are crucial for the advancement of AI-driven research in energy materials and AEMFC technologies.[160,161] When it comes to forecasting performance measures, AI-assisted models, such as XGBoost, decision trees (DT), and artificial neural networks (ANN), have proven to be quite accurate. After comparing Linear Regression (LR), *K*-Nearest Neighbors (KNN), and Support Vector Machine Regression (SVMR) over a range of humidity conditions, it was found that LR predicted the PEMFC performance with the highest accuracy.[91,97,160] This systematic perspective wraps up with the article's efforts and findings while offering some insights regarding the future directions of AI/ML-guided AEMFC technology.

1.4 Comparative analysis of AEMFC research trends: PGM catalysts and AI/ML integration

Bibliometric analysis from 2010 to 2025 identifies two distinct developmental paths influencing the progression of AEMFC research trends. The following keyword has been used to generate the data from both SCOPUS and WOS (TITLE-ABS-KEY ("key word") AND ("keyword" "anion exchange membrane fuel cell") (2010–2025)), applicable for both trend analyses. The initial trend (Fig. 2a) illustrates the disparity between the overall AEMFC articles and those particularly addressing non-precious-metal (NON-PGM) catalysts. Commencing with about 50 AEMFC articles in 2010, the domain proliferated swiftly to almost 600 publications by 2025. During the same timeframe, research on NON-PGM catalysts increased from around 5 papers ($\approx$10% of AEMFC literature) to around 170 ($\approx$28%), indicating a significant and deliberate transition towards cost-efficient, resource-sustainable, and scalable catalyst alternatives. The significant increase in NON-PGM research post-2018 corresponds with heightened corporate involvement and specific government financing aimed at facilitating alkaline fuel cell commercialization, indicating a fundamental shift in the research environment. The second trend (Fig. 2b) underscores the divergent yet converging adoption rates of AI/ML methodologies in PEMFC and AEMFC research. Although publications on AI/ML linked to PEMFCs are greater, totaling 288 in 2025 compared to 122 for AEMFCs, the increasing pace of AI/ML research related to AEMFCs is far more pronounced. The publishing disparity has decreased from a 4 : 1 ratio in 2010 to around 2.4 : 1 by 2025. This acceleration signifies a swiftly

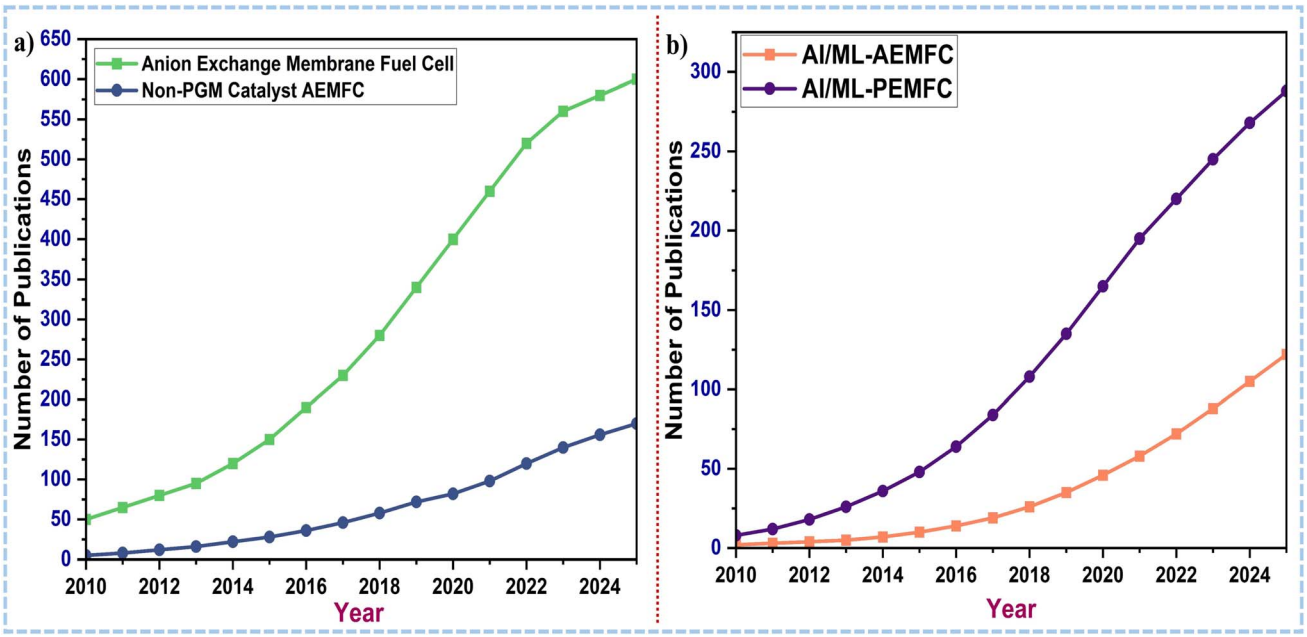

Fig. 2 Graphical analysis of annual research growth trends in (a) AEMFC development compared with non-PGM catalyst utilization in AEMFCs (2010–2025) and (b) AI/ML integration for AEMFCs compared with PEMFCs (source: SCOPUS and WOS 2010–2025).

growing acknowledgment of machine learning's contribution to advancing AEMFC innovation and facilitating predictive membrane design, catalyst optimization, degradation forecasting, and system-level performance modeling. These trends collectively underscore the technological advancement of AEMFCs and the nascent incorporation of computational intelligence to advance the field towards practical implementation.

These trends indicate the evolution of AEMFCs from a nascent research area to a more data-driven and catalyst-optimized technological platform. The concurrent advancement of non-PGM (platinum group metal) catalyst development with the increasing implementation of AI/ML techniques suggests that future advancements in AEMFCs will significantly rely on computational screening, machine learning-assisted material discovery, and predictive performance modeling. This convergence will enable the field to bridge the gap with the more established PEMFC technology and enhance the trajectory toward scalable, cost-effective, and commercially viable alkaline fuel cell systems.[210–215]

1.4.1 Synopsis. The bibliometric trends together indicate a developing AEMFC ecosystem marked by increasing material research, heightened focus on non-PGM catalysts, and rapid incorporation of AI/ML methodologies. These findings underscore the significance of this study and indicate a more data-driven trajectory for the evolution of AEMFC.

1.5 Mechanisms involved in improving the efficiency of AEM fuel cells

In AEMFCs, cell efficiency can be improved by enhancing the conductivity of the MEA, structural stability, and water management, as well as optimizing the ionomer loading.[38] The performance of anion exchange membrane fuel cells is directly influenced by the ionic conductivity, making it critical. Stretching of AEMs can greatly enhance the OH^- conductivity by aligning polymer chains and elongating water clusters, hence improving ion-transport routes.[39] The hydration level of AEMs is crucial, as a high water content often enhances ionic conductivity. This is evidenced by the superior performance of Orion and Alkymer membranes under varying hydration levels. Introducing hyperbranched structures and phase-separated morphologies improves water absorption and creates effective ion-transport pathways, resulting in increased OH^- conductivity and improved mechanical characteristics. Furthermore, the utilization of functionalized polymers and cross-linking techniques, such as those involving poly(styrene-*co*-4-vinylbenzyl chloride) and polyquaternium-10, leads to anion exchange membranes (AEMs) that exhibit both high ionic conductivity and long-term durability. These properties are crucial for ensuring the steady operation of fuel cells.[38–42] The insertion of alkyl side chains and fluorinated structures also encourages the separation of phases, resulting in the formation of linked hydrophilic channels that enhance the movement of anions while preserving dimensional stability.[29,42] Researchers have investigated different materials and structural changes to enhance the ion-exchange capacity, water absorption, and OH^- conductivity of anion exchange membranes (AEMs). This has resulted in improved performance of fuel cells. Some of the modifications include incorporating quaternary ammonium poly(vinyl alcohol) (QPVA) and poly(diallyldimethylammonium chloride) (PDDA).[43] The long-term durability of AEMs under high-pH conditions is dependent on the mechanical and thermal stability of their polymer matrix and cationic head framework. Advanced designs, such as the tripartite cationic full-interpenetrating polymer network (F-IPN) and fluorinated

poly (aryl piperidinium) (FPAP) anion exchange membranes (AEMs), have shown substantial enhancements in terms of ionic conductivity, mechanical characteristics, and chemical stability.[29,44,45] Computational models emphasize the significance of characteristics such as water diffusivity, membrane thickness, and ion-exchange capacity in maximizing the performance and lifespan of anion exchange membranes (AEMs). Together, these improvements in AEM design and material composition enhance the efficiency and longevity of fuel cells, making them more suitable for commercial use.[46,47,173,174] In this timely systematic review, the integration of artificial intelligence (AI) and machine learning (ML) techniques in AEM fuel cells, as well as the advantages, technology gaps, and pathways to overcome challenges, has been discussed.

2. Operating principles and components of AEMFCs

AEMFC can function using non-precious/non-platinum group metal electrocatalysts and low-cost anion exchange membranes (AEM). Hydrogen is allowed to pass through the anode as fuel, and oxygen is allowed to pass through the cathode as an oxidant. The anode electrode typically employs an electrocatalyst, such as Pt/C or Ru/C; nevertheless, the cathode can make use of non-precious metal catalysts, such as Fe–N–C or cobalt ferrite (CF) nanoparticles supported on Vulcan XC-72 carbon (CF-VC). The AEM enables the movement of hydroxide ions (OH^-) from the cathode to the anode, where hydrogen oxidation takes place, resulting in the production of water and electrons.[7,42,48] The primary concern in AEMFC is the inclusion of water as a reactant, alongside the O_2 oxidant, at the cathode. Oxygen is then reduced into OH^- ions while the cell load is applied; these ions subsequently traverse the membrane to the anode side and combine with H_2 to generate H_2O as the final product. Water is used at the cathode and produced twice at the anode. If water management is not correctly maintained, the cathode may get dry, and the anode may become inundated. During the redox reaction, electrons generated at the anode are gathered by the current collectors and conveyed to the cathode by the external circuits.[38] This excess water in the cell can hinder the performance of the fuel cell. More about the importance of balancing the water in the AEM fuel cell will be discussed in the upcoming section. Fig. 3 illustrates photographic images of the side view and top view of a real-time fuel cell, and the AEMFC oxidation-reduction mechanism is given below.

Anode-oxidation:

$$2H_2 + 4OH^- \rightarrow 4H_2O + 4e^-$$

Cathode-reduction:

$$O_2 + 2H_2O + 4e^- \rightarrow 4OH^-$$

Overall:

$$O_2 + 2H_2 \rightarrow 2H_2O$$

Fig. 3 Photographs of the top view and side view of a real-time fuel cell.

In AEMFCs, aqueous solutions of KOH/NaOH or K_2CO_3/Na_2CO_3 are used to conduct ions between electrodes, where the AEM acts as a separator/barrier between the anode and the cathode to avoid short-circuiting. The solid AEM electrolyte not only transports (OH^-) ions but also helps minimize the carbonation and fuel crossover related to Aq electrolytes. AEM exhibits exceptional thermal and mechanical attributes. An efficient fuel cell requires OH^- ions to be selective and to have good conductivity through the membrane. Nevertheless, the selection of the membrane and its subsequent design necessitate creative and original endeavors. The ideal membrane would be impermeable to fuel, stable in the medium of choice, and long-lasting independent of the hydration state while retaining its characteristics at the operating temperatures.[38,42] The rate of membrane degradation in PEMFCs is substantially lower when compared with that in AEMFCs, due to the extremely corrosive nature of the latter. Nevertheless, the primary benefit of the alkaline fuel cell is its reduced occurrence of fuel crossover. The primary cause of fuel crossover is the electroosmotic drag phenomenon and the disparity in concentration between the anode and cathode. The fuel crossover takes place in the opposite direction as the OH^- ion flow, resulting in a significant reduction in electroosmotic drag. Approximately around 1970, K. Kordesh was the first person to implement this technology in the automobile industry, which is what brought attention to AFCs.[38,52]

2.1 Mechanisms of anion conductivity

Anion exchange membrane fuel cells (AEMFCs) have significantly lower anion conductivities compared to the proton conductivities in Nafion-based proton exchange membrane fuel cells (PEMFCs). The anion conductivity is influenced by both the relative humidity and the cell temperature. Several mechanisms have been explained by a few research groups on anion mobility and conductivities; for example, the most common transport methods for hydroxide transfer *via* AEMs include the Grotthuss mechanism (Fig. 4a), diffusion, migration, and convection. The hypothesis that most of the OH^- ions are transported through the AEM *via* the Grotthuss mechanism is supported by the observation that OH^- ions display Grotthuss behavior in aqueous solutions, like protons. According to this mechanism, hydroxide ions move across the interconnected network of water molecules by forming or breaking covalent bonds. There is an argument claiming that the movement of the hydrated hydroxyl ion is accompanied by a water molecule with a higher coordination than usual. As shown in Fig. 4b, when another water molecule that donates electrons arrives, it causes rearrangements and reorientations of hydrogen bonds. This also leads to the transfer of hydrogen ions and the development of a water molecule that is fully coordinated in a tetrahedral shape. The hydroxide ion is transported across the membrane by a series of water molecules linked together through hydrogen bonding, which is then broken to release the hydroxide ion. In addition to the Grotthuss mechanism, diffusion and convective flow are deemed to be significant. Diffusive transport takes place when there is a gradient in the concentration and electrical potential. Convective flow occurs when hydroxides, as they migrate across the membrane, carry water molecules with them, resulting in a convective flow of water molecules across the membrane. Hydroxyl anions undergo surface site hopping on the membrane's quaternary ammonium groups. Due to the water's interaction with the membrane's fixed charges, this transport is believed to constitute a secondary kind of transport across the membrane. The tight coordination of water molecules around the ammonium groups reduces the likelihood of the ionic species interacting with the ammonium groups on the membrane.[49–51]

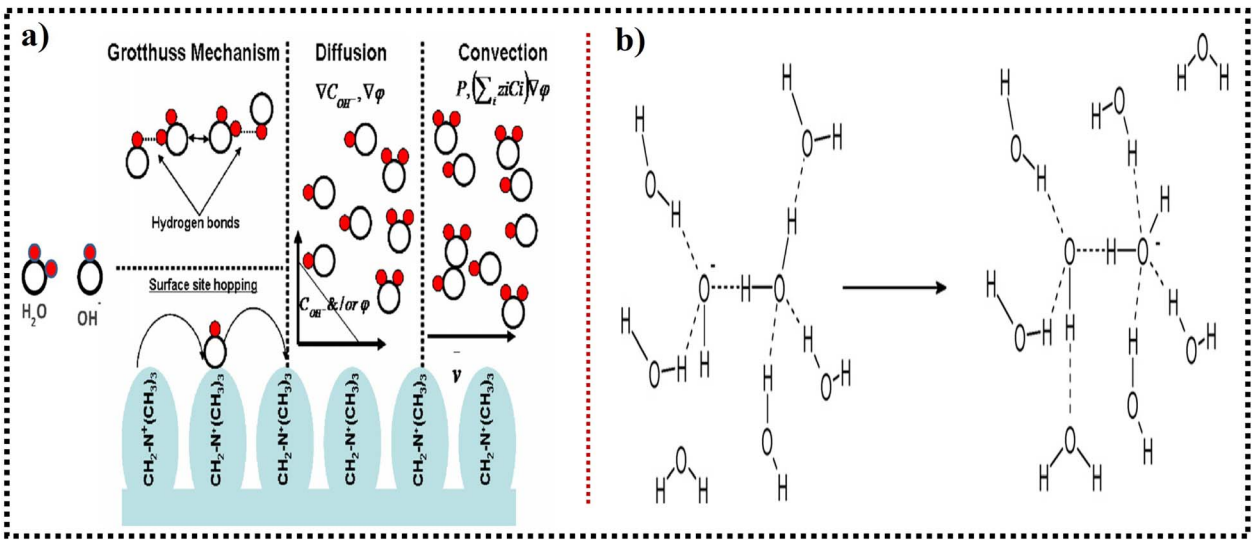

Fig. 4 (a) Grotthus, diffusion, and convection flow mechanism of OH^- transport in anion exchange membranes. Image reproduced from ref. 49 with permission from IOP Publishing, Kyle N. Grew and Wilson K. S. Chiu 2010 *J. Electrochem. Soc.* **157** B327, copyright © 2010. (b) Mechanism of hydrated OH^- ion transport in aqueous media. Image reproduced with permission from ref. 51. Copyright © 2011 Elsevier B.V. All rights reserved. https://doi.org/10.1016/j.memsci.2011.04.043.

The primary hurdle faced by AEMFCs is carbonation, which occurs when hydroxide ions react with CO_2 to produce bicarbonates. This process leads to increased resistivity and decreased power production, posing a significant obstacle for AEMFCs working with ambient air. *Operando* electrochemical measurements and neutron imaging have been suggested for use in gaining a deeper understanding of water distribution and its influence on performance, resulting in the achievement of unprecedented peak power densities. High performance and durability in AEMFCs are achieved through the methodical design and optimization of cell components, such as the use of ionomers with high water permeability and appropriate catalyst mixtures. While polymer degradation, which results in performance degradation, is negligible in high hydration states, long-term operation tests have shown that catalyst agglomeration is the other main source of performance degradation.[38,53,54]

2.1.1 Synopsis. This section clarifies the fundamental principles governing AEMFC operation, emphasizing the significance of hydroxide-ion transport, membrane–electrode interactions, and water-management dynamics in influencing cell efficiency. The foundational ideas support the ensuing discourse on material innovation and require improved computational methods to address current design and operational constraints.

2.2 Durability of anion exchange membranes (AEMs)

Poor chemical stability is one of the many limitations of AEMs, especially when subjected to environments with high pH and high temperatures. Emerging synthetic methodologies encompass controlled radical polymerization, grafting-from procedures, side-chain engineering, crosslinking tactics, heteroatom-functionalized backbones, and interpenetrating polymer networks (IPNs). To make AEMs last longer, researchers have investigated a variety of approaches. One example is the persistent problem of quaternary ammonium (QA) cationic group decomposition; nevertheless, new *ex situ* methods have been developed to assess the alkaline stability of soluble and insoluble AEMs in low-hydration environments, with encouraging outcomes for AEMs that have been grafted with radiation. Scientists have devised a novel technique to assess the resistance of anion-exchange membranes (AEMs) to alkaline conditions, even when they are not soluble in DMSO. This method involves utilizing Raman spectroscopy to track alterations in the characteristics of the membranes. The researchers employed two variants of radiation-grafted anion exchange membranes (AEMs), namely poly(ethylene-*co*-tetrafluoroethylene)-(ETFE)-based poly(vinylbenzyltrimethylammonium) and poly(-vinylbenzyltriethylammonium) ETFE-TEA, together with a crosslinked polymer derived from a random copolymer and

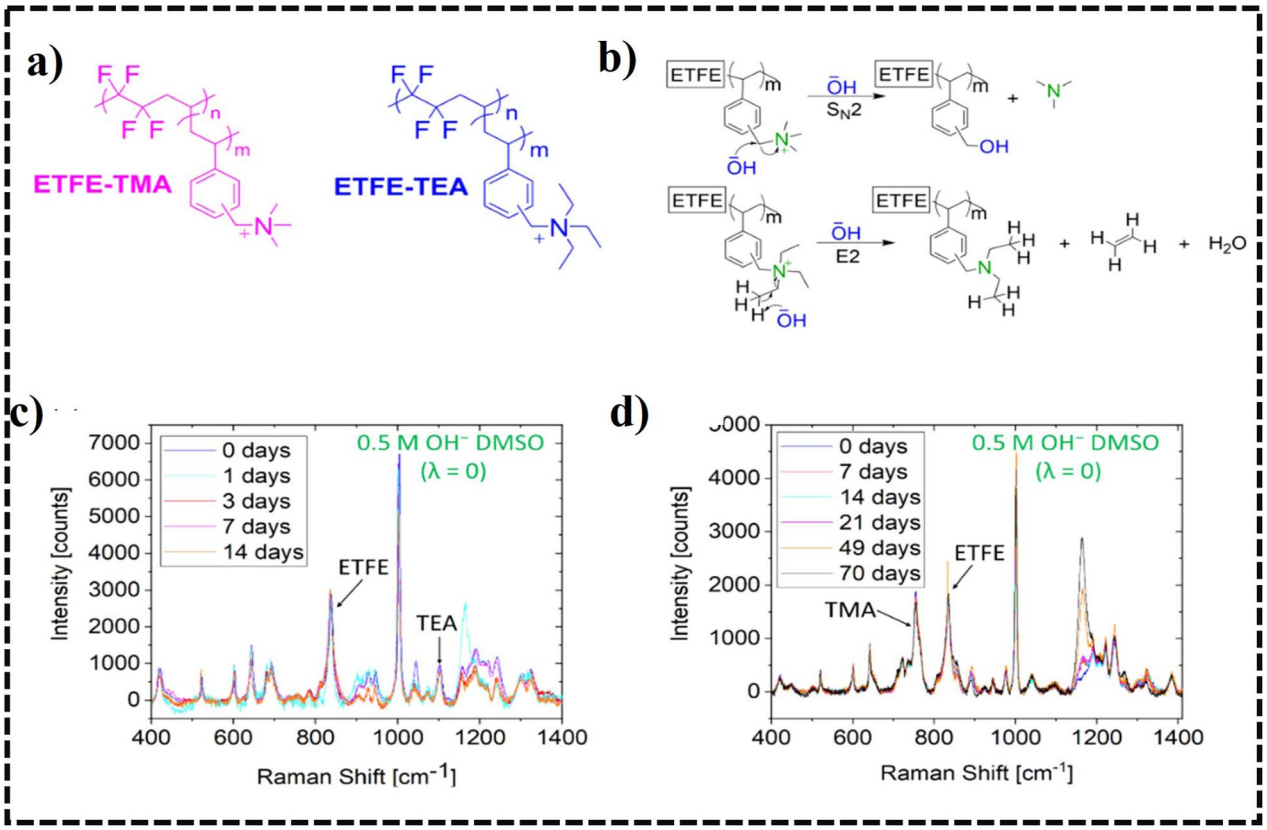

Fig. 5 (a) Structures of ETFE-TMA and ETFE-TEA. (b) Degradation mechanisms of ETFE-TMA by nucleophilic attack (SN_2) and ETFE-TEA by Hofmann elimination (E_2). (c) Raman spectra of ETFE-TEA. (d) Raman spectra of ETFE-TMA immersed in 0.5 M OH^- DMSO. Image reproduced with permission from ref. 55. Copyright © 2023 the American Chemical Society. This publication is licensed under CC-BY 4.0. https://doi.org/10.1021/acsaem.2c03689.

N,*N*,*N*′,*N*′-tetraethyl-1,3-propanediamine (TEPDA). The objective was to evaluate the durability of these materials in alkaline environments. The study revealed that the AEMs exhibited excellent stability in very alkaline settings, as evidenced by their preserved ion-exchange capacities and OH^- conductivities (Fig. 5). This is a crucial characteristic for ensuring their long-term effectiveness in real-world applications.[55]

Researchers previously discovered that the catalyst and ionomer in the cathode of anion exchange membrane fuel cells (AEMFCs) degrade dramatically over time, although the membrane remains reasonably robust. This finding suggests that the cathode environment significantly contributes to the performance loss that occurs in these fuel cells. Catalyst and ionomer degradations happen over time; however, membrane stability plays an important role, and the membrane does not degrade significantly over time. The alkaline environment and the presence of the cathode catalyst layer are recognized as the primary factors contributing to the deterioration of both the catalyst and ionomer, resulting in a decline in the performance of the fuel cell. The utilization of an alkaline-stable ionomer that possessed an *N*,*N*-dimethylhexylamine group, which was developed based on density functional theory (DFT) calculations, led to an increase of 87% in the fuel cell's endurance.[56] Enhanced water management was achieved by utilizing functionalized carbon (fluorinated carbon) as an additive in the catalyst layer (CL) of the anode, which helped to tune the hydrophobicity and hindered water flooding. On the other side, the cathode is modified with fluoroalkyl-functionalized and hydroxyl-functionalized carbons to optimize water management (Fig. 6).

To prevent the cathode from drying out, the cathode contains hydroxyl-functionalized carbon. Because the integration of the hydrophobic anode CL and the hydrophilic cathode CL reduces the water imbalance between the cathode and the anode, the maximum current density is increased by 1.7 times in comparison with the current density in carbon-additive-free MEA systems. Additionally, the pairing ensures stable, constant current operation for more than 1000 hours. Carbon materials aid in the efficient management of water, thereby mitigating the issues of flooding, which can impede gas flow due to excessive water, and drying, which can hinder the chemical reactions necessary for power generation due to insufficient water. Functionalized carbon modifications enhance the number of active sites available for chemical reactions, leading to increased fuel cell efficiency and improved water management by promoting water production and consumption processes.[57] In another study, it was demonstrated that incorporating fluorine atoms into carbon-based materials can increase the catalyst performance in low-temperature fuel cells. The incorporation of fluorine atoms into carbon-based materials enhances their surface area, improves their pore structure, and safeguards them from deterioration during the redox process in fuel cells. This further enhances the interaction between the carbon support and platinum group metals, hence increasing the efficiency of the catalyst in promoting the required redox processes, corrosion resistance, and thermal stability.[58] Another interesting study revealed that altering the cell temperature/operational temperatures enhances the performance of fuel cells. Increasing the operational temperature of anion exchange membrane fuel cells (AEMFCs) to 120 °C enhances their performance and efficiency by accelerating reaction and mass-transfer rates. The increased temperature further boosts the water diffusivity, leading to better hydration levels at the cathode and resulting in a decrease in the ionomers' chemical degradation rate.[59,175–177] Chen *et al.* reported poly(fluorenyl aryl piperidinium) membranes and ionomers exhibiting exceptional OH^- conductivity, minimal H_2 permeability, and superior

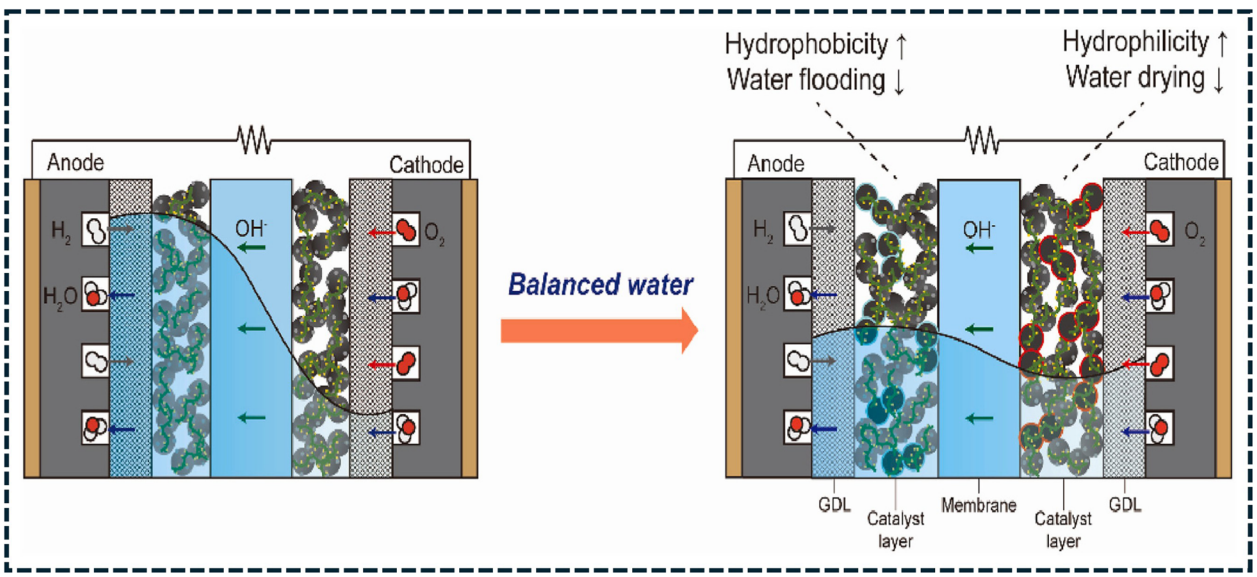

Fig. 6 Illustration of the hydrophobicity-tuned MEA by pairing a hydrophobic anode and a hydrophilic cathode. Image reproduced with permission from ref. 57. Copyright © 2022 Elsevier B.V. All rights reserved. https://doi.org/10.1016/j.jpowsour.2022.231835.

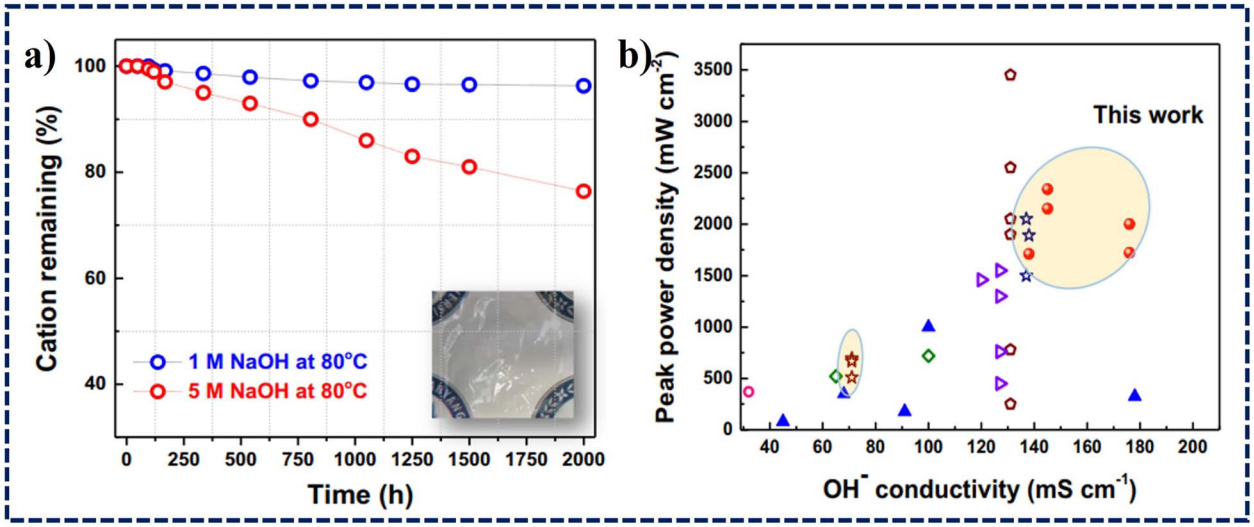

Fig. 7 (a) Cations (%) of the PFTP-13 AEMs at different concentrations of NaOH (1 and 5 M) at 80 °C after 2000 hours, detected by ^{1}H NMR, along with the picture of the membrane after alkaline treatment in 1 M NaOH for 2000 h. Notably, 3% and 22% losses in the ion-conducting groups (piperidinium) were detected by ^{1}H NMR testing after immersion in those alkaline solutions. (b) Comparison of OH^- conductivity and PPDs at 80 °C for representative AEIs in the current research. PFAP (red cycle) and FAA Fumion ionomers (brown star) in this work. PSF/PPO ionomers (blue triangle symbols): BMTA-polysulfone, BTMA-PPO, DMP-PPO, ASU-PPO, and multi-cation side chain PPO. PBI ionomers (pink circle symbols): HMT-PBI; BTMA-ETFE ionomers (brown pentagon symbols). BTMA-SEBS ionomers (green tetragon symbols), PAP ionomers (blue star symbols): PFTP-0 and PFBP-0 ionomers (but the OH^- conductivity of PFBP-0 is currently missing). PF/PP ionomers (purple triangle symbols): sidechain polyfluorene and polyphenylene. Image reproduced with permission from ref. 32, copyright 2021 © Nature publishing group under Creative Commons Attribution 4.0. https://doi.org/10.1038/s41467-021-22612-3.

mechanical characteristics. They exhibited a significant OH^- conductivity of 208 mS cm^{-1} at 80 °C, with low H_2 permeability, and they continued to exhibit *ex situ* durability for 2000 hours in 1 M NaOH at 80 °C. The poly(fluorenyl aryl piperidinium) membranes and ionomers demonstrated impressive power densities of 2.34 W cm^{-2} in H_2–O_2 and 1.25 W cm^{-2} in H_2–air (CO_2-free). These newly developed membranes have exceptional tensile strength, elongation at the point of rupture, and Young's modulus. This allows for effortless fabrication into thin membranes while maintaining a high level of rigidity and thermomechanical stability.[32] Fig. 7a illustrates the ^{1}H NMR spectra of PFTP-13 AEMs at different concentrations of NaOH (1 and 5 M) at 80 °C after 2000 h and Fig. 7b presents a comparative study of OH^- conductivity and PPDs for typical AEIs at 80 °C. This work utilizes PFAP (red cycle) and FAA Fumion ionomers (brown star). The PSF/PPO ionomers are represented by blue triangle symbols and include BMTA-polysulfone, BTMA-PPO, DMP-PPO, ASU-PPO, and multication side-chain PPO. PBI ionomers are represented by pink circle symbols, whereas BTMA-ETFE ionomers are represented by brown pentagon symbols. BTMA-SEBS ionomers, which are represented by green tetragon symbols, and PAP ionomers, which are represented by blue star symbols, are identified as PFTP-0 and PFBP-0 ionomers, respectively. However, the OH^- conductivity of PFBP-0 is missing. PF/PP ionomers are represented by purple triangle symbols and consist of sidechain polyfluorene and polyphenylene.[32]

A poly(fluorenyl-*co*-aryl piperidinium) ionomer with a side chain grafted onto it exhibited an impressive peak power density of 2.6 W cm^{-2} at 80 °C. By maintaining a low voltage decay rate of 0.4 mV h^{-1} under a current density of 0.6 A cm^{-2} at 70 °C, these ionomers show remarkable long-term *in situ* stability, suggesting that they can be used for extended periods in real-world settings.[60]

2.2.1 Synopsis. The current advancement of AEM materials has facilitated notable improvements in polymer backbone architecture, cation stability, mechanical resilience, nanophase segregation, and hydroxide conductivity. Notwithstanding these developments, persistent chemical deterioration and the trade-offs between conductivity and stability continue to pose significant obstacles. The problems at the material level provide a compelling justification for the incorporation of AI-driven screening and prediction capabilities, as discussed in the subsequent section.

3. Different catalyst electrode materials, oxygen reduction reaction (ORR) and hydrogen oxidation reaction (HOR)

The engineering of effective cathode catalysts is a key goal of fuel cell research, as the electrochemical oxygen reduction process (ORR) has intrinsically slow kinetics. The ORR is a multi-step reaction whose route is determined by the electrolyte type and catalyst type. In an alkaline solution, molecular oxygen can be reduced by either the 4e$^-$ or 2e$^-$ routes.[38,64] The reduction route should be either direct (4e$^-$) or two-step (2e$^-$), and peroxide generation should be minimized if the catalyst is to promote the reaction and maximize energy gain. Corrosion of fuel cell components due to peroxide generation leads to

unstable performance, which, in turn, reduces operating potential and current efficiencies.[64] Another significant benefit of AEMFCs is their capacity to employ non-precious metal (NPM)/non-platinum group (NPG) catalysts for the oxygen reduction process (ORR), which is essential for their economic feasibility and effectiveness. Their hierarchical porous structure allows for the transfer of reactants and products (O_2 and H_2O) through the macro- and mesopores, and the high microporosity allows for the hosting of many electroactive surface sites. Several investigations have examined diverse catalyst electrode materials to improve the activity of the oxygen reduction reaction (ORR) and the performance of fuel cells. Specifically, Fe–N–C catalysts produced from porous organic polymers and metal–organic frameworks have demonstrated encouraging results in anion exchange membrane fuel cells (AEMFCs), exhibiting significant ORR activity and power densities.[16,38,64,171] Fe–N–MPC and FeMn–N–MPC, which are mesoporous carbons doped with transition metals and nitrogen, have shown remarkable activity and stability in oxygen reduction reactions (ORR). These materials have achieved peak power densities of around 470 mW cm^{-2}.[61] Buggy *et al.* investigated various compositions of ionomers and catalysts to enhance the efficiency of water electrolysis systems through electrode optimization. The chemical composition of ionomers has a considerable impact on the transfer and movement of ions and neutrals in the electrode. This is essential for maximizing the efficiency of Anion Exchange Membrane (AEM) devices.[62] In microbial fuel cells, porous carbons that have been co-doped with copper and nitrogen have been produced. These carbons exhibit strong ORR activity and stability, and their power densities are equivalent to those of Pt-based catalysts.[63,64] Carbon materials with hetero atom (N, S, P, *etc.*) dopants are reported to show high electrocatalytic activity. The bandgap may be shifted, and the charge distribution may be modulated by nitrogen, which has a stronger electronegativity and an additional electron compared to carbon, causing the carbon atoms that are close to nitrogen to become more positively charged, which ultimately leads to an increase in the dissociative adsorption of oxygen molecules. The best-performing electrocatalyst for the oxygen reduction reaction (ORR) was the one that was annealed at 900C, and it was made utilizing N-doped ordered mesoporous graphitic arrays derived from *N*,*N*′-bis(2,6-diisopropylphenyl)-3,4,9,10-perylenetetracarboxylic diimide using ordered mesoporous silica SBA-15 as a template.[65] Pajarito Powder, LLC manufactured a mesoporous transition metal–nitrogen–carbon type catalyst utilizing a process called VariPore™. This catalyst incorporates iron and nitrogen as dopants. The catalytic performance is enhanced by the material's high specific surface area and very porous structure, with an average pore size of around 7 nanometers. Because of its mesoporous structure and the fact that it combines iron with nitrogen groups (pyrrolic-N, pyridinic-N, and graphitic-N), it performs very well when paired with the HMT-PMBI anion-exchange membrane. The use of Pt–Ru/C as the anode catalyst is also investigated with the Fe–N–C material as the cathode catalyst, affording peak current densities of 450 mA cm^{-2} at 0.4 V (Fig. 8a).[66]

Using an aluminum oxide template, N@CNTs (nitrogen-doped carbon nanotubes) were developed. At −1.2 V *vs.* Ag/AgCl, implausible ORR current densities were achieved in RDE (rotating disc electrode) mode, above the predicted limits of current densities for a 4-electron reduction of oxygen (O_2) by a factor of three. Fig. 8b illustrates N@CNTS and Pt/C electrodes at 50 °C, which exhibit current densities of 150 mA cm^2 and 170 mA cm^2 at 0.2 V, respectively.[67] A study on electrocatalysts using carbon nanotube/heteroatom-doped carbon was conducted by a group of researchers. For the synthesis, compound 1-butyl-3-methylimidazolium bis(trifluoromethyl sulfonyl)imide (BMITFSI) (ionic liquid) and tetraethyl orthosilicate (TEOS) were

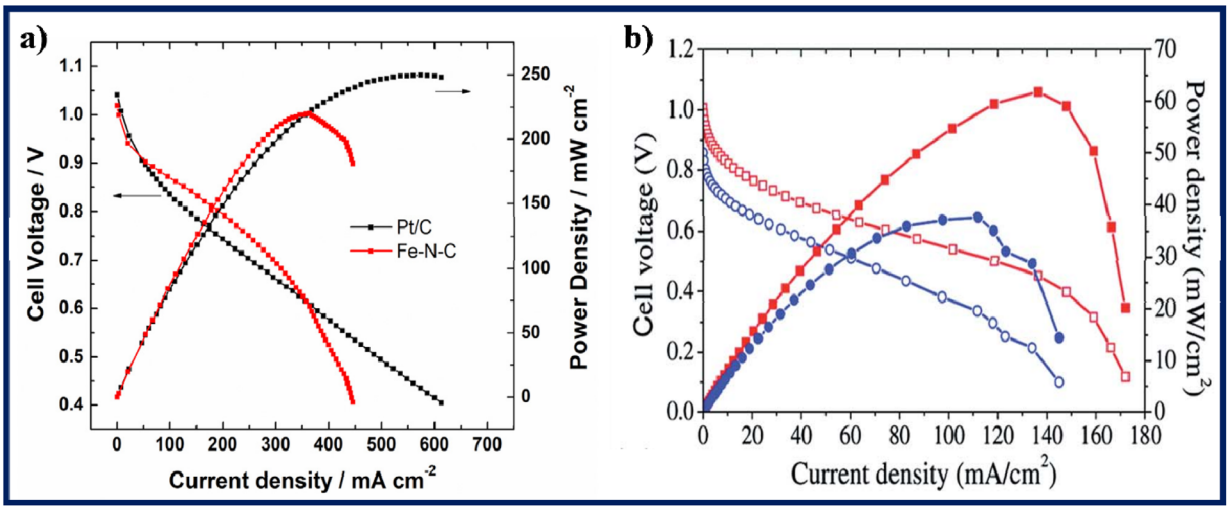

Fig. 8 (a) Polarization and power density curves for H_2/O_2 AEMFCs using the HMT-PMBI anion exchange membrane. The anode and cathode catalysts were Pt–Ru/C and Fe–N–C or Pt/C, respectively. $T = 60$ °C. Image reproduced with permission from ref. 66, copyright © 2021 The Author(s). Published by Elsevier Ltd. Under a Creative Commons license. https://doi.org/10.1016/j.powera.2021.100052. (b) MEA with N@CNTs and Pt/C as cathodes at 50 °C (red corresponds to Pt/C and blue to N@CNTs). Image reproduced with permission from ref. 67. Copyright © 2012 the American Chemical Society. https://doi.org/10.1021/jp210840a.

introduced into a mixture of CNTs (all suspended in the IL). Formic acid was used to initiate the synthesis of silica gel. After the solvent evaporated, a composite of carbon nanotubes (CNT), ionic liquid, and silica was created. This composite was then subjected to heat treatment at temperatures ranging from 800 to 1000 °C. The silica component was subsequently eliminated using hydrofluoric acid (HF). The resulting composite is referred to as CNT-HDC-*X*, where *X* is the carbonization temperature. To make an analogy, N-doped carbon nanotubes (CNTs) were also synthesized employing NH_3 and urea as the sources of nitrogen. TEM measurements confirmed the creation of a core-sheath nanostructure consisting of CNT/HDC. According to the XPS results, the HDC sheath had three different heteroatom dopants: N, S, and F. An inherent benefit of the IL-based technique is the potential to effectively regulate the kind and number of heteroatoms prevalent in the CNT/HDC composite. The deposition of HDC layers on CNTs significantly boosted the rate of progression of the oxygen reduction reaction (ORR). The oxygen reduction reaction (ORR) activity of the nitrogen-doped carbon nanotubes (CNTs) was lower than that of the platinum/carbon (Pt/C) catalyst in a 1 M potassium hydroxide (KOH) solution. The MEA with the CNT/HDC-1000 cathode achieved a maximum power density of 270 mW cm^{-2}.[68]

Some Pt-group catalysts showed excellent performance for AEMFCs, highlighting the potential of bimetallic catalysts, such as Pt–Ru. Research has demonstrated that a specific power output of 25 W per mg PGM may be achieved by combining low-loading Pt–Ru anodes with Fe–N–C cathodes.[69] With strong activity for both the oxygen evolution reaction (OER) and the oxygen reduction reaction (ORR), Pt–$Pb_2Ru_2O_{7-x}$ has demonstrated great potential as a bifunctional oxygen electrocatalyst.[70] Low-load Pd/CeO_2 bifunctional electrocatalysts, which can substitute platinum, have been characterized by life-cycle assessments as having positive effects on the environment.[71] However, to achieve zero PGM by 2030, the U.S. Department of Energy (DOE) has established massive goals to reduce PGM loadings. One approach that has been used to achieve these goals is the Switch Solvent Synthesis (SWISS) process, which has been able to lower PGM loading by a factor of 12 while retaining performance that is equivalent to those of commercial catalysts. Another approach is the development of atomically dispersed catalysts. The new techniques for making electrodes have cut the amount of anode catalysts by 85%, bringing the performance near 1 W cm^{-2}, in line with goals set by the DOE.[72,73]

3.1 Hydrogen oxidation reaction (HOR)

The hydrogen oxidation reaction (HOR) in anion exchange membrane fuel cells (AEMFCs) is the principal anodic mechanism that determines cell performance, which occurs when hydrogen combines with hydroxide ions to produce water and release electrons. In alkaline environments, the hydrogen oxidation reaction (HOR) follows the Tafel–Volmer–Heyrovsky mechanism; however, its kinetics are markedly slower by about 2–3 orders of magnitude compared to those in acidic PEMFCs, attributable to poorer hydrogen binding, competitive hydroxide ion (OH^-) adsorption, and protracted water-production stages. The hydrogen oxidation reaction (HOR) in alkaline systems demonstrates much slower kinetics than in acidic systems, presenting a substantial obstacle to the AEMFC performance. This kinetic discrepancy results from many mechanistic changes in the alkaline environments. The contact between hydrogen intermediates and catalyst surfaces diminishes in alkaline fluids, weakening the adsorption strength and obstructing the subsequent reaction steps, including dissociation and recombination. This boosts the activation energy and diminishes the overall reaction rates. The involvement of hydroxide ions adds complexity: OH^- species affect the surface adsorption energetics and impact both the Volmer step and hydrogen desorption, frequently contending for active sites. Consequently, surmounting these kinetic impediments necessitates the creation of highly efficient HOR catalysts specifically designed for alkaline conditions, particularly those that can optimize hydrogen and hydroxide binding energies to promote high AEMFC performance.[251,252] Innovative machine learning methodologies enhance the identification of HOR catalysts by forecasting essential characteristics, including the HBE (hydrogen binding energy), OHBE (hydroxide binding energy), and interfacial charge-transfer dynamics. Enhancing the hydrogen oxidation reaction (HOR) activity is crucial, as it directly affects the anode overpotential, water management, current density, and overall durability of fuel cells, hence facilitating the development of high-performance, cost-effective, and commercially viable AEMFC technologies.[236,252] Men *et al.* examined a PdNiRuIrRh high-entropy alloy (HEA) catalyst *via* machine learning-driven Monte Carlo simulations to elucidate its catalytic properties. Utilizing a dual-network deep potential model, iteratively trained with DFT-generated data, they attained precise mapping of the alloy's high-dimensional potential energy surface. This method facilitated the precise identification of surface atomic configurations, encompassing catalytically significant Pd–Pd–Ni, Pd–Pd–Pd ensembles, and oxophilic Ni/Ru sites. Their studies revealed a dramatic improvement in HOR activity, with a mass activity of 3.25 mA mg^{-1}, substantially surpassing that of Pt/C. Moreover, machine learning-based simulations of surface dissolution elucidated the high-entropy alloy's exceptional stability, exemplifying how artificial intelligence expedites catalyst development and enhances mechanistic comprehension.[236,262] In another study, machine learning was utilized in a guided experimental process to expedite the identification of HOR catalysts, implementing high-throughput fluorescence screening over an extensive compositional range of alloy electrocatalysts. Through the integration of catalyst composition, onset potentials, and comprehensive characterization data, their machine learning models not only forecasted novel active formulations but also elucidated critical mechanistic descriptors, namely the significance of average work function and metal–oxygen bond enthalpy in influencing catalytic activity. This data-driven technique discovered Pt_6Sn_4 as a notably promising alloy, which attained a power density of 132 mW cm^{-2} mg_{Pt}^{-1} in alkaline polymer membrane fuel cells, surpassing traditional Pt/C. These findings underscore the considerable potential of machine learning in enhancing the

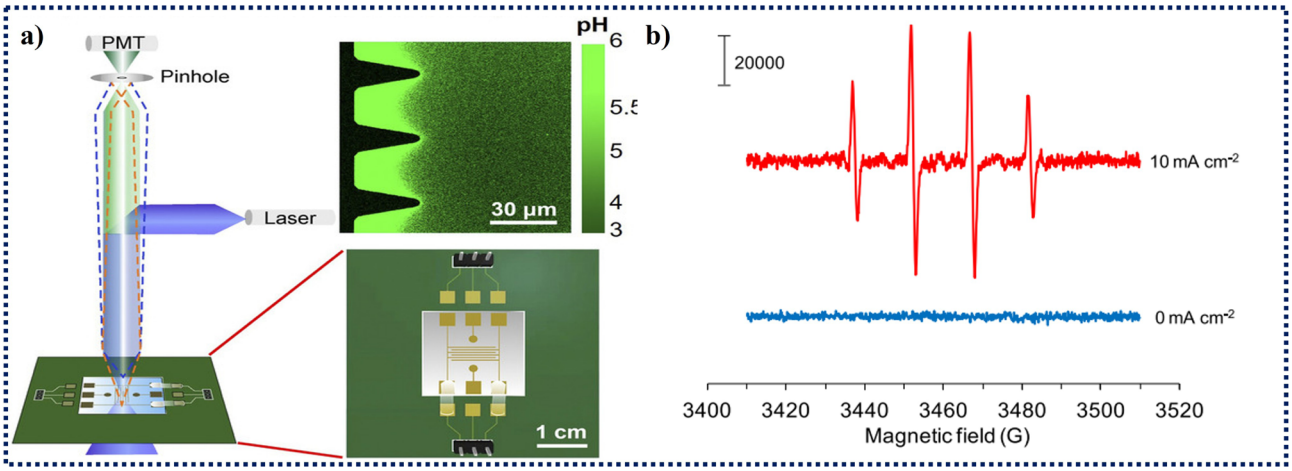

Fig. 9 (a) Novel *in operando* microfabricated electrochemical cell (MEC) combined with laser scanning confocal microscopy (LSCM) fluorescence detection system. Image reproduced with permission from ref. 74. Copyright © 2022 Wiley-VCH GmbH. https://doi.org/10.1002/anie.202206236. (b) ESR characterization of the ˙OH radicals produced electrochemically at the TiSO anode. Image reproduced with permission from ref. 75. Copyright © 2019 the American Chemical Society. https://doi.org/10.1021/acs.est.8b06773.

inadequately explored hydrogen oxidation reaction in alkaline environments, especially in addressing intricate alloy chemistries and revealing principles that regulate activity.[236,263]

4. Interfacial phenomena at the electrode–AEM interface

4.1 Optimization of ion-transport mechanisms in AEMs

If we want to learn how to optimize electrochemical processes, we need to know what happens at the interface between the electrode and the anion exchange membrane (AEM). Utilizing state-of-the-art methods, like laser scanning confocal microscopy (Fig. 9a), we can observe the dynamic activities occurring at this interface, including potential-induced ion redistribution. These processes include the creation and modification of the Nernst diffusion layer in response to pulsed voltage, which, in turn, facilitates ion transport.[74] The phenomenon of interfacial Joule heating (IJH) occurs at the interface between the anode and the solution during electrochemical advanced oxidation processes (EAOPs). This IJH effect causes an increase in the temperature at the interface, which, in turn, enhances the diffusion of hydroxyl radicals and the rates of oxidation. However, it also results in lower concentrations of hydroxyl radicals due to their conversion into H_2O_2 through a process called dimerization.

The higher temperature that occurs as a result of the interfacial Joule heating (IJH) effect results in a reduced concentration of OH that is accessible for oxidation. However, this results in an increase in the diffusion and reaction speeds, which makes the process more effective for notable organic molecules. The impact of temperature rise on the concentration and activity of OH radicals, the rate of pollutant degradation, and the overall efficiency of the EAOP process has been reported. Fig. 9b illustrates the formation of ˙OH radicals and their ESR (electromagnetic resonance) characterization at 10 mA cm^{-2} at the TiSO anode.[75] The pH effect on ion transport study revealed that carbonate ions play a major role in the kinetics of the hydrogen oxidation reaction (HOR) and the methanol oxidation reaction (MOR) at the AEM/Pt microelectrode interface. Site blockage and inadequate hydroxyl ion availability at low pH levels cause both processes to be suppressed.[76] Interfacial phenomena, such as water management and two-phase transport, are critical in proton exchange membrane fuel cells (PEMFCs), with mechanisms including "eruptive water expulsion" managing water movement within the fuel cell components.[77] Electrochemical measurements are often used to study the electrochemical double layer and adsorption processes at immiscible liquid interfaces, such as that between liquid metal and slag. This allows for an evaluation of the reaction kinetics and adsorption mechanisms, yielding valuable insights. *Ab initio* molecular dynamics simulations were used to study the behavior of electrified Au(111) slabs in contact with liquid water. The simulations showed that the electrochemical interface is not uniform, indicating the significance of comprehending the movement of the solvent under an applied voltage.[78,79] Surface analyses conducted using advanced techniques, such as Raman microscopy and atomic force microscopy, aided the identification of harmful processes occurring at the interface between the electrode and electrolyte. These processes can result in the deterioration and malfunction of the electrode.[80] A researcher investigated the interactions between electroless-plated Ni–P/Au UBM and Sn–Bi eutectic solder. The study found that Ni_3Sn was formed at the interface between the P-rich Ni layer and Ni_3Sn_4. This identification was made using the CBED (Convergent Beam Electron Diffraction) technique. The volume of the primitive unit cell of the Ni_3Sn phase was determined to be 104.10 $Å^3$, which closely approximates the theoretical value of Ni_3Sn (103.19 $Å^3$). This suggests the existence of the Ni_3Sn phase rather than Ni_2SnP. The interface was found to consist of three distinguishable layers. The Ni_3Sn_4 layer mostly consisted of Ni and Sn, with a minor presence of Au, as confirmed by STEM-EDS and CBED methods.[81] The

efficient operation of the cell is limited by the recombination rate of proton-hydroxyl groups. The occurrence of a concentration gradient of ions enhances the rate at which recombination occurs at the interface.[82] Electrochemical atomic layer epitaxy (ECALE) has successfully proven the controlled generation of compound semiconductors, such as CdTe. This technique has improved our knowledge of interfacial dynamics.[83] The relevance and complexity of the events occurring at the interface between the electrode and the AEM in different electrochemical systems are highlighted by these findings taken as a whole.

4.2 Interactions between AEM and electrode surfaces

The interactions between the active electrode materials and the electrode surfaces are complex, encompassing mechanical, electrical, and chemical dynamics. Surface electrodes that are both mechanically and electrically stable are essential for reliable biopotential signal capture; this is proven by the self-similar designed configurations that improve skin conformability and stretchability while decreasing motion artifacts and noise.[84] The presence of palladium nanoparticles with transition-metal oxides, such as RuO_2, improves the efficiency of the hydrogen oxidation reaction (HOR) by promoting the accumulation of OH^- groups on the surface of the palladium at lower overpotentials. The ionomer present in the electrode catalyst layer regulates the movement of ions and neutral particles toward the catalyst surface, hence exerting a substantial influence on charge transfer and the overall efficiency of the cell. The electrochemical interface is enhanced, and the kinetics of the oxygen reduction reaction (ORR) are improved by modifying the Ag catalysts with transition-metal phthalocyanine (MPc) molecules.[85–87] A two-dimensional model is used to investigate the impact of modifications of electrode parameters, such as porosity, catalyst loading, and ionomer content, on water transport and the overall performance of AEMFCs. Because anion exchange ionomers (AEI) swell to such a high degree and balanced water flow between electrodes is essential for AEMFC integrity and performance, these interactions also affect AEMFC water management. The study also found that a greater difference in porosity near the interface between the cathode gas-diffusion layer (GDL) and the electrolyte membrane increases the movement of mass and the removal of water, leading to improved performance of the anion exchange membrane fuel cell (AEMFC).[88] By optimizing the relative humidity and applying a hydrophobic treatment to the anode, problems such as anode flooding and cathode dry-out may be addressed, leading to a considerable increase in power density.[89] The chemical stability of anion exchange membranes (AEMs), specifically the deterioration of quaternary ammonium groups under alkaline conditions, continues to be a significant concern, especially when the membrane is exposed to ambient air and carbonation processes. Advanced modeling and experimental approaches, such as the incorporation of humidity sensors, allow for a deeper understanding of water dynamics and facilitate the optimization of operational parameters. Overall, understanding and engineering the chemical reactions between AEMs and electrode surfaces are essential for advancing AEMFC technology, enabling the use of non-precious metal catalysts, and improving long-term performance and reliability. Using modeling techniques like Artificial Intelligence and machine learning can help predict the issues in the cell earlier, a concept that is discussed in a later section.[90,91]

4.3 Water management

Anion exchange membrane fuel cells' (AEMFCs) capacity to handle water is a key factor that greatly affects how well and how long they last. Due to the unique nature of AEMFCs, wherein water is created at the anode and consumed at the cathode, a careful equilibrium is required to prevent dehydration and flooding, in contrast to the requirements for PEMFCs.[38,265] An effective approach for managing water involves utilizing hydrophilic gas diffusion layers to improve the hydration of the membrane. However, it is important to note that this method also raises the possibility of flooding. Moreover, employing humidity sensors to oversee and regulate the relative humidity at the gas outputs might offer significant insights regarding the water equilibrium at each electrode, hence facilitating the enhancement of operational circumstances and materials.[38,92,93] Omasta T. J. *et al.* demonstrated that anion exchange membrane fuel cells (AEMFCs) are dependent on the water content and balance, as they attained a very high-power density of 1.4 W cm^{-2} at 60 °C. They were able to do this by paying more attention to the delicate balance between hydrating the membrane and avoiding electrode flooding (Fig. 10a and b), which, interestingly, can happen at either the anode or the cathode. In order to investigate how the feed gas flow rate, gas feed dew points, and the usage of hydrophobic *vs.* hydrophilic gas diffusion layers affect the AEMFC performance, radiation-grafted ETFE-based anion exchange membranes and anion exchange ionomer powder functionalized with benchmark benzyl trimethylammonium groups were employed. During electrode optimization, the cell temperature was kept at 60 °C with a flow rate of 1 L min^{-1} for the hydrogen and oxygen reactant gases. Fig. 10c and d shows polarization curves illustrating the relationship between the applied cell voltage (V) and the current density (mA cm^{-2}). Fig. 10c shows the incorporation of Pt/Ru catalyst and 5% PTFE GDL in the anode (anode: 0.69 mg_{PtRu} cm^{-2} on 5% PTFE, cathode: 0.35 mg_{Pt} cm^{-2}; different cathode dew points, such as 60/60, 59/60, 58/60, 57/60, were reported). Fig. 10d shows that the cathode gas diffusion layer (GDL) was modified by including 5% polytetrafluoroethylene (PTFE). The dew points of the anode and cathode were set at 60/60 (anode: 0.6 mg_{PtRu} cm^{-2} with 5% PTFE, cathode: 0.4 mg_{Pt} cm^{-2}) and 54/57 (anode: 0.67 mg_{PtRu} cm^{-2} on 5% PTFE, cathode: 0.53 mg_{Pt} cm^{-2}).[38] The proposed distribution of water inside the AEM and the electrodes in an AEMFC is based on the hypothesis that there is a high-conductivity AEM with significant water back-diffusion. This distribution is expected to change as the relative humidity of the gas stream increases. Advanced modeling approaches have been used to forecast how AEMFCs would react to changes in operational factors, such as inlet humidity and temperature. This helps to identify performance limitations and develop ways to overcome them.[94]

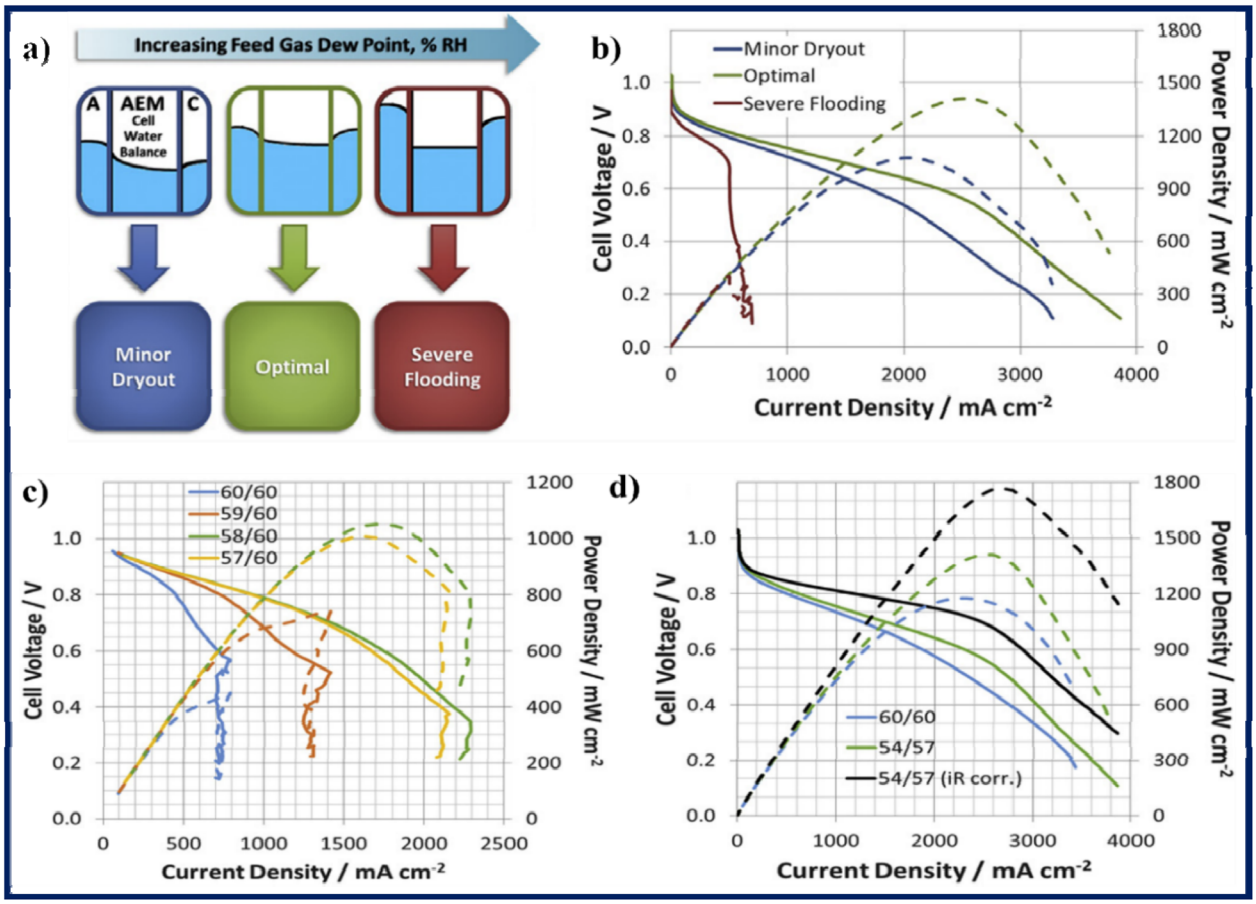

Fig. 10 (a and b) Illustration of the proposed distribution of water inside the AEM and electrodes in an AEMFC, based on the hypothesis that there is a high-conductivity AEM with significant water back-diffusion. This distribution is expected to change as the relative humidity of the gas stream increases along with the graph of the cell polarization curve. (c) Incorporating Pt/Ru catalyst and 5% PTFE GDL in the anode (anode: 0.69 mg_{PtRu} cm^{-2} on 5% PTFE, cathode: 0.35 mg_{Pt} cm^{-2}), with different cathode dew points. (d) The cathode gas diffusion layer (GDL) was modified by including 5% polytetrafluoroethylene (PTFE). The dew points of the anode and cathode were set to 60/60. Image reproduced with permission from ref. 38, copyright © 2017. Published by Elsevier B.V. https://doi.org/10.1016/j.jpowsour.2017.05.006.

The fabrication of ionomers and hydrophilic membranes, along with the control of dew points and flow rates, has demonstrated potential in preserving the required water content of the membranes without leading to instability.[95] The mobile hydroxide anions react with the CO_2 in AEMFCs to produce bicarbonate and carbonate anions. Carbonate ions undergo a chemical reaction with the potassium cations that are freely moving in the liquid KOH/K_2CO_3 electrolyte. This reaction causes the formation of solid potassium carbonate on the cathode electrode. Over time, the accumulation of potassium carbonate solids renders the cell non-functional. Transporting carbonates through the AEM does not absolve CO_2 from concern in these systems. The presence of CO_2 is known to reduce the attainable current in AEMFCs. The anion transport mechanism allows the cell to quickly change from the hydroxide form to the carbonate form. The proton-hopping process is available to OH^-, but not to carbonate and bicarbonate anions. Consequently, carbonates have significantly less inherent mobility compared to OH^-. The fact that AEMs formed from bicarbonate only display approximately 20–25% of the conductivity of equivalent membranes in the hydroxide state is particularly worrisome because, like hydroxide, bicarbonate is monovalent but somewhat bigger. Carbonate exhibits lower mobility than OH^-, although it benefits from being divalent and smaller than bicarbonate.[95,96,98] The influence of water flooding on the AEMFC performance has been studied, and several experiments have been done by Professor William E. Mustain's group; a more detailed discussion on water management is provided in ref. 16 and 96. Mass transport concerns are similarly crucial for good performance, but they are often disregarded in the development of novel catalysts and membranes. Excessive buildup of water may be prevented by utilizing hydrophobic polymers in the catalyst layer, according to research. This improves water management.[96] In summary, attaining ideal water management in AEMFCs requires a careful equilibrium between sustaining membrane hydration, avoiding flooding, and guaranteeing effective water-transport routes. This may be assisted by the use of sophisticated diagnostic techniques and inventive material designs.[96–99]

4.3.1 Synopsis. Advancements in electrode design are transforming the performance and cost structure of AEMFCs. Nonetheless, enhancing catalyst–ionomer interactions, active-

site longevity, and MEA integration necessitates considerable research. This encourages the implementation of data-driven design and machine learning frameworks to expedite catalyst discovery and membrane electrode assembly optimization.

5. Integration of artificial intelligence (AI) and machine learning techniques

In the multidisciplinary area of artificial intelligence (AI), researchers strive to build computers that can mimic human intellect in areas including thinking, learning, perceiving, and decision-making. A wide variety of technologies are included in the artificial intelligence field, such as robots, computer vision, machine learning (ML), and voice and natural language processing.[100] Intelligence, according to a group of scientists in "Mainstream science on intelligence," is a broad mental capacity that encompasses many different areas of study and practice, such as reasoning, planning, problem-solving, abstract thought, grasping complicated concepts, rapid learning, and experience-based learning. We present Artificial Intelligence (AI) as an interdisciplinary study focusing on how to teach computers to think and behave intelligently.[100–102] Machine Learning (ML) is a subfield of AI. There has been a revolutionary technological evolution in human society thanks to machine learning (ML), which incorporates many different fields, including the theory of algorithm complexity, convex analysis, approximation theory, statistics, and probability theory. Successful applications of ML tools in workflow management and execution have led to improvements in dimensionality reduction, feature extraction, clustering, classification, and advanced regression for incredibly huge dimensional datasets.[91,102–104]

In the application of machine learning to AEMFC research, meticulous control of overfitting and underfitting is crucial for ensuring dependable model predictions. Underfitting generally occurs when the model or chosen features do not adequately represent the complexity of AEMFC datasets, including nonlinear relationships among membrane chemistry, ion transport, and operational parameters, leading to elevated training error. Conversely, overfitting transpires when the model assimilates noise rather than significant patterns, resulting in inadequate generalization to novel settings (*e.g.*, new catalyst compositions/catalyst design with respect to materials science or MEA topologies). It is essential to monitor both training and validation errors throughout training; a discrepancy between these measures frequently signifies the emergence of overfitting, illustrating the traditional bias-variance trade-off. To evaluate generalization, models must be tested on novel data using suitable validation methods. Although basic holdout or *k*-fold cross-validation approaches are frequently employed, more rigorous techniques, such as Monte-Carlo cross-validation or leave-one-cluster-out, are advisable for materials datasets to prevent overly optimistic performance evaluations. Robust validation techniques are crucial in AEMFC modeling because datasets are frequently restricted, varied, and susceptible to experimental variability.[253–256] A wide array of ML methods may be utilized to simulate structure–property correlations and enhance system performance.[257] Fundamental methodologies encompass linear and kernel-based regression and classification techniques, which are effective instruments for elucidating essential patterns in membrane conductivity, catalyst performance, and cell-level operational parameters. Accompanying these are feature selection and extraction techniques that assist in isolating the most significant descriptors and diminishing model complexity, an imperative step when dealing with constrained or diverse AEMFC datasets. In addition to these linear frameworks, more sophisticated nonlinear learning models provide further flexibility. Tree-based techniques, like Random Forests and Extremely Randomized Trees, proficiently elucidate intricate connections within experimental and computational datasets. Neural network methodologies enhance modeling capabilities: feed-forward networks and convolutional neural networks (CNNs) facilitate high-dimensional pattern recognition, whereas variational autoencoders (VAEs) and generative adversarial networks (GANs) assist in representation learning and synthetic data generation. These algorithms collectively constitute the methodological foundation for expediting materials discovery, enhancing MEA design, and attaining predictive optimization in next-generation AEMFC systems.[218,220,254–256]

There are three main types of ML algorithms, each with its own unique approach to model training: supervised, unsupervised, and semi-supervised (reinforced) learning. It is possible to utilize machine learning techniques to foretell acceptable expectations, and accordingly, experimental outcomes may be utilized to confirm the predictions made by the machine learning models. To aid in research concerning new material discovery, design, synthesis, and optimization, qualitative and quantitative approaches rooted in autonomous processes and high-throughput computations are utilized.[104,105] However, supervised and unsupervised learning are two principal kinds of machine learning methodologies.[216,217] Supervised learning encompasses a diverse array of methods, including eXtreme Gradient Boosting (XGB), Random Forests (RF), Multiple Linear Regression (MLR), Support Vector Machines (SVM), and Artificial Neural Networks (ANN). In supervised learning, models are trained with labeled datasets that include input variables (X) and their associated output variables (Y).[219,220] Multiple Linear Regression (MLR) serves as a significant baseline approach when the correlation between predictor variables and the target response is nearly linear. Its simplicity, low computing expense, and rapid training render it particularly appropriate for datasets of moderate size. Gaussian Process Regression (GPR) enhances this functionality using a nonparametric Bayesian framework, facilitating more adaptable modeling of nonlinear connections and offering uncertainty quantification.[218] Decision Trees (DTs) provide a clear, interpretable framework that can accommodate both numerical and categorical data with few preprocessing requirements. Random Forests (RF) consolidate several decision trees to enhance prediction accuracy and resilience, proving useful for both regression and classification problems. The three main categories of machine learning, *i.e.*, supervised learning, semi-supervised learning, and unsupervised learning,

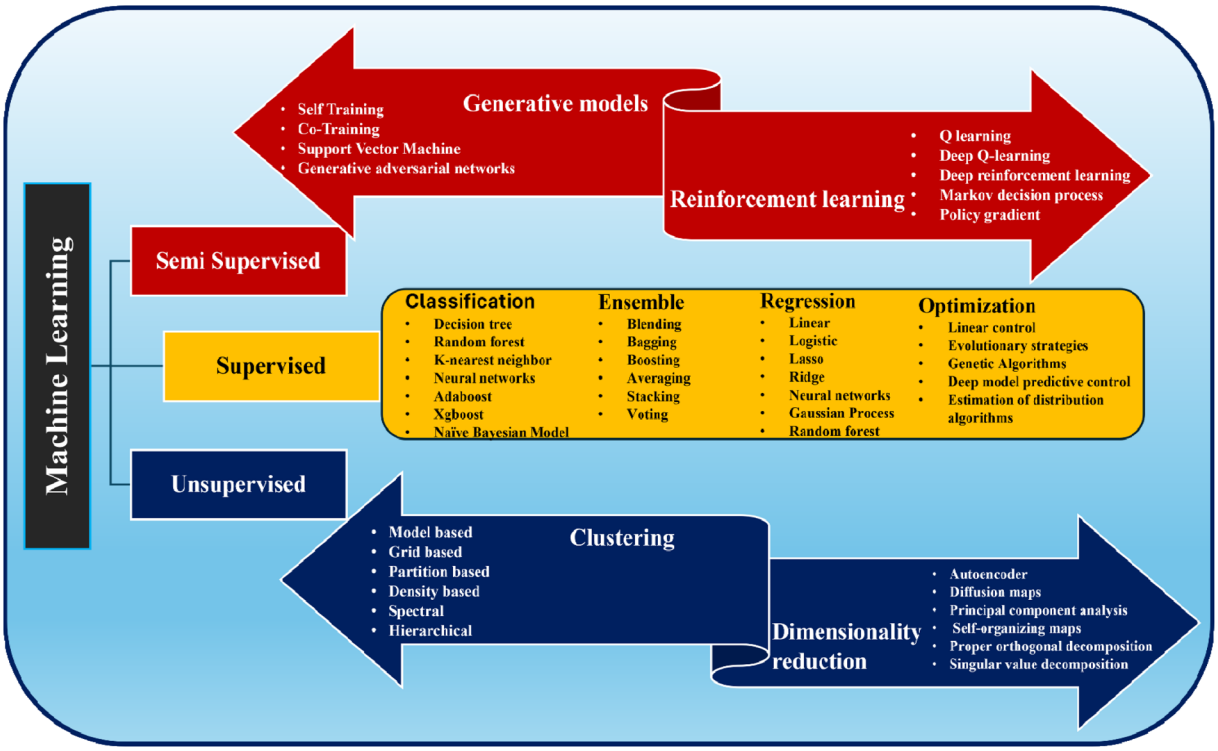

Fig. 11 Illustration of the various machine learning (ML) algorithms that can be used for fuel cells.

are illustrated in Fig. 11, using a flow chart. For problems involving continuous or categorical value prediction, supervised learning makes use of known inputs and outputs. Random Forest and *k*-nearest neighbor are two algorithms that can handle both tasks; however, Naïve Bayes is only good for classification. Algorithms like *k*-nearest neighbor and support vector machine determine the structure of the model in supervised learning. For a model to learn how to predict new data, it needs features (inputs) and targets (outputs) during training.[103,105]

The most important supervised learning algorithms for fuel cell applications are given in Scheme 1 below.[103–106] Unsupervised learning, which detects concealed patterns in data without predetermined labeling, offers considerable promise in promoting the progress of anion exchange membrane fuel cells (AEMFCs). Conventional approaches for creating anion exchange membranes (AEMs) often involve either trial and error or simulations, which may be time-consuming and expensive. Through the utilization of unsupervised learning, scientists may discover new associations between the molecular compositions of AEMs and their characteristics, such as chemical stability and ion conductivity, without requiring huge datasets for training.[107,108] Researchers can find new connections between AEM molecular shapes and their attributes, like ion conductivity and chemical stability, using unsupervised learning, which does not require large training databases. This method can be used in conjunction with others that have demonstrated potential in predicting and directing the synthesis of high-stability AEMs, such as supervised learning and the virtual module compound enumeration screening (V-MCES). Another important problem that prevents alkaline membrane fuel cells from being used in the real world is the degradation processes in AEMs. Unsupervised learning can help shed light on this issue.[108,109] Additionally, it can aid in the discovery of hidden patterns in degradation data, which can guide the development of stronger membranes. In addition, parametric models that estimate AEMFC performance with different variables (*e.g.*, temperature and pressure) may be merged with unsupervised learning to optimize their dynamic behavior. As another example, direct ammonia anion-exchange membrane fuel cells (DAFCs) can benefit from this integration through the enhancement of performance and extension of the lifetime of the cells while tackling issues like ammonia crossover. The use of unsupervised learning in AEMFC research might speed up the process of finding high-performance materials and improving fuel cell designs. This, in turn, could help bring this promising technology closer to manufacturing and increase its acceptance.[110]

Data-constrained modeling in AEMFC research. Recent research in data-constrained settings, such as the "comparative investigation of learning algorithms for image classification with small datasets," indicates that even restricted experimental datasets may successfully train strong prediction models if suitable architectures are selected. This mirrors the difficulties in AEMFC modeling, where material and performance databases frequently remain limited.[208]

Transferability of hybrid neural models to energy systems. Hybrid neural architectures, shown as transformer-enhanced

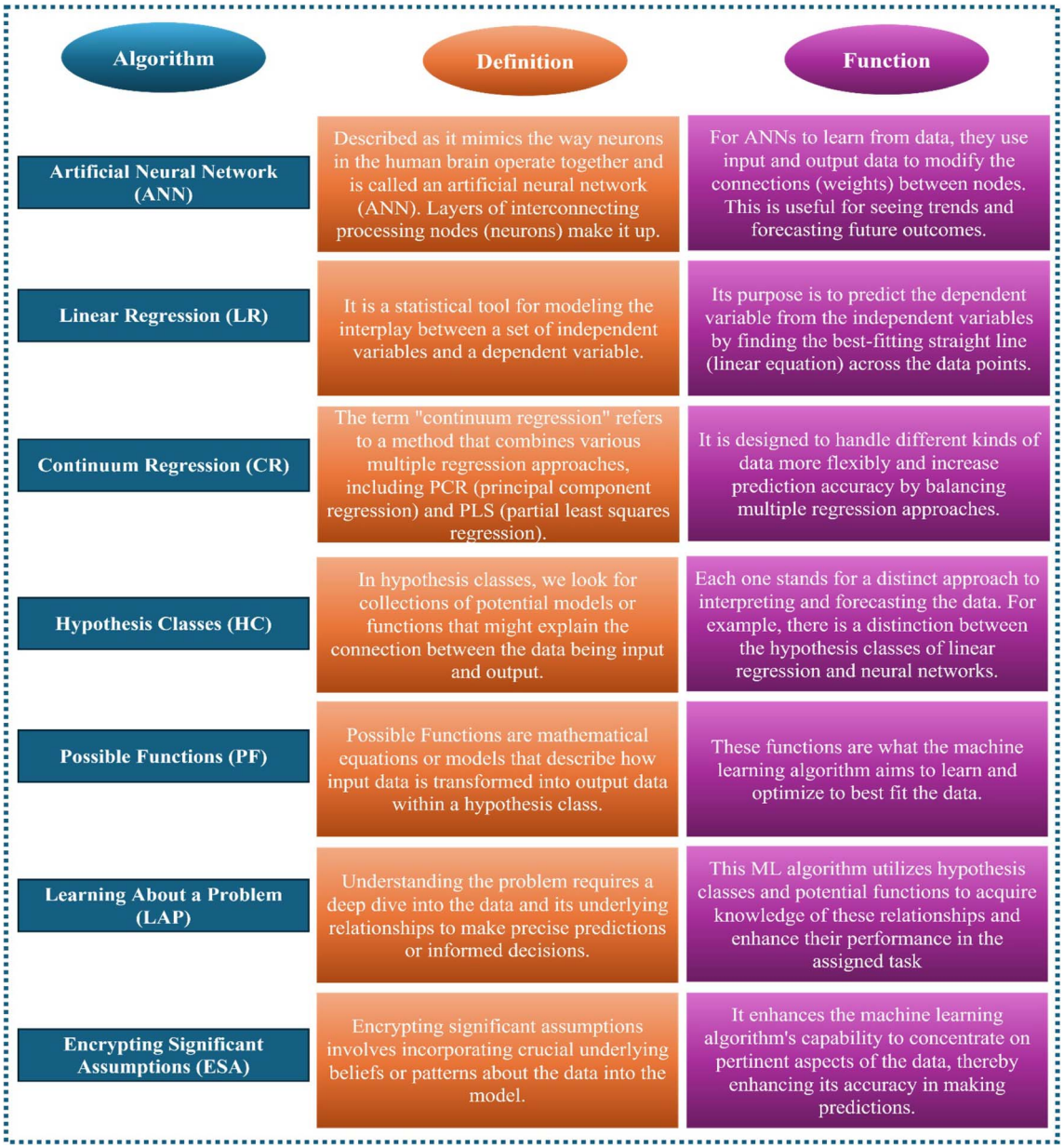

Scheme 1 Important supervised algorithms and functions.

recurrent neural networks employed in sophisticated solar irradiance forecasting, underscore the efficacy of integrating temporal learning mechanisms with attention frameworks to simulate intricate physical systems. These approaches are adaptable to AEMFC behavior prediction, including current density evolution, water-management transients, and performance decay.[209]

5.1 Real-world use of machine learning algorithms in AEMFC research

(a) Artificial Neural Networks (ANNs) have been utilized to forecast current density–voltage characteristics, AEM hydroxide conductivity, and MEA deterioration patterns using nonlinear correlations extracted from experimental data.[190]

(b) Decision trees and ensemble methods (Random Forest, XGBoost) have been employed to identify the principal descriptors (IEC, water uptake, cationic headgroup chemistry, electrode loading, relative humidity, operating temperature) that significantly affect cell efficiency, ohmic resistance, and oxygen reduction reaction (ORR) kinetics. These models facilitate the rating of material and operational criteria.[190–197]

(c) Unsupervised clustering methods, such as *k*-means and hierarchical clustering, have been employed to categorize AEM chemistries, degradation processes, and catalyst microstructures according to similarities in transport behavior or alkaline stability.[190–197]

(d) Semi-supervised learning handles the amalgamation of limited experimental datasets with extensive simulated or

synthetic AEMFC datasets to enhance ion-transport prediction and longevity assessment.[190–197]

5.2 Benchmark studies between traditional physics-based modeling and data-driven learning approaches

Conventional physics-based modeling: the conventional physics-based modeling (NEA equations, Nernst–Planck transport, multiphysics CFD, kinetic ORR modeling) and its constraints under integrated thermodynamic, hydrodynamic, and electrodynamic circumstances are covered.

Data-driven models: data-driven models provide rapid predictions with minimal physical parameterization and perform excellently when extensive multidimensional datasets are accessible.

Hybrid physics-informed neural networks (PINNs): PINNs serve as an interface between first-principles models and machine learning, facilitating enhanced generalizability and reduced data requirements.[196–200]

By combining labeled and unlabeled data, semi-supervised learning may optimize anion exchange membrane fuel cells (AEMFCs) and greatly improve their development and optimization. This reduces the requirement for large experimental datasets while simultaneously improving model accuracy. An example of a methodology that successfully predicts the chemical stability of AEMs and guides the fabrication of extremely stable membranes is virtual module compound enumeration screening (V-MCES). This method combines supervised learning with feature selection of molecular descriptors.[111] A more elaborate study on virtual module compound enumeration screening (V-MCES) discloses that V-MCES involves searching a chemical space with over 4.2 × 105 candidates without the need for costly training datasets. More clear information about its functionality and advantages is given in Scheme 2. The schematic of the virtual module compound enumeration screening (V-MCES) integration for AEM fuel cells is visualized in Fig. 12.[111]

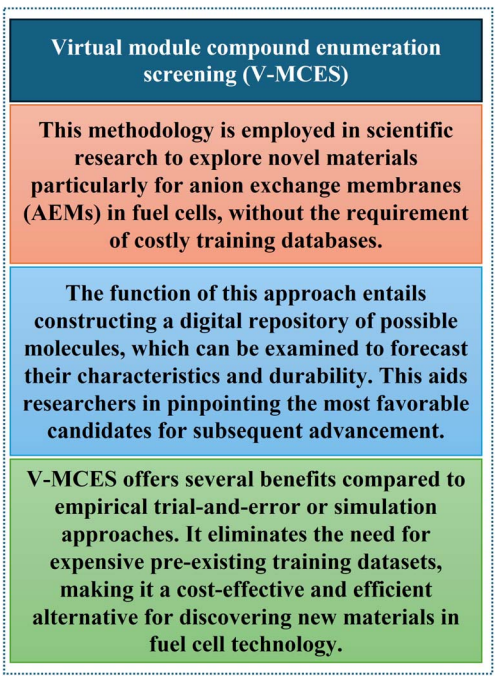

Scheme 2 Virtual module compound enumeration screening (V-MCES) functionality and advantages.

Applying supervised learning approaches to V-MCES improves its accuracy. These techniques aid in choosing the most relevant molecular descriptors, which, in turn, improve the chemical stability prediction for AEMs. Discovering novel compounds that would not be easily found through standard approaches becomes a breeze with V-MCES, since it can search a huge chemical space comprising over 420 000 possibilities. The use of V-MCES allows for the generation of a prioritized list of possible AEMs with high stability. This list then directs the synthesis of AEMs with very high stability, taking AEM research to new heights in terms of building performance and design.[111]

5.3 Integration of neural networks (NNs) and artificial neural networks (ANNs) in AEMFC technologies

Although neural network algorithms in ML are not new to computer engineers and AI engineers, the supervised neural network model has become very important in chemistry and electrochemistry, especially for fuel cell applications. However, very limited literature is available on AI and ML applications for fuel cells, especially AEM fuel cells. Considering this perspective, I would like to put forward some of my thoughts and views about using specific machine learning algorithms trained on long-term experimental data to provide predictions on planned experiments and schemes. In recent years, neural networks have emerged as a helpful tool to improve the performance and stability of anion exchange membrane (AEM) fuel cells. These fuel cells are an essential component of sustainable energy solutions. Predicting and improving critical performance characteristics, such as chemical stability and voltage consistency, is the primary objective of utilizing artificial neural networks (ANNs) for anion exchange membrane (AEM) fuel cells.

Artificial neural networks (ANNs) are a subcategory and a more advanced version of neural networks. They have the potential to think and make decisions on their own after receiving certain training using varied data. Further, they have shown great potential for use in enhancing the development and improvement of anion exchange membrane (AEM) fuel cells by tackling issues related to chemical stability and performance. ANNs are used to predict the chemical stability of AEMs by linking molecular structures with stability metrics, like Hammett substituent constants, obtaining good prediction accuracy (R^2 = 0.9978). To evaluate fuel cell conditions and optimize control techniques, artificial neural networks (ANNs) have been used to predict the cell voltage distribution in commercial-size fuel cell stacks, drastically decreasing the calculation time without sacrificing accuracy.[112]

The components that make up artificial neural networks are similar to neurons in the real world. The whole Artificial Neural Network of a system is made up of these units organized in a succession of layers. The number of units in a layer can range from a few hundred to millions, depending on the complexity of

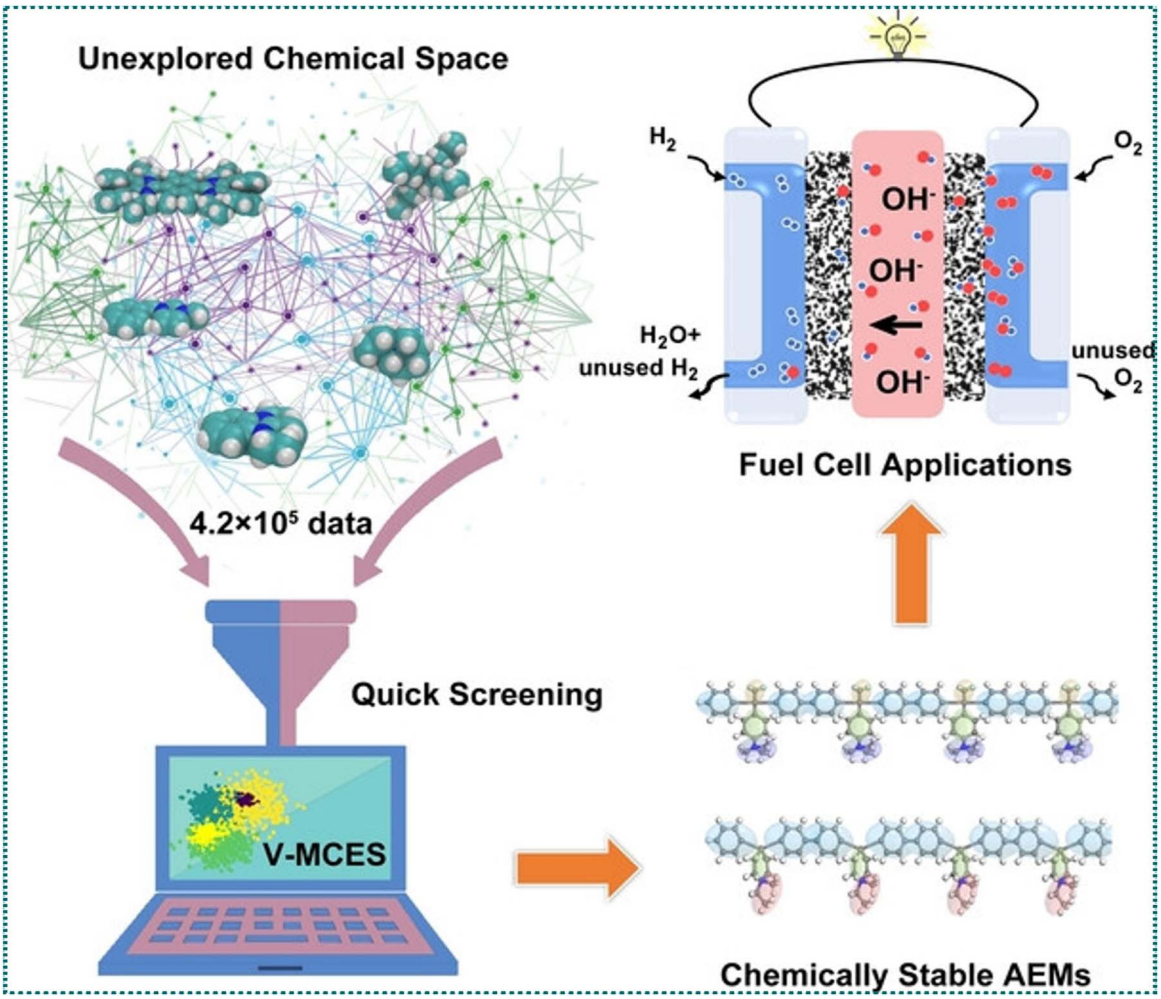

Fig. 12 Visualization of virtual module compound enumeration screening (V-MCES) integration for AEMFC applications. Image reproduced with permission from ref. 111. Copyright © 2023 Wiley-VCH GmbH. https://doi.org/10.1002/anie.202300388.

the neural networks needed to uncover the dataset's hidden patterns. An input layer, an output layer, and hidden layers are the typical components of an artificial neural network. The data that the neural network needs to learn or evaluate comes from the outside world and is received by the input layer. The input data are then transformed into valuable output data by passing them through one or more hidden layers. Lastly, the output layer delivers the result of the Artificial Neural Networks' reaction to the input data. The vast majority of neural networks use linked units that span many layers. A unit's impact on another is determined by the weights of each of these links. With each data transmission, the neural network gains a deeper understanding of the inputs, which is then used to generate an output at the output layer.[112,129,130] The architecture of artificial neural networks with input layers, hidden layers, and output layers for the prediction of the AEMFC performance is illustrated in Fig. 13a. Neural networks (NNs) consist of interconnected layers of input and output nodes, with each connection transmitting a weighted signal that is progressively modified during training. By iteratively optimizing these weights and biases, the network reduces the discrepancy between anticipated and desired outputs until sufficient convergence is attained. Neural networks, while often necessitating extensive training datasets and prolonged training durations, have several benefits: robust resilience to noisy data, the capacity to model highly nonlinear connections, and adaptability to forecast both continuous and categorical outcomes. Notwithstanding their restricted interpretability, neural networks have demonstrated considerable efficacy in various scientific applications, such as predicting electrochemical performance, screening catalysts, conducting molecular dynamics simulations, and forecasting synthesis routes, rendering them an invaluable asset for the progression of data-driven AEMFC research. Fig. 13b illustrates forward feed and error backpropagation of a neural network.[225,258] The most prevailing neural network architecture is the backpropagation neural network, in which the discrepancy between the predicted output and the target value is sent backward through the layers to repeatedly adjust the connection weights and biases (Fig. 13c). A standard backpropagation network has an input layer, one or more hidden layers, and an output layer, with each layer comprising several nodes or neurons. Fig. 13b demonstrates that the descriptors from the training dataset are

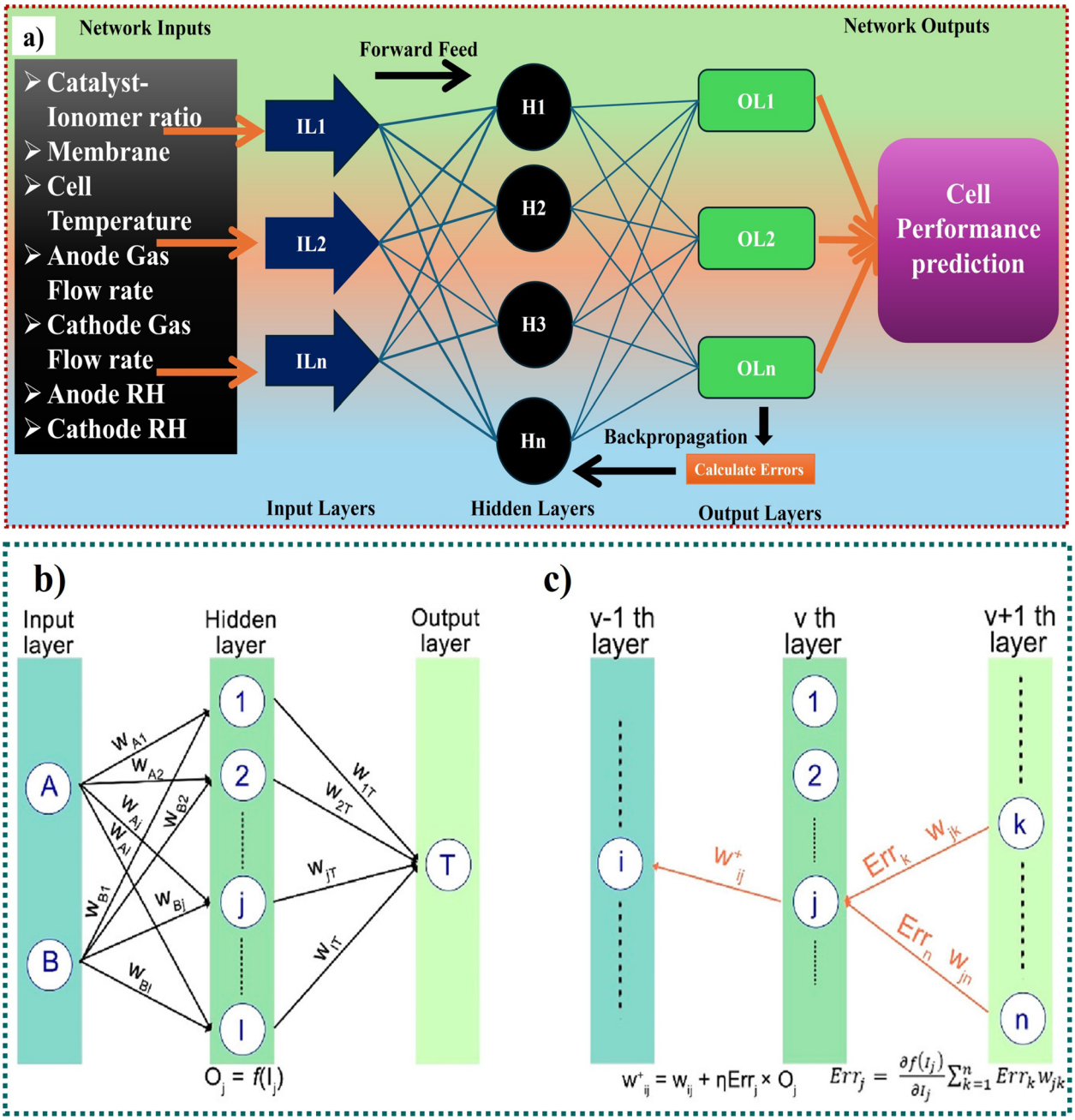

Fig. 13 (a) The organization of the artificial neural network utilized in the process of constructing the model for AEMFC performance prediction. (b) Schematic of the forward feed. Image reproduced with permission from ref. 225, copyright © 2022 the American Chemical Society. https://doi.org/10.1021/acs.chemrev.2c00061. (c) Schematic of the error backpropagation of a neural network. Image reproduced with permission from ref. 225, copyright © 2022 the American Chemical Society. https://doi.org/10.1021/acs.chemrev.2c00061.

transmitted from the input layer to the hidden layer, where they undergo transformation *via* activation functions before being relayed to the output layer to provide predictions. The quantity of input nodes is directly proportional to the number of descriptors, but the output layer may have a singular node for regression or binary classification tasks, or several nodes for multiclass or multi-objective predictions. Due to the absence of a uniform guideline for ascertaining the ideal quantity of hidden layers or neurons, the design of the network generally necessitates empirical adjustment. Bayesian regularization can autonomously adjust network complexity and maximize the quantity of trainable parameters, facilitating robust and highly predictive performance across various material-property datasets.[225,259–261]

There are many kinds of Artificial Neural Networks (ANNs), and they all have different uses and designs. There are five most common kinds. One type of feedforward neural network is the (a) multilayer perceptron (MLP), which consists of two or more output and input layers separated by hidden layers. Solar irradiance and rainfall forecasting are only two examples of the many

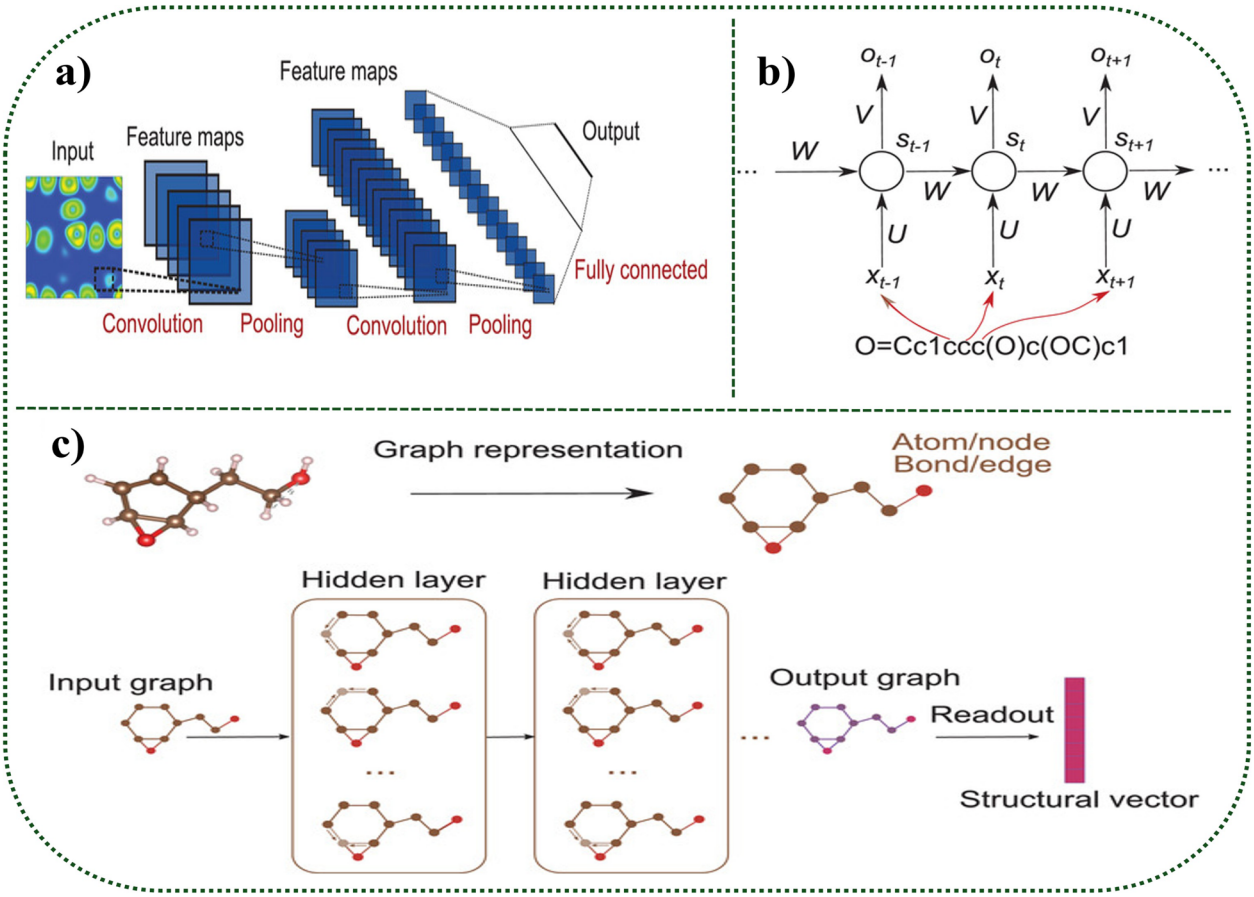

Fig. 14 (a) Convolutional neural networks (CNNs). (b) Example of recurrent neural networks (RNNs). (c) Graph convolutional neural networks on the molecule graph. Image reproduced with permission from ref. 229, copyright © 2020 WILEY-VCH Verlag GmbH & Co. KGaA, Weinheim. https://doi.org/10.1002/aenm.201903242.

categorization, regression, and forecasting jobs for which MLPs are extensively used. (b) Convolutional Neural Networks (CNNs): CNNs are mostly employed in computer vision and image processing; they are built to learn feature hierarchies from input pictures in an automated and flexible manner. Pattern recognition and medical picture analysis are other areas where they find use.[226] CNNs have garnered significant attention in recent years because of their remarkable efficacy in image identification tasks, where they routinely surpass most conventional machine learning methods. In CNN architectures (Fig. 14a), uniform convolutional filters are utilized over all areas of an input picture, producing feature maps that encapsulate local patterns. The notion of confined receptive fields corresponds to the location of interactions seen in several material systems. A direct approach to implementing CNNs in materials science is transforming material structures into image-like representations and subsequently training CNN models on these modified inputs. This direct method is frequently insufficient, as ordinary CNNs do not intrinsically accommodate the rotational and permutational invariances essential for physically relevant material descriptors. Although rotational data augmentation can somewhat alleviate these limits and enhance model resilience, more sophisticated symmetry-aware architectures are often required for precise and generalizable predictions in materials research.[227–229] (c) Recurrent Neural Networks (RNNs): RNNs are a great choice for time series forecasting, language modeling, voice recognition, and other jobs that require processing sequences of data. Applications needing contexts, such as robotics and natural language processing, are well-suited to their memory-preserving capabilities. In contrast to CNNs, which utilize spatially restricted convolutions, Recurrent Neural Networks (RNNs) handle input in a sequential manner by linking computational nodes across temporal intervals while maintaining weight sharing across the sequence. RNNs are very proficient at modeling sequential data and have been extensively utilized in fields such as natural language processing and speech recognition. Nonetheless, their utilization in materials research is constrained due to the non-sequential nature of most material descriptors. An anomaly occurs in molecular informatics, where linear string-based representations, such as SMILES, offer a sequential format conducive to RNN structures, facilitating tasks, such as molecular property prediction and generative design (Fig. 14b).[229] (d) Radial Basis Function (RBF) network: this network type is commonly used for function approximation, time series prediction, and control systems; it employs radial basis functions as activation functions. When it comes to optimizing chemical processes and

performing multi-objective controls, RBF networks are famous for their powerful nonlinear mapping capabilities. (e) The fifth type of generative model is the Deep Belief Network (DBN), which consists of several layers of latent, stochastic variables. Its applications include dimensionality reduction, feature learning, and unsupervised learning. Speech recognition and bioinformatics are two domains where DBNs find use.[130,131] (f) Graph convolutional neural networks are a specific type of graph neural network (GNN, discussed in a later section). The initial Graph Convolutional Neural Network (GCNN) models facilitated information sharing predominantly among linked atoms, employing deep learning elements, usually multilayer perceptrons (MLPs), as local function approximators. With the introduction of supplementary graph convolutional layers, each atom acquires access to increasingly expansive chemical surroundings, hence augmenting its receptive field. Subsequent innovations provided structures that may modify bond characteristics according to the atomic states they link, thereby improving the depiction of chemical interactions. Recent graph network frameworks extend GCNNs by integrating global qualities that coexist with atom- and bond-level features, facilitating information propagation across all three hierarchical levels. These advancements have markedly enhanced the expressive capacity of graph-based models, which now exhibit state-of-the-art efficacy in predicting molecular and crystalline characteristics relative to conventional machine learning techniques (Fig. 14c).[229–232]

Training and learning of ANNs: the process of learning in artificial neural networks (ANNs) involves altering weights through either supervised or unsupervised learning experiences. Unsupervised learning finds patterns in input data without intended outputs, whereas supervised learning minimizes mistakes using a training set with input–output pairings. Training set: to get dependable results from supervised learning, the training set must be a good representation of the model. The operational weights of the network are set after training is complete. Schemes for learning: one typical approach to learning is error correction, which frequently makes use of the closest neighbor and backpropagation techniques. Finding the discrepancy between the node's output and the desired output and adjusting the weights accordingly is the process of error correction (Fig. 13).[130]

5.4 Hebbian's theory of neural network learning

The idea of learning through the change of synaptic connections between neurons was proposed by Hebb in his 1949 hypothesis, which was based on nervous system physiology. This assumption is known as Hebb's theory. Neuron A's axon can strengthen its connection to neuron B through a development process if it helps fire neuron B several times, according to Hebbian learning. In single-layer networks with input and output units, the majority of neural network learning methods are variations of Hebbian learning, which states that the synchronous activity of two neurons enhances their connections.

5.5 Perceptron neural network learning

The perceptron is a standard neural network that is taught with the perceptron-learning algorithm to partition input vectors into target outputs, which are generally either +1 or −1. Because of this, it is well-suited for performing fundamental pattern categorization tasks. Both online and batch training options are available for neural networks. To get a cumulative update that closely tracks the gradient, we use batch mode to store and apply weight adjustments after an entire epoch, as opposed to updating them after each data sample in online mode. To train, one must input samples, compute the output error, and then tweak the weights so that the error is as small as possible. The selection of hidden neurons in a neural network is critical as an excessive number might result in subpar performance on novel input, but an insufficient number can impede the network's ability to learn successfully.[130–132]

5.6 Real-time working model of artificial neural networks (ANNs)

ANNs are computer models that aim to solve complicated issues by learning from data in a way similar to the way the human brain works. ANNs have been around for almost fifty years, but they've just recently been popular because of how much faster and more powerful computers are. Similar to biological neurons, ANNs analyze data through a network of linked neurons, which allows them to efficiently deal with input–output nonlinearities. Applications necessitating pattern identification, data categorization, and predictive modeling find ANNs particularly helpful due to these capabilities. Applications ranging from system control to facial recognition might benefit from ANNs because of their self-organizing nature, resilience, parallelism, and capacity to handle imprecise input. Although ANNs have many benefits, they may be difficult to model and require careful training-phase control to avoid problems like overfitting and local minima.[114]

The study analyses the output of artificial neural network (ANN) models trained with three distinct learning methods, utilizing critical input parameters, such as stack current, cathode inlet temperature, anode inlet pressure, and flow rates. To find out how well the models forecast stack voltage and temperature, this evaluation is crucial. The models were trained using over 90% of the 400 data points, whereas testing and validation accounted for less than 10%. Each model only included one hidden layer, and several models were tested by adjusting the hidden layer's neuron (processing unit) count; an example of a neural network model is given in Fig. 15a. To maximize the model's efficiency, various learning techniques were evaluated. One way to compare anticipated and actual values is with the Mean Squared Error (MSE), which is calculated as the average of the squares of all the errors. An improved model performance is indicated by a low MSE. The R^2 coefficient shows how closely the model's predictions fit the observed data. Performance is improved when the value is closer to 1. The algorithm type, range of neurons in the hidden layer, R^2 values, and MSE values are all listed in the columns. The x-axis shows time (s), and the y-axis shows the voltage (V) in Fig. 15b–d. Finding the optimal model for PEMFC performance prediction requires comparing several techniques and neuron counts.[112,114]

Despite their benefits, ANNs are difficult to mimic and may overfit and exhibit local minima, which must be managed

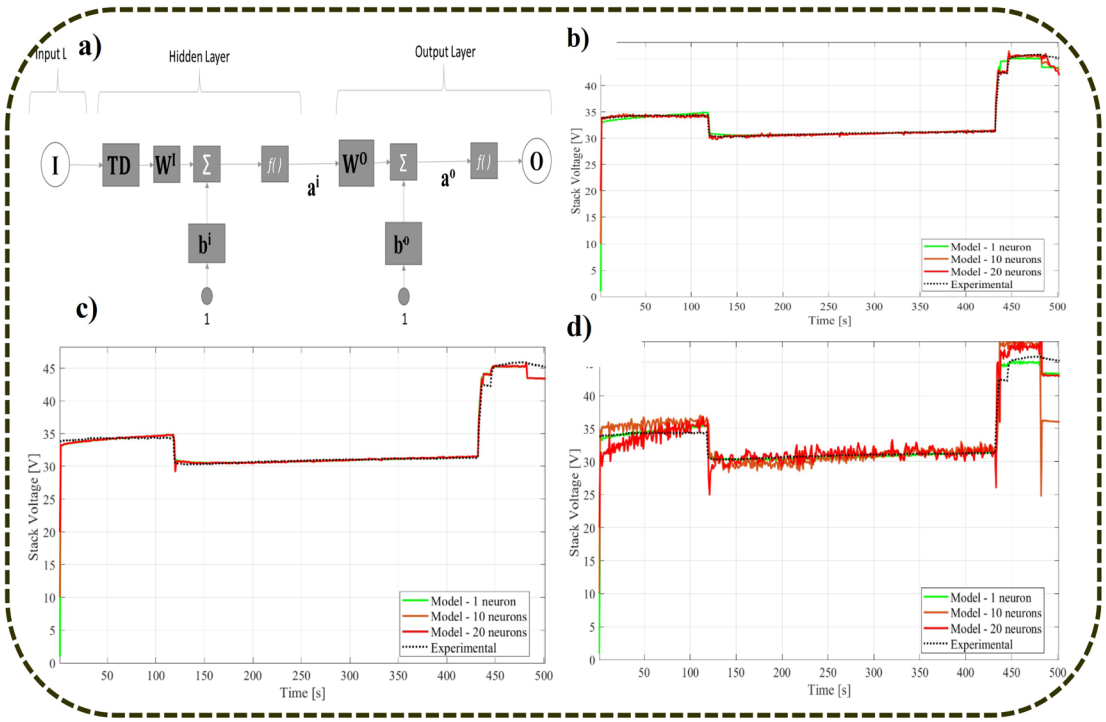

Fig. 15 (a) Neural network model illustrating a three-layer architecture with an input, a hidden, and an output layer. (b) The stack voltage's experimental and modeled responses using an ANN and the LM algorithm. (c) Experimental and model stack voltage responses with a Bayesian-based ANN. (d) Model and experimental stack voltage responses using an ANN and the SCG algorithm. Image reproduced with permission from ref. 112. Copyright © 2022 by the authors. Licensee MDPI, Basel, Switzerland under Creative Commons Attribution (CC BY) license. https://doi.org/10.3390/en15155587.

during training. The use of Artificial Neural Networks (ANNs) in resolving mathematical programming difficulties further emphasizes their adaptability and promises for future investigation. The ongoing progress and use of ANNs are primarily motivated by their capacity to simulate intricate patterns and make informed choices, resembling the adaptive learning mechanisms of the human brain. Consequently, their extensive utilization in several influential domains has established them as a fundamental component of contemporary artificial intelligence and machine learning investigations.[115,116] Hinton G. E. *et al.* reported working with high-dimensional data and reducing the dimensionality; notably, data that contain a great number of characteristics or variables are called high-dimensional data. A dataset with many measurements for each sample and a picture with many pixels are two examples. Codes with fewer dimensions: these encode the most important aspects of high-dimensional data using a less complex representation. Automatic encoders and multilayer neural networks are examples. Neural network with multiple layers: refers to an AI model that uses a network of interconnected nodes or neurons to perform computations on input data. The data are transformed by each layer, making pattern recognition simpler. An autoencoder is a specialized kind of neural network that can learn to code input data efficiently. It contains two parts: an encoder that compresses the data and a decoder that reconstructs the original data from the compressed form. Dimensionality reduction makes it easy to classify data into multiple groups; enhanced classification results in reduced data complexity, facilitating better visualization and comprehension. Less data mean simpler storage and sharing, improving communication.[113]

6. Novel artificial intelligence predictive modeling and approaches for fuel cells

6.1 Predictive modeling

Predictive modeling substantially boosts the operation and efficiency of anion exchange membrane fuel cells (AEMFCs) by optimizing several parameters and minimizing the requirement for extensive experimental trials. Researchers can investigate the effects of membrane properties, such as water diffusivity, membrane thickness, ion exchange capacity, and hydroxide conductivity, on the AEMFC performance and stability using computational methodologies, such as the one-dimensional isothermal and time-dependent models. They concluded that the most important factors affecting the AEMFC lifetime are water diffusivity and the maximum hydration level.[117–119] The chemical stability of anion exchange membranes (AEMs) and the performance of membrane electrode assemblies (MEAs) have been predicted using artificial intelligence (AI) and machine learning techniques, such as artificial neural networks (ANNs) and decision trees. This has resulted in a high level of accuracy and a reduction in the number of unnecessary experiments. These models can accurately anticipate the distribution

of cell voltage and the consistency of cell voltage in commercial-size fuel cell stacks. As a result, the amount of time required for calculation is greatly reduced, and they also help in the assessment and improvement of control systems.[121,122]

The global modeling process (GMP) has reportedly been applied to DMFCs, and the efficiency of direct methanol fuel cells (DMFCs) depends on a wide range of variables. It is possible to ruin the model by attempting to characterize all these elements with just one electrochemical formula. Using computational fluid dynamics models: by taking varying values of these elements into account, CFD (Computational Fluid Dynamics) models aid in calculating the performance of fuel cells. It takes a long time to run these simulations. Difficulty in handling variations in parameters: rebuilding the CFD models is necessary when there are changes to the geometric and MEA physical parameters. Metamodel for Kriging: one mathematical tool for developing a global model that considers several factors is the Kriging metamodel. The importance of reliable samples: it takes a lot of time and money to conduct experiments to construct these models. A novel approach to efficient data sampling for model generation is required (Fig. 16).[117,121]

Computational modeling studies on PEM fuel cells revealed through analysis and optimization of their performance, models aid in the improvement of PEM fuel cells. An effective model may collect crucial data from within the program, much like a software sensor. Issues arise, however, when relying on empirical data to define the proper parameters for these models, as this area has not been thoroughly investigated. The

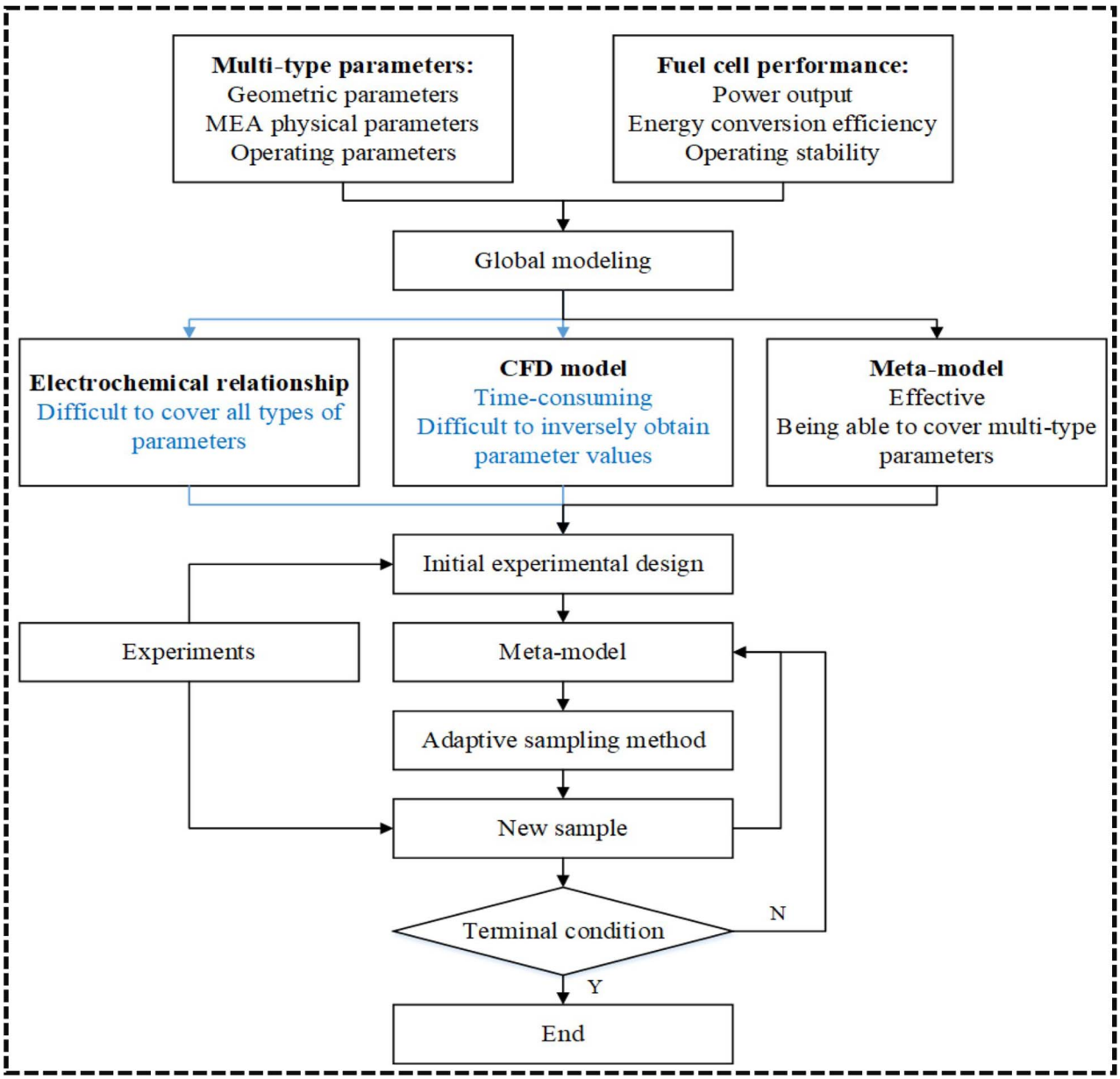

Fig. 16 Illustration of the global modeling process. Image reproduced with permission from ref. 117. Copyright © 2022 by the authors. Licensee MDPI, Basel, Switzerland under Creative Commons Attribution (CC BY) license. https://doi.org/10.3390/en15228549.

model's accuracy for real operating settings might be limited by the current parameterization approaches, which require substantial resources and intrusive procedures. Because of this, it is difficult to establish reliable predictions about the behavior of fuel cells. Despite the high computing costs, optimization-based approaches can assist in identifying fuel cell model parameters using non-invasive measurements. More accurate parameterization of electrochemical systems may be possible, according to new studies on batteries. To parameterize PEM fuel cell models, improve parameter identifiability, and solve structural identifiability difficulties with extra data, a study has offered appropriate experimental designs and a systematic procedure.[123] The model investigations concentrate on chemical degradation, transport processes, and electrochemical reactions. These studies include a one-dimensional isothermal and time-dependent model of the operations of an anion exchange membrane fuel cells (AEMFC). Key findings indicate that membrane water diffusivity and $\lambda_{(max)}$ have a significant impact on the lifespan of an anion exchange membrane fuel cell (AEMFC). Additionally, membrane thickness and IEC play roles owing to their ability to improve water distribution. Enhancing the stability of functional groups is essential for maintaining performance stability, whereas the conductivity of AEM hydroxide has little effect on the longevity of the material. The study discovered a connection that helped estimate the lifespan of an AEMFC and compare it to the actual operating times. This highlighted critical aspects that should be considered while designing improved AEMs.[122] In addition, global modeling tools that combine adaptive sampling with the Kriging approach have been created, guaranteeing accurate performance forecasts throughout the whole design space and increasing prediction accuracy by around 26% when compared to conventional models.[121,124] A mathematical model was developed to analyze the impact of various operating variables, such as temperature and pressure, on the voltage and efficiency of a single cell in an anion exchange membrane (AEM) water electrolyzer. The model considers many crucial aspects that impact the effectiveness of the electrolyzer, such as electrolyte conductivity, AEM thickness, catalyst layer porosity, and the existence of double layers at liquid–gas interfaces. The model has determined that the ideal temperature for running the AEM water electrolyzer is 75 °C, while the optimal pressure is 1.8 MPa. These values align with the experimental results, confirming the dependability of the model. The model assesses the electrolyzer's present performance and efficiency and suggests ways to enhance these parameters in the future. These suggestions might lead to more efficient and cost-effective assembly and operation of single-cell AEM water electrolyzers.[125] By improving operating circumstances and system design, AEMFCs may be made even more efficient using AI-aided models and adaptive neuro-fuzzy inference systems (ANFIS), which show promise for making accurate and dependable performance forecasts. All things considered, predictive modeling is a potent tool for enhancing AEMFC performance and efficiency with less experimental effort through better design, control, and operation.[126] In another report, in Matlab, a model was used to make predictions about the operation of a solid polymer electrolyte fuel cell. This model makes use of electrical and thermal models to anticipate the behavior of the fuel cell, particularly temperature variations. The findings demonstrate how performance varies with different factors, such as temperature and pressure.[127]

6.2 Optimization algorithms

The performance and efficiency of anion exchange membrane fuel cells (AEMFCs) may be significantly improved by the utilization of optimization algorithms. These algorithms are responsible for precisely calculating and fine-tuning the parameters that regulate the functioning of these fuel cells. It has been demonstrated that the hybrid particle swarm optimization puffer fish (HPSOPF) algorithm has superior performance in parameter estimation for proton exchange membrane fuel cells (PEMFCs). This algorithm can be adapted for anion exchange membrane fuel cells (AEMFCs) to achieve a minimal sum of square errors and improved voltage–current characteristics.[128] A MATLAB-Simulink model has been developed to simulate the behavior of proton exchange membrane fuel cells. This model, which considers design and environmental parameters, can anticipate the impact of these elements without performing tests. For precise parameter identification, the model employs a GA-PSO hybrid optimization approach, guaranteeing an error margin of less than 1% between the experimental and simulation data. Dynamic simulations validate the model's correctness and dependability by displaying dependable voltage and power responses.[119,120] Rui Ding *et al.* demonstrated that when it comes to parameter extraction, the Coyote Optimization Algorithm (COA) demonstrates a substantial level of precision, which is necessary for improving the performance of fuel cells under a variety of operating conditions. They worked on optimizing different ML algorithms to predict the current density at 0.6 V and the precious platinum consumption of the PEMFC. They compiled a database comprising 126 entries that describe the PEMFC performance across four operating conditions, *i.e.*, cathode and anode flow rates, cell temperature, and back pressure, with an emphasis on variables like flow rate and membrane thickness. Additionally, the dataset tracks 15 parameters for MEA preparation, including active area, drying temperature, membrane thickness, type of MEA fabrication, ink stirring method, ink stirring temperature, I/C ratio, equivalent ionomer weight, anode Pt loading and cathode Pt loading.[264] Fig. 17a illustrates the machine learning-assisted algorithm optimization flow chart for the PEMFC experimental data. Fig. 17b presents a collection of graphical data for the prediction of the current density of PEMFC at 0.6 V using different ML-assisted algorithms.

Fig. 18 shows a graphical data representation of various machine learning techniques that were evaluated for their performance in predicting Pt usage at 0.6 V. The regression modeling utilized all 19 initial characteristics as input.[126] In addition, innovative algorithms, such as the opposition-based arithmetic optimization algorithm (OBAOA) and the coyote optimization algorithm (COA), have shown that they are capable of accurately retrieving and optimizing the parameters of

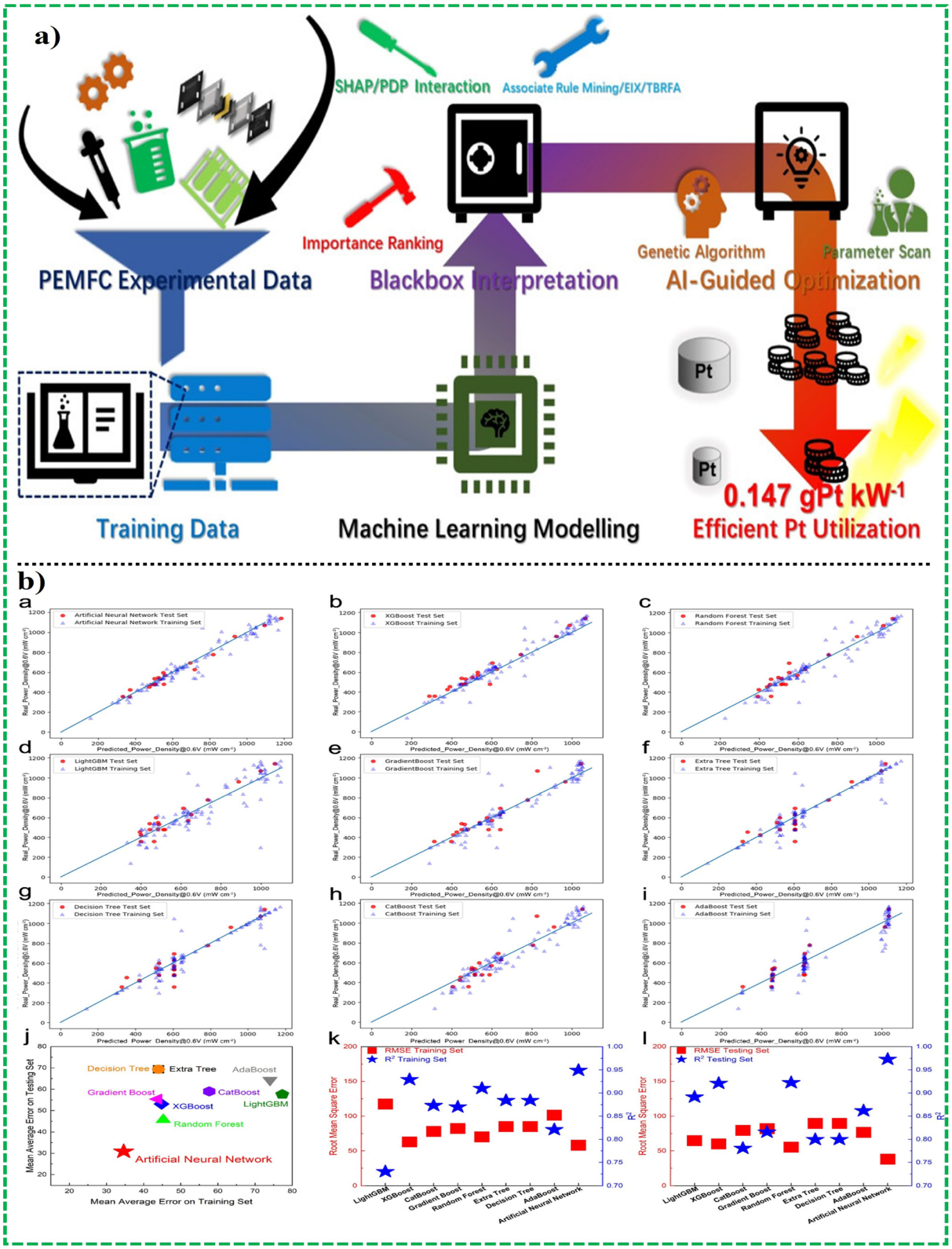

Fig. 17 (a) Machine language-guided optimization flow chart. (b) Different graphs of different machine language algorithms predicting the current density at 0.6 V; ((b) a–i) regression modeling inputs with 19 feature algorithms for predicting the current density at 0.6 V; ((b) j) different ML algorithms' MAEs on the training set and testing set; ((b) k) various RMSE and R^2 values obtained from the training set using different machine learning (ML) methods; ((b) l) the R^2 and RMSE values of several ML methods on the test set. Image reproduced with permission from ref. 264, copyright © 2022 the American Chemical Society. https://doi.org/10.1021/acsami.1c23221.

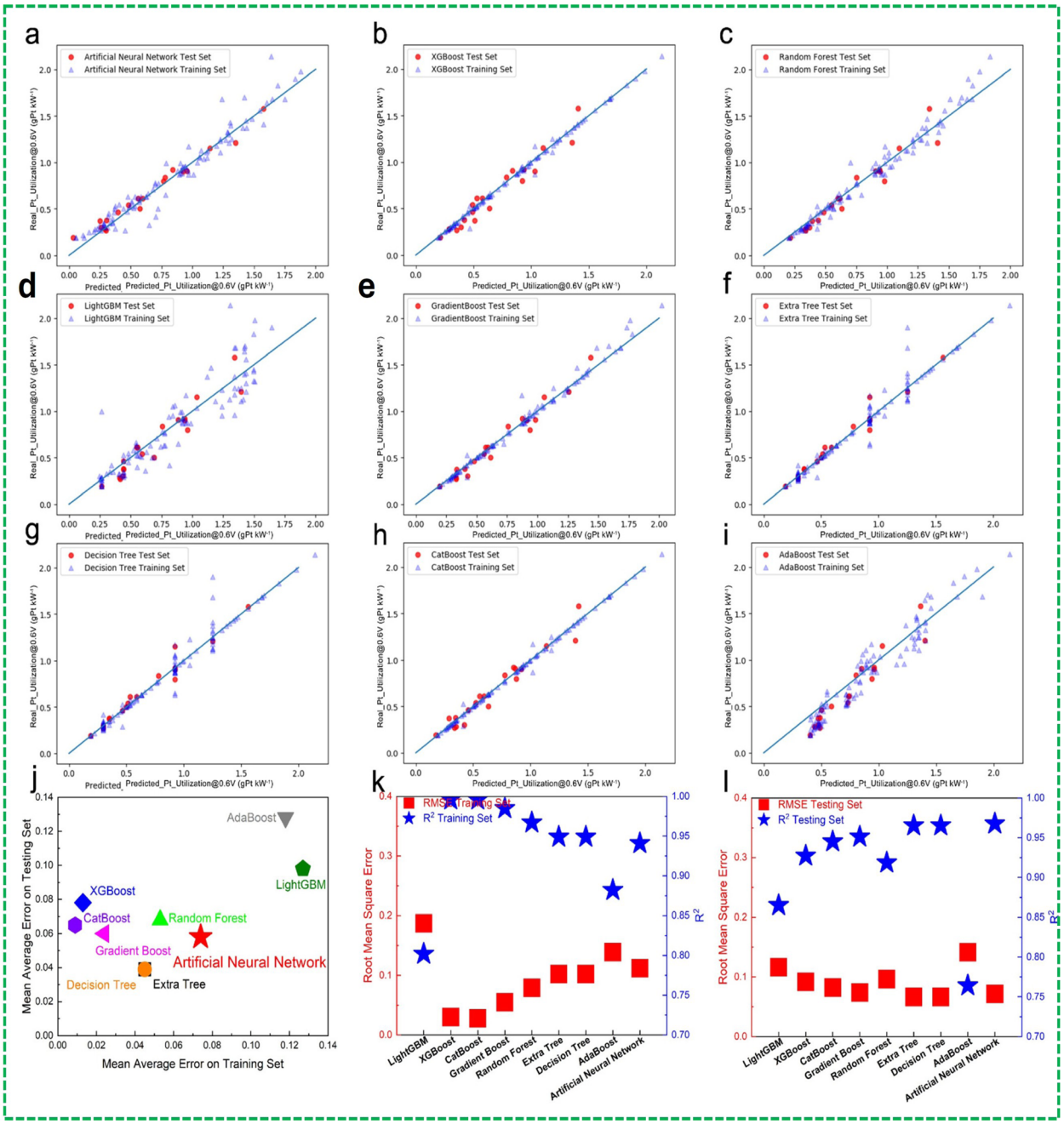

Fig. 18 (a–i) Various machine learning techniques were evaluated for their performance in predicting Pt usage at 0.6 V. The regression modeling utilized all 19 initial characteristics as input. (j) Mean absolute error (MAE) values of several machine learning (ML) algorithms on both the training and testing sets. (k) RMSE and R^2 values of several machine learning methods on the training set. (l) RMSE and R^2 values of several machine learning methods on the test set. Image reproduced with permission from ref. 264, copyright © 2022 the American Chemical Society. https://doi.org/10.1021/acsami.1c23221.

PEMFCs. These algorithms can be extended to AEMFCs to improve their efficiency and performance.[133] The horse herding optimization algorithm (HHOA) and the seagull optimization algorithm (HSOA) are two examples of hybrid algorithms that have demonstrated their usefulness in terms of convergence speed and final correctness. These two aspects are essential for the practical application of anion exchange membrane fuel cells (AEMFCs). By optimizing operational conditions and decreasing dependence on precious metals, the incorporation of these sophisticated optimization approaches makes AEMFCs more economically viable while simultaneously improving their performance and durability.[126,264]

6.2.1 Model training for AEMFC. After identifying the best feature subset, including ion-exchange capacity, membrane water absorption, hydroxide conductivity, catalyst loading, and MEA operating conditions, it may be utilized to train various linear and nonlinear machine learning algorithms specifically designed for AEMFC research.[134] Datasets are often partitioned

into training and test sets: the training set is utilized for constructing the prediction model, while the test set is designated for assessing its generalization performance. Based on the characteristics of the data and the desired outputs, machine learning in AEMFC investigations can be executed using supervised, unsupervised, or semi-supervised learning methodologies. In supervised learning, models discern correlations between input variables (*e.g.*, polymer backbone chemistry, quaternary ammonium stability, electrode porosity, gas feed parameters) and goal outputs, such as membrane conductivity, degradation rate, peak power density, or AEMFC efficiency. Regression and classification models modify their internal parameters to reduce prediction errors, enabling swift evaluation of performance metrics for new membrane materials or MEA configurations, thus providing a robust alternative to laborious experiments and resource-demanding physics-based simulations. In the absence of labeled identifiers, unsupervised learning facilitates clustering and dimensionality reduction to reveal latent patterns, like polymer family classifications, stability-conductivity trade-offs, or similarities in catalyst structures. These insights facilitate the formulation of logical design strategies and indicate which material categories or operational conditions warrant further investigation.[229,233–235]

6.3 Data-driven insights using AI

Using data-driven insights and developing innovative materials can greatly improve the performance and efficiency of anion exchange membrane fuel cells (AEMFCs). Improvements in anion exchange membranes (AEMs), binders, and catalyst layers (CLs) have allowed AEMFCs to reach performance levels similar to those of proton exchange membrane fuel cells (PEMFCs), with power densities reaching 3 W cm^{-2}.[135] The adjustment of operating parameters, such as the cell temperature and reactant humidification, is particularly important. This is due to the fact that higher temperatures and adjusted gas dew points can reduce the risk of flooding and dehydration, which ultimately leads to an improvement in cell performance. Furthermore, the synthesis of ionomers that are highly water-permeable and the implementation of hydrophobic treatments inside the catalyst layer have the potential to tackle the issues of anode flooding and cathode dry-out, enabling peak power densities of up to 2.70 W cm^{-2}. Key membrane parameters, such as water diffusivity and ion-exchange capacity, have been identified as significant elements that influence the lifetime and performance stability of an anion exchange membrane fuel cell (AEMFC) through the use of computational models.[135,136] Similarly, the implementation of novel techniques, such as applying textures to membranes to augment surface roughness, has demonstrated the ability to boost the three-phase boundary, resulting in a notable increase in power density of up to 17%. Empirical equations relating ionic conductivity and hydration level have been created, and these relationships will be crucial in guiding future developments in membrane technology and water-management approaches. Together, these data-driven insights and technology developments offer a complete foundation for enhancing the performance and efficiency of AEMFC, thereby making them commercially viable.[108,137]

Karam Yassin *et al.*'s findings demonstrate that the maximum hydration level (λ_{max}) significantly impacts the lifetime of AEMFCs, with ion-exchange capacity (IEC), water diffusivity, and membrane thickness following in influence. Improving the stability of functional groups is essential, while the conductivity of AEM hydroxide has a negligible impact. Furthermore, establishing an algebraic functional relationship among essential dimensionless parameters and utilizing machine learning (ML) regression analysis to evaluate the lifetime of AEMFCs are important. A wide neural network (WNN) model, trained and validated with MATLAB's Regression Learner Toolbox (2022a), predicts the influence of AEM parameters (λ_{max}, IEC, thickness, diffusivity, and reaction rate constant) on AEMFC durability. The comparison of model predictions with reported membrane lifetimes offers significant insights for the optimization of AEM design, aimed at improving fuel cell stability.[172]

6.4 AI in fault detection and maintenance of fuel cells

Analogous to proton exchange membrane fuel cells, anion exchange membrane fuel cells (AEMFCs) rely on fault detection and maintenance to improve efficiency and performance. Reliable problem diagnostic systems are necessary to guarantee consistent performance and prevent deterioration. Hybrid deep learning networks that combine ResNet and LSTM have demonstrated exceptional accuracy in fault detection, achieving a remarkable 99.632%. These networks utilize characteristic impedance and other vehicular measurement signals to identify different fault categories, such as membrane drying and flooding.[138] During the fuel cell testing process, non-invasive approaches that are based on the coefficient of variability, imprecise membership values, and wavelet transform have also been verified experimentally for fault identification and isolation. This ensures that the fuel cell is not damaged in any way.[139] Diverse artificial intelligence (AI) and machine learning (ML) methods have been utilized to improve the precision and effectiveness of defect diagnostics. For example, the use of deep learning frameworks that combine Electrochemical Impedance Spectroscopy (EIS) with neural networks has demonstrated enhanced performance in diagnosing faults. These frameworks utilize a small amount of EIS data to forecast the parameters of an analogous circuit model and create reliable diagnostic characteristics.[140] The diagnostic accuracy and generalizability of Support Vector Machines (SVM) improved with adaptive particle swarm optimization (APSO) have been shown to be superior for common defects, such as flooding and drying.[141] The integration of swift EIS measurements with enhanced *k*-nearest neighbor classifiers has proven to be successful in differentiating between various conditions, such as flooding and membrane drying. By employing sensor pre-selection and artificial neural networks (ANNs), data-driven methods have successfully attained exceptional diagnosis accuracy (99.2%) and recall rates (98.3%). This has been accomplished by eliminating fewer sensitive sensors and employing efficient training techniques.[142] Stacked autoencoders (SAE) have demonstrated strong identification capabilities for several fault circumstances, including

hydrogen leaking. Furthermore, the utilization of multi-stage fault detection models employing Support Vector Machines (SVM) in conjunction with binary trees has proven to be highly accurate in classifying fault kinds and degrees. Algorithms such as the square root unscented Kalman filter (SRUKF) and Bayesian inference have been employed to detect and isolate faults at an early stage, especially in cases of floods and catalytic degradation. The progress in artificial intelligence (AI) and machine learning (ML) applications for proton exchange membrane fuel cells (PEMFCs) establishes a strong basis for creating fault detection algorithms for AEMFCs, guaranteeing enhanced dependability and longevity.[143,144]

6.5 AI/ML in materials discovery for fuel cells

Artificial intelligence (AI) and machine learning (ML) technologies combine fast calculations and interpretable models to forecast and interpret the capacity to create and the functioning of materials. This helps to connect the predictions made by computer simulations with the practicality of real-world experiments. Previously, energy materials like fuel cell components were developed through time-consuming and costly trial-and-error processes. However, with the help of AI and ML, massive datasets can be rapidly analyzed to reveal patterns and forecast material features. For example, convolutional neural networks (ConvNets), which are a type of deep learning model, are used to analyze particle-size distribution in catalyst layers. This helps to improve the efficiency of polymer electrolyte fuel cells.[145,146] The fast identification of superionic conductors, which are necessary for solid-state electrolytes and cathode materials, is made possible by AI platforms, such as AI-IMAE, which accurately anticipate the ion migration activation energy. Also, cost-effective oxygen evolution reaction (OER) catalysts have been developed using ML-guided materials discovery and high-throughput synthesis; these catalysts are essential for boosting the efficiency of electrochemical technologies.[147] Artificial intelligence (AI) has shown great promise in improving proton exchange membrane fuel cell (PEMFC) efficiency by detecting critical parameters in membrane electrode assemblies (MEAs) without requiring laborious trial-and-error procedures. Artificial intelligence (AI) can transform material design and performance knowledge; for example, a fuel cell anion exchange membrane (AEM) designed using virtual module compound enumeration screening (V-MCES) in conjunction with supervised learning shows impressive stability. To sum up, artificial intelligence and machine learning play crucial roles in revolutionizing fuel cell material discovery by facilitating the creation of innovative energy materials at a lower cost, with greater efficiency, and in less time.[140,148] However, the materials science community has access to a wide range of DFT and MD software, including both private and publicly licensed software. The methods, basis sets, exchange–correlation functionals, and potentials used by these codes vary. Table 1 of ref. 157 illustrates a variety of DFT and MD software, along with their descriptions.[157]

Recently, researchers proposed the PrISMa platform as an all-encompassing answer that combines life cycle assessment, techno-economics, process design, and materials. Its goal is to bring together stakeholders at the beginning of carbon-capture technology development in order to speed up the process. Technological progress relies on the identification of high-performing materials. Density functional theory and molecular simulations provide reliable material property predictions; however, they are resource-intensive. To get around this, researchers employed a machine learning feedback loop to efficiently screen a bigger area of chemical designs.[158] Data analysis, computer methods, and domain knowledge are all part of machine learning's systematic approach to materials chemistry, which aims to speed up the process of discovering and synthesizing novel compounds. Each of the many critical steps in this intricate procedure is essential to the final result. The first step is to gather a large amount of chemical data. After that, they are processed and polished to make them more useful for materials chemistry analysis and prediction. The first step is to determine which machine learning algorithms will be most effective for solving the challenge. The available data are used to train these algorithms, and their performance is fine-tuned by adjusting their parameters. Validation and testing are carried out utilizing new, unseen data to guarantee the dependability of the model. Understanding the connections between the input features and the attributes that are predicted is made easier with the aid of these models. Fig. 19a and b illustrate the systematic flow of the ML process.[161]

6.5.1 Differentiating between real-time adaptive control and materials discovery for AEMFCs. Predictive modeling, empirical performance estimation, and parameter optimization have been the focus of recent AI and ML frameworks in fuel cell research. Beyond these conventional uses, AI plays a more expansive transformational function in the context of AEMFCs.[178–180] It is possible to distinguish two different domains.

6.5.1.1 Data-driven screening of membranes, catalysts, and electrode components. Machine learning enables rapid, high-throughput screening of next-generation anion exchange membranes by learning complex, nonlinear relationships between polymer structure, morphology, and electrochemical performance. Using supervised learning models, such as random forests, support vector regressors, and neural networks, researchers can predict key AEM properties, including hydroxide conductivity, alkaline stability, water uptake, swelling ratio, and mechanical robustness directly from molecular descriptors or polymer fingerprints. Unsupervised clustering techniques help identify hidden structure–property trends, classify polymer backbones based on stability signatures, and reveal design motifs associated with enhanced OH^- transport. Neural network-based structure–property prediction, graph neural networks (GNNs), and polymer informatics platforms enable the exploration of large chemical spaces encompassing cationic head groups, spacer architectures, side-chain lengths, and backbone rigidity. These approaches significantly reduce the reliance on traditional trial-and-error synthesis by enabling *in silico* prioritization of polymers with higher alkaline stability, suppressed Hofmann elimination, improved microphase separation, and optimized hydration levels. ML-guided screening

Table 1 Important databases providing the structural and physicochemical properties of materials

Database	Data and insights offered	Source information	Link to the database
Materials Project	Provides high-throughput DFT-computed structural, thermodynamic, electronic, and mechanical properties for experimentally known and theoretically predicted materials	Computed using high-throughput density functional theory (DFT) workflows developed and maintained by LBNL under the U.S. DOE Materials Genome Initiative	https://materialsproject.org/
ChemSpider	Aggregates chemical structures, properties, spectra, and bibliographic data for millions of small molecules from multiple curated sources	Provided by The Royal Society of Chemistry (RSC), integrating data from commercial, academic, and publicly contributed chemical databases	http://www.chemspider.com
Open Quantum Materials Database	Contains DFT-calculated thermodynamic, structural, and stability data for hundreds of thousands of inorganic crystalline materials, enabling large-scale materials screening and discovery	Generated using automated high-throughput DFT workflows developed at Northwestern University and Argonne National Laboratory	http://oqmd.org/
NOMAD (novel materials discovery)	Provides compliant, curated materials-science data, including raw and processed outputs from DFT, MD, and electronic-structure calculations supporting large-scale ML modeling and benchmarking	Hosted by the NOMAD Laboratory (EU Centre of Excellence), aggregating worldwide computational materials data submitted by researchers through a standardized, open-access infrastructure	https://nomad-coe.eu/
ZINC	Provides a curated library of purchasable small molecules with 3D structures, physicochemical properties, and ready-to-dock formats for virtual screening and computational drug/materials discovery	Developed and maintained by the Irwin Lab at the University of California, San Francisco (UCSF), sourcing compounds from commercial chemical suppliers	https://zinc15.docking.org/
Khazana	Provides curated, standardized datasets for chemistry and materials science, including reaction data, molecular properties, and materials informatics benchmarks, supporting reproducible AI/ML model development	Developed by DeepChem and the broader open-source scientific ML community, compiling datasets from peer-reviewed literature and public repositories into machine-learning-ready formats	https://khazana.gatech.edu/
CMR	Hosts curated computational materials datasets, including crystal structures, electronic properties, and DFT-calculated energies, enabling benchmarking, reproducibility, and ML-driven materials discovery	Developed by the Computational Materials Science Group at the University of Copenhagen, aggregating standardized DFT datasets generated using high-throughput simulation workflows	https://cmr.fysik.dtu.dk/
MatNavi	Integrated materials-database system for polymers and inorganic materials	Developed by the National Institute for Materials Science (NIMS), Japan, providing experimental and computational data on polymers, inorganic materials	https://mits.nims.go.jp/
HTEM	Provides experimental data on inorganic thin-film materials, including composition, synthesis/deposition conditions, structural information (*e.g.*, X-ray diffraction), and optoelectronic properties, enabling high-throughput materials discovery and machine learning applications	Maintained by the National Renewable Energy Laboratory (NREL), USA; publicly accessible through the HTEM web portal and API under an open-access license	https://htem.nrel.gov/
MatWeb	Provides comprehensive material property data for metals, polymers, ceramics, and composites,	Hosted and maintained by MatWeb, Inc., offering an open-access platform with subscription options	http://matweb.com/

Table 1 (*Contd.*)

Database	Data and insights offered	Source information	Link to the database
	including mechanical, thermal, electrical, and chemical properties, as well as processing information	for extended features and commercial use	
AiiDA/Materials Cloud	Provides curated datasets, workflows, simulation archives, and provenance-tracked results from high-throughput computational materials science, including structural, electronic, and thermodynamic properties generated *via* automated workflows	Developed and maintained by the NCCR MARVEL consortium at EPFL (École Polytechnique Fédérale de Lausanne), Switzerland; accessible through the open-access Materials Cloud platform integrated with the AiiDA workflow management framework	https://materialscloud.org/
Citrine Informatics	Provides curated materials data, including composition-property relationships, processing histories, experimental results, and computational datasets, enabling data-driven materials design and machine learning model development	Offered through the Citrine Platform developed by Citrine Informatics (USA), which hosts both open datasets and proprietary enterprise tools for materials informatics and AI-driven materials development	https://citrine.io/
Ansys Granta (MaterialUniverse Repository)	Provides validated engineering data for metals, polymers, ceramics, composites, and functional materials, including mechanical, thermal, electrical, processing, environmental, and cost-related properties, along with predictive models for material performance	Maintained by Ansys Granta, part of Ansys Inc., delivering structured, industry-grade materials data through the MaterialUniverse repository within the Granta MI and Granta EduPack platforms	https://www.ansys.com/

also assists in predicting catalyst layer compositions, binding energies, pore structures, and metal–support interactions relevant to AEMFC electrodes. Collectively, this data-driven domain focuses on rationally designing intrinsically stable, high-performance AEM materials with tunable transport pathways, reduced degradation, and improved operational durability, accelerating discovery cycles and guiding experimental work toward the most promising membrane chemistries (Fig. 19a).[181–183]

6.5.2 From Sabatier principle to ML models: catalyst design. The design and development of effective, robust, and cost-effective electrocatalysts is crucial for the progress of AEMFC technology, especially for essential reactions like the oxygen reduction reaction (ORR) and hydrogen oxidation reaction (HOR) in alkaline environments. In AEMFC catalyst engineering, material selection conventionally adheres to the Sabatier principle, which posits that optimal catalytic activity is achieved when the contact between intermediates (*e.g.*, OH*, OOH*, and O*) and the catalyst surface is of moderate strength (Fig. 20a). This connection is typically represented by volcano plots that associate catalytic activity with adsorption energies (Fig. 20b). While alkaline conditions facilitate the investigation of non-precious metal catalysts, including transition-metal oxides, perovskites, spinels, and M–N–C structures, numerous candidates continue to exhibit inadequate activity, instability at elevated pH levels, or excessive overpotential demands. Machine learning has become an effective instrument for expediting AEMFC catalyst development by forecasting adsorption energetics, stability ranges, and active-site characteristics without necessitating comprehensive high-fidelity simulations. Traditional methodologies, such as the d-band model, which correlates the d-band center of transition-metal surfaces with bonding strength and catalytic reactivity, continue to be essential for comprehending ORR/HOR processes in alkaline environments. Nevertheless, acquiring precise d-band descriptors often necessitates computationally demanding DFT computations, which impose constraints on extensive screening efforts. Machine learning-based surrogate models provide an alternative by directly learning structure–activity connections from computed or experimental datasets, facilitating the fast discovery of promising PGM-free catalysts characterized by low overpotential, high intrinsic activity, and enhanced alkaline durability (Fig. 20c).[236–241] The major databases providing structural and physicochemical property information for materials research are listed in Table 1.[221–225]

A significant challenge arises in correlating the intricate porous architecture of AEMFC electrodes, specifically the catalyst layer (CL) and microporous layer (MPL), with their respective effective transport properties, including tortuosity, ionic conductivity, gas diffusion resistance, and water-management characteristics. The electrode meso/micro-structure is established during manufacture, considering factors such as ink formulation, ionomer ratio, solvent composition, and deposition process. Consequently, a more profound inquiry arises about the impact of certain manufacturing factors on the ultimate 3D architecture of the catalyst layer. In a specific catalyst system (PGM or PGM-free), alterations in the meso/micro-structure properties, such as the pore-size distribution,

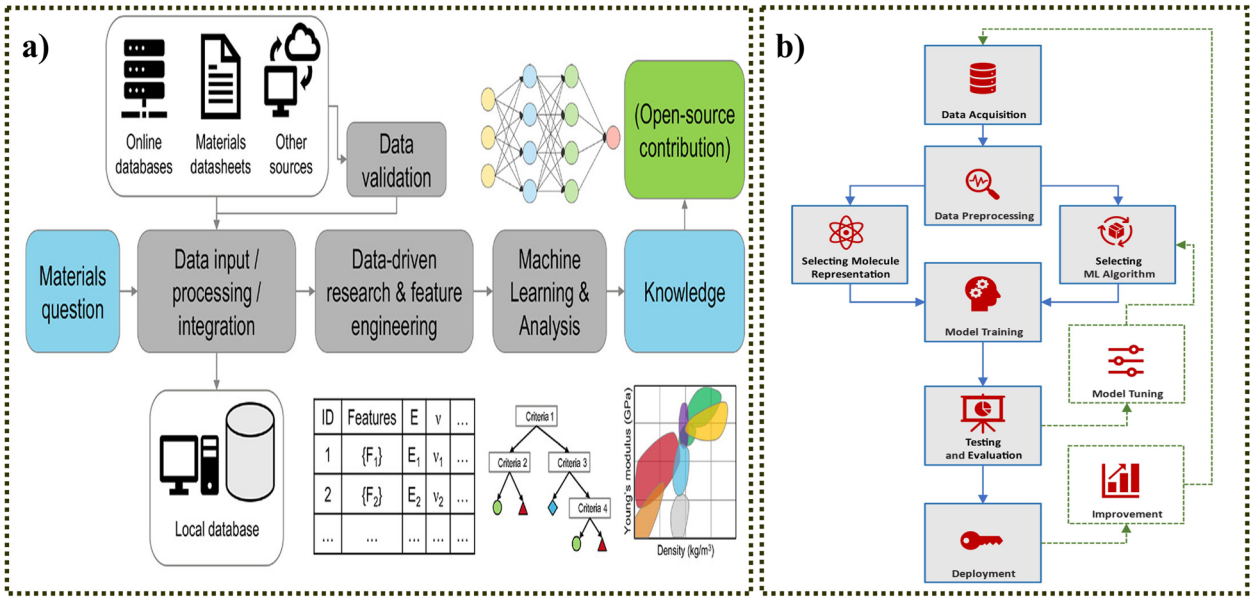

Fig. 19 (a) Application of machine learning in materials science. Image reproduced with permission from ref. 183, copyright © 2020 the American Chemical Society. https://doi.org/10.1021/acs.chemmater.0c01907. (b) Schematic of the systematic process of ML. Image reproduced with permission from ref. 161, copyright © 2024 The Author(s). Published by Elsevier B.V. https://doi.org/10.1016/j.aichem.2024.100049.

connectedness, and ionomer distribution, significantly affect the AEMFC performance, including its ORR kinetics, mass-transfer efficiency, and water retention. While physics-based modeling of electrode manufacture processes, including slurry dynamics, drying, ionomer migration, and layer compression, has gained prominence, data-driven approaches for comprehending these interactions are just starting to develop. This domain is characterized by two interconnected challenges: (i) quantifying the impact of fabrication variables (ink composition, ultrasonication energy, spraying speed, hot-pressing conditions) on the meso/micro-structure of the catalyst layer, and (ii) assessing how these meso/micro-structural attributes affect the cell-level performance under different humidity and loading conditions (Fig. 21a–c).[245,250] Conventional methodologies employ sequential multiscale models to simulate discrete processing steps, like slurry formulation, solvent evaporation, ionomer redistribution, and pore formation, and integrate their outputs into mesoscale electrode models and continuum-level AEMFC performance simulators. Machine learning now provides robust capabilities to evaluate, expedite, and rectify multiscale operations. For instance, machine learning models may be developed to deduce meso/micro-structural descriptors from constrained experimental or simulation data, improve slurry compositions, forecast ionomer dispersion patterns, or enhance force-field parameters in coarse-grained simulations of catalyst–ionomer interactions (Fig. 21c). Hybrid physics-machine learning frameworks are poised to provide reliable linkages between manufacturing, meso/micro-structure, and performance for next-generation anion exchange membrane fuel cell electrodes.[242–250] Some recent advancements by Rashen Lou Omongos *et al.* illustrate the emergence of (ML)-based optimization frameworks for gas diffusion layer (GDL) microstructure engineering, providing robust alternatives to conventional physics-based characterization. One significant method involved training ML models to accurately predict essential GDL morphological and transport features, attaining $R^2 = 95\%$ for six of the seven functional qualities and $R^2 \approx 90\%$ for the GDL–MPL interfacial resistance. The validation of digitally rebuilt GDL structures shows substantial concordance with physics-based simulations while diminishing computing time significantly from 3 to 4 hours of physical modeling to around 3 seconds of machine learning inference (Fig. 21a and b). The design insights indicate distinct structure–property relationships: low fiber concentration and low compression ratio optimize gas transport by maximizing diffusivity and minimizing interfacial contact resistance, while high fiber concentration and high compression ratio enhance electrical and thermal conductivities while maintaining controlled contact resistance. These findings demonstrate how machine learning-based optimization can swiftly traverse intricate manufacturing–structure–performance interactions, facilitating enhanced gas transfer, water management, and thermal control. This technique, originally proven for PEMFC GDLs, offers a transferable foundation for AEMFC electrode design, where microstructural optimization is essential for improving hydroxide transport, catalyst efficiency, and long-term durability.[250]

6.5.1.2 Real-time adaptive control and diagnostic. Adaptive machine learning frameworks, such as digital-twin architectures, reinforcement learning, and Bayesian optimization, continually modify operational variables, like temperature, humidity, reactant flow rates, and current density, in contrast to static prediction models. Additionally, these models provide dynamic state-of-health monitoring unique to AEMFC systems,

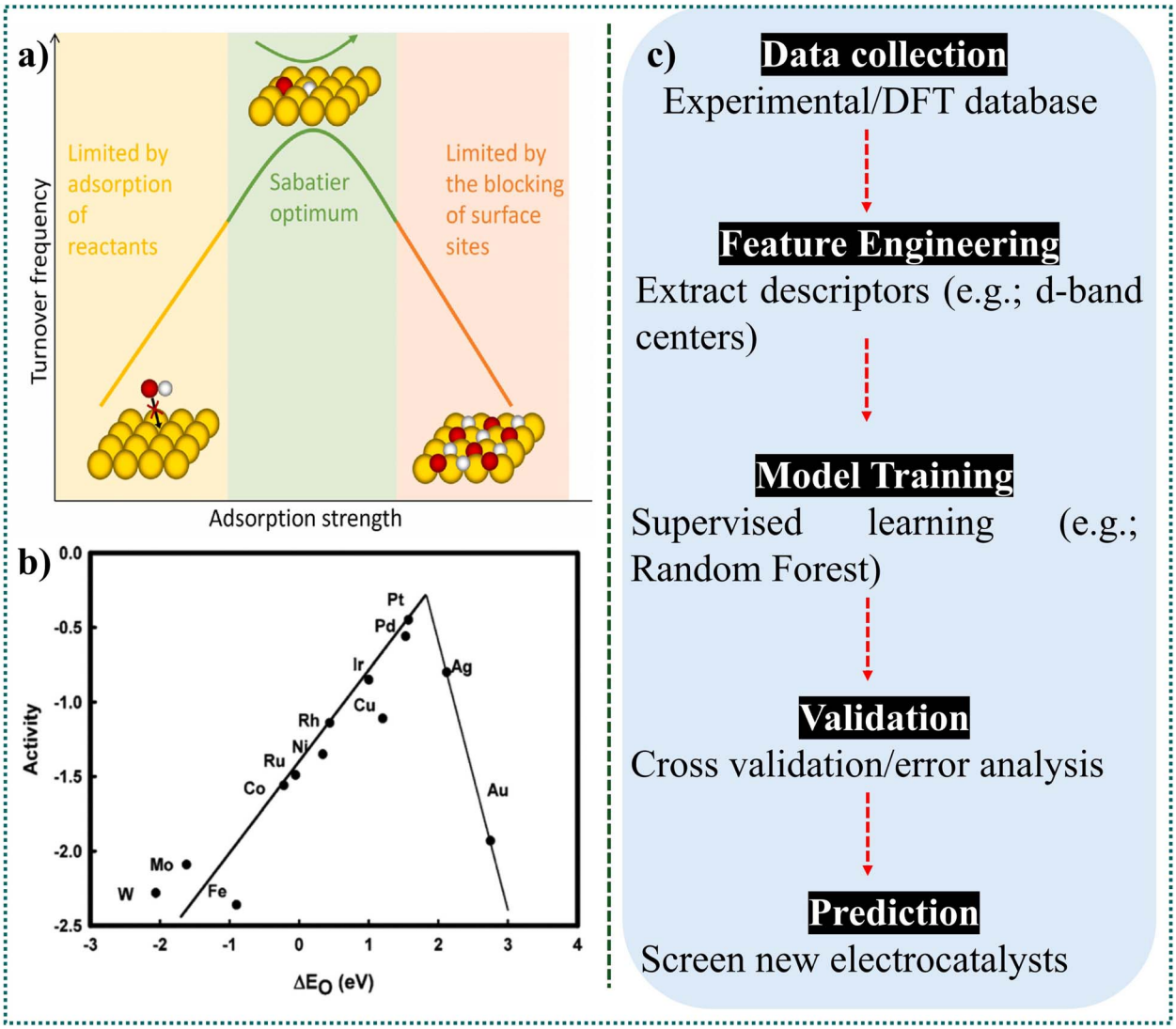

Fig. 20 (a) Illustration of the Sabatier principle; catalysts that exhibit excessive binding affinity are constrained by sluggish product synthesis or desorption, whereas those with insufficient binding affinity are hindered by delayed reactant adsorption or activation. Optimal catalysts demonstrate intermediate binding strength. Image reproduced with permission from ref. 240. Copyright © 2023 The Authors. Published by Elsevier B.V. https://doi.org/10.1016/j.surfrep.2023.100597. (b) Theoretical volcano plot of the ORR activity for various metal catalysts as a function of the oxygen-binding energy in alkaline media. Image reproduced with permission from ref. 241. Copyright © 2021 Elsevier B.V. All rights reserved. https://doi.org/10.1016/j.coelec.2021.100923. (c) Machine learning (ML) workflow for the catalyst design.

anomaly prediction, and early failure identification. When combined, these methods show that AI integration in AEMFCs provides a dual pathway: (i) accelerating material innovation and (ii) enabling intelligent operation, rather than just performance prediction. There are still restrictions, though, such as a lack of standardized reporting, a lack of data, and the requirement for open datasets and benchmarking procedures unique to AEM.[184–189] Despite the rapid progress, there are still several obstacles and subtle risks encountered when using machine learning (ML) methods in materials science. Standardized best practices for using machine learning (ML) in materials research are still developing. Fig. 22 provides a clear, step-by-step workflow for carrying out a typical machine learning project, including data loading, preprocessing, dataset segmentation, feature engineering, model training, performance evaluation, cross-model comparison, and visualization, to assist materials scientists who are just starting out in this field. By forecasting mechanical, electronic, thermodynamic, and transport properties, as well as by speeding up discovery in a variety of application areas, such as photovoltaics, energy-storage materials, electrocatalysts and photocatalysts, thermoelectrics, superconductors, high-entropy alloys, and metallic glasses, machine learning has already shown substantial value across materials science. This demonstrates the wide range of applications and revolutionary possibilities of machine learning while highlighting the need for easily available guidelines to help more academics successfully and consistently implement data-driven methodologies.[183]

To facilitate reproducible and transparent implementation of machine learning in AEMFC research, we delineate a generic

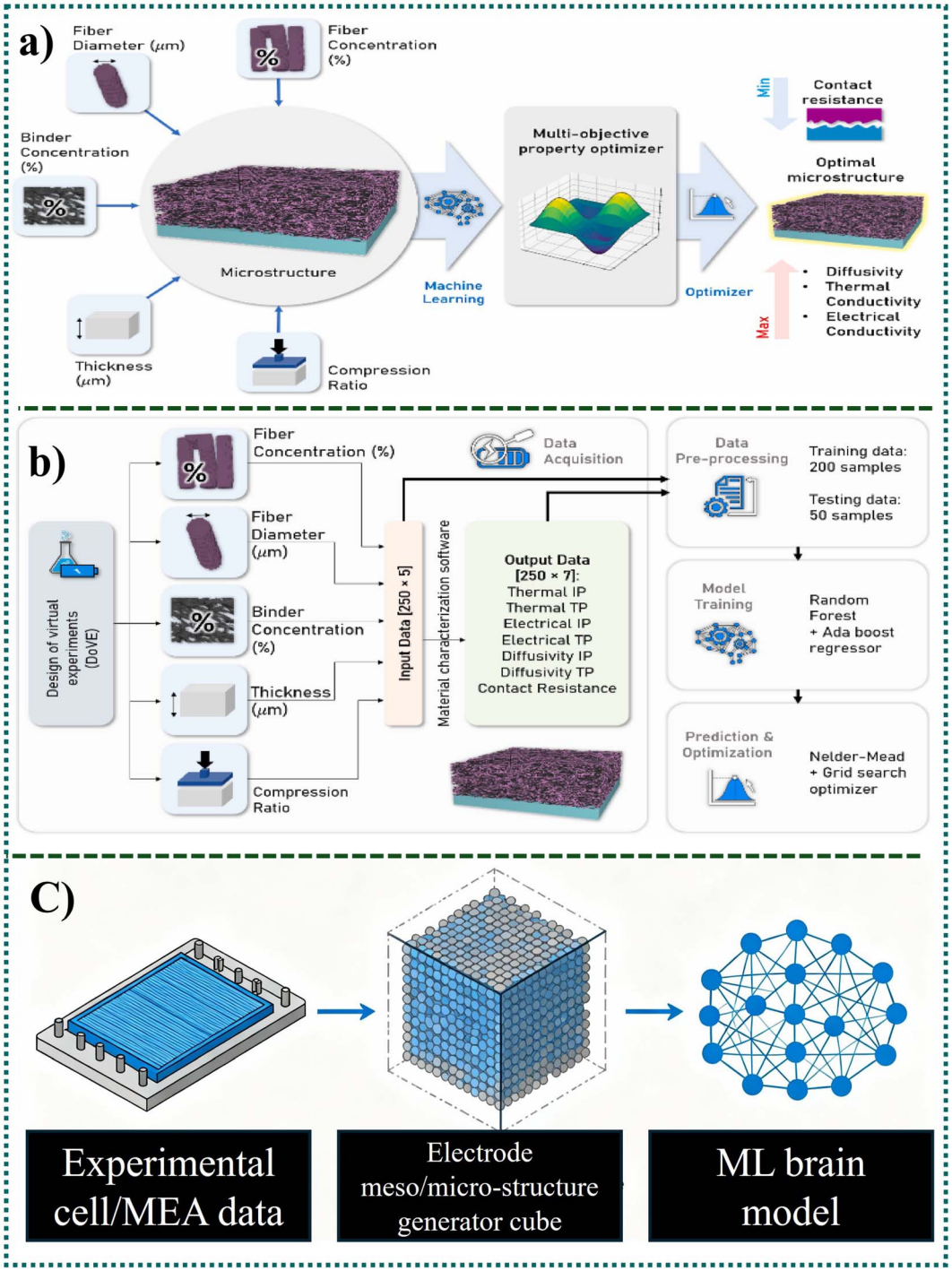

Fig. 21 (a) Schematic of the multi-objective optimization of manufacturing parameters, including the optimization of variations in fiber morphology, binder loading, electrode thickness, and compression ratio to achieve minimum contact resistance under multiple operating conditions. Image reproduced with permission from ref. 250. Copyright © 2024 The Authors. Published by Elsevier B.V. https://doi.org/10.1016/j.jpowsour.2024.235583. (b) Illustration of the ML data-driven study workflow. Image reproduced with permission from ref. 250. Copyright © 2024 The Authors. Published by Elsevier B.V. https://doi.org/10.1016/j.jpowsour.2024.235583. (c) Schematic of the coupling experimental data and ML/deep learning.

process that encapsulates the interaction between AI algorithms and experimental or simulated datasets. The pipeline starts with data collection, encompassing membrane characteristics, electrode morphology, operational parameters, and performance indicators. This is succeeded by data preparation, which includes noise elimination, normalization, and feature extraction. Subsequently, diverse machine learning models, such as regression techniques, neural networks, or ensemble methods, are trained and refined utilizing curated datasets. The trained models are subjected to validation and hyperparameter

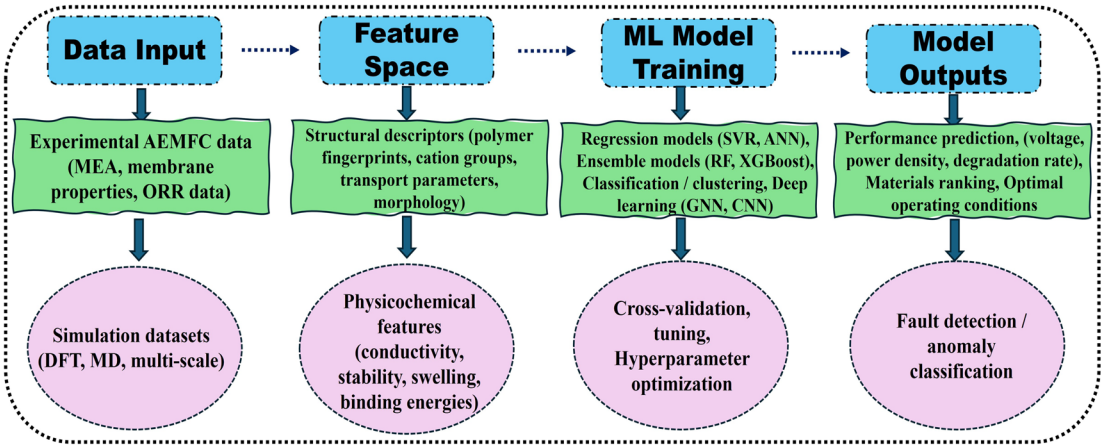

Fig. 22 Schematic of the AI/ML workflow for the AEMFC.

optimization to guarantee generalizability, followed by the assessment of performance measures (*e.g.*, RMSE, MAE, and R^2). The verified models are ultimately used for prediction, optimization, or adaptive control of AEMFC systems. This methodology offers a systematic approach for incorporating machine learning into experimental AEMFC research.

6.5.3 Graph neural networks (GNNs) and graphical neural networks (GNNs). Graph neural networks and graphical neural networks are similar, developed for the processing of data that are arranged in a graph, where nodes represent entities and edges reflect the interactions between those entities. In reality, there is not much of a difference between these terms. Graph neural networks (GNNs) are a class of machine learning models specifically designed to handle graph-structured data, such as molecular graphs. These architectures operate directly on graphs, learning to process and extract information from them. GNNs consist of layers that iteratively update node representations by aggregating information from neighboring nodes, effectively capturing both local and global structural features within the graph. Due to their ability to model complex graph data, GNNs have become increasingly popular for tasks such as molecular property prediction, drug discovery, and molecular property optimization; a more detailed molecular representation of ML is discussed in ref. 161 and 162. The graphs depict abstract structures where entities or things are represented as vertices (nodes) and their relationships as edges. A graph is formally defined as a tuple $G = (V, E)$, where V is a collection of vertices and E represents a set of edges, ev, $w = (v, w)$, that indicate connections between vertices. Graph neural networks (GNNs) are capable of addressing challenges like graph-level property prediction (*e.g.*, predicting chemical properties), node-level classification (*e.g.*, identifying members of temperature graphs), and edge-level prediction (*e.g.*, determining relationships in temperature and pore size/volume graphs). In materials chemistry, graph-level predictions are highly important.[161–163] Fuel cell materials should be selected to provide good beginning-of-life performance and durability in order to facilitate efficient hydrogen oxidation reactions (HOR) and oxygen reduction reactions (ORR). As an example, a number of previously mentioned challenges, such as the need for a durable electrocatalyst, as well as reduced catalyst loading, improved water-management and degradation strategies, reduced reactant/membrane contamination, and mitigated transport losses, must be addressed in order to increase activation. Research and development efforts pertaining to fuel cells should prioritize the advancement and enhancement of materials, as well as the establishment of basics that define material attributes and fuel cell performance under different operating conditions.[164,165]

6.5.4 Generative AI in fuel cell design and optimization. As a game changer in fuel cell technology optimization and design, generative AI provides novel approaches for solving long-standing problems. Generative AI enhances fuel cell performance and efficiency by exploring large design spaces effectively using sophisticated machine learning models, optimized microstructures, and so on.[166,167] Optimizing the nanostructures of catalyst layers (CLs) in hydrogen fuel cells has been accomplished by the development of the GLIDER framework, which is a deep generative artificial intelligence model. The Pt–carbon–ionomer nanostructures are the primary focus of this model, which combines generative artificial intelligence with data-driven surrogate methodologies in order to search for optimal CL designs in an efficient capacity. The fact that the framework is able to produce multiscale CL digital models that are realistic suggests that it has the potential to dramatically increase the design and performance of hydrogen fuel cells.[166] In the field of automobile fuel cells, a hybrid technique that combines physical modeling with artificial intelligence has been proven. A neural network is trained with data from comprehensive physical models in order to accomplish this procedure. The neural network is then utilized as an alternative model in order to facilitate efficient simulation. With this method, fuel cell models are improved in terms of their accuracy and performance, which, in turn, enables more accurate prediction of fuel consumption and range under a variety of scenarios.[168] In an effort to maximize the efficiency of electric vehicles powered by hydrogen fuel cells, scientists have implemented machine learning strategies. Machine learning has the ability to improve fuel cell system efficiency by combining conventional multi-physics analysis with AI, which allows for the precise prediction

of fuel consumption peaks.[169] To realize the full potential of generative artificial intelligence, it is necessary to overcome difficulties, such as the availability of data, interpretability of models, and integration of systems. This is notwithstanding the fact that generative AI has delivered breakthroughs in fuel cell technology. For the purpose of overcoming these obstacles and finding solutions that are both scalable and sturdy for the future of fuel cell technology, interdisciplinary collaboration will be vital.

6.5.5 Advantages of sustainability and cost in AI-enhanced discovery for AEMFC development. (i) AI-driven materials discovery minimizes waste by facilitating virtual screening of many membrane chemistries, catalyst compositions, and electrode architectures prior to physical manufacturing. This lowers the frequency of unsuccessful trials, decreases chemical usage, and eliminates resource-intensive trial-and-error testing.

(ii) Machine learning expedites prototype evaluation by precisely predicting ion conductivity, alkaline stability, ORR performance, and MEA durability across various operating conditions. This considerably reduces the development period for new AEMFC components, facilitating expedited iteration and transition to pilot-scale manufacturing.

(iii) AI predictions reduce experimental costs by selecting only the most impactful material and operational characteristics for enhancement. Models like ANN, Random Forest, and XGBoost enable researchers to make viable choices and discard superfluous measurements, thereby reducing energy, labor, and material expenses during scale-up.[202–207]

(iv) AI predicts AEM chemical stability: in a recent study, researchers illustrated the application of AI in forecasting the chemical stability of anion exchange membranes (AEMs) for fuel cells. This study measured the AEM stability using Hammett's substituent constants within a materials-genomics framework and subsequently categorized the results for five machine learning techniques using decision tree analysis. Artificial neural networks (ANNs) attained the greatest prediction accuracy, evidenced by an R^2 value of 0.9978. ANNs have been successfully utilized to forecast the alkaline stability of AEMs, due to their capacity to understand intricate nonlinear correlations from experimental data, manage many output variables, and provide enhanced regression performance (Fig. 23a). This work characterized the chemical structure of AEMs for the first time using Hammett's substituent constants, offering a significant descriptor for both polymer backbones

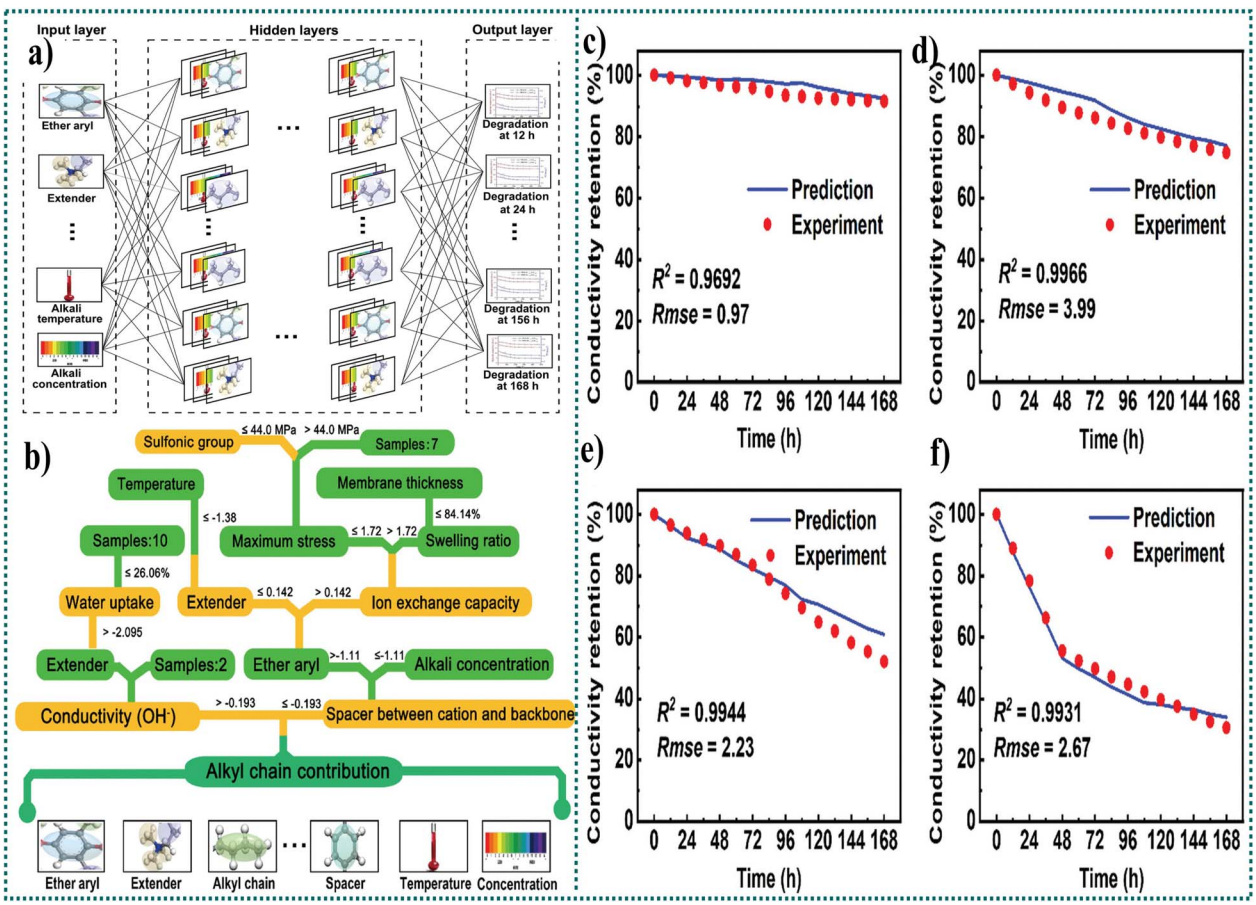

Fig. 23 (a) ANN structure. (b) Simplified partial decision tree structure derived from Hammett's substituent constants, illustrating the key structural requirements for achieving high chemical stability in the AEMs. Predicted *versus* experimentally validated conductivity retention curves for the reported AEM materials: (c) poly(*p*-phenylene-co-aryl ether ketone), (d) poly(ether sulfone)-based, (e) PPO-based AEMs, and (f) polystyrene-*N*,*N*-diethyl-3-(4-vinylphenyl)propan-1-amine. Image reproduced with permission from ref. 108. Copyright © The Royal Society of Chemistry. https://doi.org/10.1039/D1EE01170G.

and cationic side chains. Before model training, a characteristic analysis of the dataset was conducted to assess the quality and representativeness of the input samples. A decision tree model was employed alongside the ANN to assess feature significance, utilizing its interpretability and computational efficiency. Although atomic numbers were evaluated as structural descriptors, the Hammett constants provided superior selective capability. The decision tree framework identified essential structural conditions for high chemical stability, with the root node emphasizing the significant impact of the alkyl-chain contributions on the polymer backbone, an observation aligned with known degradation pathways in alkaline environments (Fig. 23a and b). Fig. 23c–f shows the predicted *versus* experimentally validated conductivity retention curves for the reported AEM materials: poly(*p*-phenylene-*co*-aryl ether ketone), poly(ether sulfone)-based, PPO-based AEMs, and polystyrene-*N*,*N*-diethyl-3-(4-vinylphenyl)propan-1-amine. Collectively, machine learning-derived findings offer explicit directions for the systematic design and production of more chemically resilient anion exchange membranes. The AI predictions were confirmed using long-term chemical stability studies, proving the resilience and practical dependability of the AI-based technology. This combined computational-experimental methodology underscores the capacity of machine learning to expedite the evaluation and formulation of chemically stable anion exchange membrane materials.[108]

6.5.6 Potential challenges and future directions. When it comes to the development of anion exchange membrane fuel cells (AEMFCs), the inclusion of artificial intelligence (AI) and machine learning (ML) algorithms presents not only substantial hurdles but also exciting prospects. Achieving accurate prediction of chemical stability and ion-migration activation energy (E_a) in aqueous electrolyte membranes (AEMs) is one of the key problems. These two factors are essential for the performance and durability of anion exchange membrane fuel cells (AEMFCs). Artificial intelligence models, such as artificial neural networks (ANNs) and crystal graph neural networks, have demonstrated high accuracy and efficiency in predicting these parameters, thereby significantly reducing the need for extensive experimental trials. Traditional methods for determining these properties are time-consuming and complex.[108] Notwithstanding these progressions, the ever-changing characteristics of electrolyte solutions and the requirement for extensive simulation durations and vast system dimensions to obtain precise sampling remain unresolved concerns.

6.5.7 Numerous significant hurdles persist in the use of AI in AEMFC research. Data scarcity continues because of the scarcity of high-quality, publicly accessible datasets pertaining to AEM materials, MEA structures, and operational diagnostics. This limits model training and diminishes generalizability.

Model bias can emerge from limited or skewed datasets, resulting in ML algorithms overfitting prevalent chemistry or membrane types while neglecting atypical yet possibly high-performing alternatives.

Model interpretability remains a significant obstacle, especially for deep neural networks, whose intricate designs occasionally hide the fundamental physical–chemical dynamics. Interpretability can be enhanced by the use of feature-importance assessments, SHAP values, or physics-informed machine learning frameworks; nevertheless, these technologies remain underutilized in AEMFC research.

Researchers can utilize machine learning algorithms to evaluate extensive datasets, identifying trends and forecasting the long-term performance of various membrane materials under operating settings. This predictive capacity may result in the creation of more durable membranes that resist deterioration over time. Furthermore, the enhancement of electrocatalysts is another domain in which AI may make substantial contributions.

The advancement of platinum group metal (PGM)-free electrocatalysts is crucial for lowering fuel cell expenses. However, new developments in deep learning, particularly neural network potentials (NNPs), present potential resolutions. Achieving good anion exchange membrane conductivity and durability, as well as finding appropriate OH^- ion-conducting polymers, constitutes additional material and processing hurdles that need creative engineering solutions for the advancement of AEMFCs. Improving AEMFC durability procedures and performance degradation processes is crucial for developing AEMFCs with extended lifespans, as particular component degradations have been identified as limiting factors. Both artificial intelligence and machine learning have the potential to speed up the process of discovering and optimizing novel materials. This has been demonstrated by the speed with which prospective superionic conductors (SCs) for solid-state electrolytes and cathode materials are immediately identified. To avoid problems like anode flooding and cathode dry-out, AI can help optimize operational parameters, like cell temperature and gas humidification levels. Optimizing multi-objective functions, such as input pressure and temperature, for maximum output current density and power efficiency, may be achieved through the use of deep neural networks and genetic algorithms. The increased funding for research and the growing number of papers, which indicate an overwhelming dedication to this technology, both point to a bright future for artificial intelligence integration in anion exchange membrane fuel cell (AEMFC) research. To satisfy the ever-changing needs, artificial intelligence models may be continually modified through transfer learning as additional experimental and high-precision theoretical data become available. This paves the way for substantial breakthroughs in the performance and sustainability of anion exchange membrane fuel cells (AEMFC). AI can also assist the integration of AEM systems into carbon capture, utilization and storage (CCUS) frameworks, optimizing the whole process and enhancing environmental remediation results.

Conflicts of interest

The author declares no competing interests.

List of nomenclature

A_{cell} Membrane electrode assembly geometrical area (m^2)

AEM	Anion exchange membrane
AEMFC	Anion exchange membrane fuel cell
AFC	Alkaline fuel cell
AEMWE	Anion exchange membrane water electrolyzer
AI	Artificial intelligence
DMFC	Direct methanol fuel cell
DAFCs	Direct ammonia anion-exchange membrane fuel cells
E_a	Activation energy, J mol^{-1}
f	Frequency, Hz
F	Faraday's constant (96485C mol^{-1})
i	Current density, A m^{-2} or mA cm^{-2}
I	Current (A) or mA
IEC	Ion exchange capacity
M	Molecular weight
ML	Machine learning
n	No. of electrons
P	Pressure (atm)
P	Power (W)
PEFC	Polymer electrolyte fuel cell
PEMFC	Polymer electrolyte membrane fuel cell
PFOA	Perfluorooctanoic acid
PFOS	Perfluorooctane sulfonic acid
PFBSA	Perfluorobutane sulfonamide
PDDA	Poly(diallyldimethylammonium chloride)
RH	Relative humidity (%)
R_Ω	Ohmic resistance, Ω or Ω m^2
SOFC	Solid oxide fuel cell
T	Temperature (K or °C)
t	Time (S)
ξ	Stoichiometric ratio
ρ	Density (kg m^{-3})
a	Anode
c	Cathode
H_2	Hydrogen
O_2	Oxygen

Data availability

No primary research data, software or code were generated for this study. The bibliometric data were obtained from searches of the Scopus and Web of Science Core Collection databases, using identical query strings applied to titles, abstracts, and keywords. The retrieved records were merged and duplicate entries were removed to generate a unique dataset. The dataset supporting the findings of this study are openly available in the Zenodo repository at https://doi.org/10.5281/zenodo.18401509.

Acknowledgements

Dr Srikanth Ponnada would like to express his sincere gratitude and dedicate this article to his postdoctoral advisor, Prof. Andy M. Herring, on his 60th birthday, for his invaluable mentorship, including providing hands-on training and futuristic insights into fuel cell technologies and acknowledge the Colorado School of Mines, U.S.A., for resources, technical, and postdoctoral funding assistance.

References

1 S. Chu, Y. Cui and N. Liu, The path towards sustainable energy, *Nat. Mater.*, 2017, **16**(1), 16–22.
2 M. K. Debe, Electrocatalyst approaches and challenges for automotive fuel cells, *Nature*, 2012, **486**(7401), 43–51.
3 B. P. Setzler, Z. Zhuang, J. A. Wittkopf and Y. Yan, Activity targets for nanostructured platinum-group-metal-free catalysts in hydroxide exchange membrane fuel cells, *Nat. Nanotechnol.*, 2016, **11**(12), 1020–1025.
4 A. R. Motz, M. C. Kuo, G. Bender, B. S. Pivovar and A. M. Herring, Chemical stability via radical decomposition using silicotungstic acid moieties for polymer electrolyte fuel cells, *J. Electrochem. Soc.*, 2018, **165**(14), F1264.
5 A. R. Motz, M. C. Kuo, J. L. Horan, R. Yadav, S. Seifert, T. P. Pandey, S. Galioto, Y. Yang, N. V. Dale, S. J. Hamrock and A. M. Herring, Heteropoly acid functionalized fluoroelastomer with outstanding chemical durability and performance for vehicular fuel cells, *Energy Environ. Sci.*, 2018, **11**(6), 1499–1509.
6 C. G. Arges, V. K. Ramani and P. N. Pintauro, The chalkboard: Anion exchange membrane fuel cells, *Electrochem. Soc. Interface*, 2010, **19**(2), 31.
7 C. Kim, I. Wu, M. C. Kuo, D. J. Carmosino, E. W. Bloom, S. Seifert, D. A. Cullen, P. Ha, M. J. Lindell, R. Jiang and C. S. Gittleman, Improved Fuel Cell Chemical Durability of an Heteropoly Acid Functionalized Perfluorinated Terpolymer-Perfluorosulfonic Acid Composite Membrane, *J. Electrochem. Soc.*, 2023, **170**(2), 024505.
8 C. Y. Ahn, J. E. Park, S. Kim, O. H. Kim, W. Hwang, M. Her, S. Y. Kang, S. Park, O. J. Kwon, H. S. Park and Y. H. Cho, Differences in the electrochemical performance of Pt-based catalysts used for polymer electrolyte membrane fuel cells in liquid half-and full-cells, *Chem. Rev.*, 2021, **121**(24), 15075–15140.
9 L. Carrette, K. A. Friedrich and U. Stimming, Fuel cells: principles, types, fuels, and applications, *ChemPhysChem*, 2000, **1**(4), 162–193.
10 G. Hoogers, *Fuel Cell Technology Handbook*, CRC press, 2002.
11 L. Carrette, K. A. Friedrich and U. Stimming, Fuel cells: principles, types, fuels, and applications, *ChemPhysChem*, 2000, **1**(4), 162–193.
12 Y. Zhao, Y. Mao, W. Zhang, Y. Tang and P. Wang, Reviews on the effects of contaminations and research methodologies for PEMFC, *Int. J. Hydrogen Energy*, 2020, **45**(43), 23174–23200.
13 A. Serov and C. Kwak, Review of non-platinum anode catalysts for DMFC and PEMFC application, *Appl. Catal. B Environ.*, 2009, **90**(3–4), 313–320.
14 A. Sarapuu, E. Kibena-Põldsepp, M. Borghei and K. Tammeveski, Electrocatalysis of oxygen reduction on heteroatom-doped nanocarbons and transition metal–nitrogen–carbon catalysts for alkaline membrane fuel cells, *J. Mater. Chem. A*, 2018, **6**(3), 776–804.

15 Y. M. Zhao, L. M. Liao, G. Q. Yu, P. J. Wei and J. G. Liu, B-Doped Fe/N/C Porous Catalyst for High-Performance Oxygen Reduction in Anion-Exchange Membrane Fuel Cells, *ChemElectroChem*, 2019, **6**(6), 1754–1760.
16 D. R. Dekel, Review of cell performance in anion exchange membrane fuel cells, *J. Power Sources*, 2018, **375**, 158–169.
17 H. Chen, K. T. Bang, Y. Tian, C. Hu, R. Tao, Y. Yuan, R. Wang, D. M. Shin, M. Shao, Y. M. Lee and Y. Kim, Poly (ethylene piperidinium) s for anion exchange membranes, *Angew. Chem.*, 2023, **135**(38), e202307690.
18 M. A. Hickner, A. M. Herring and E. B. Coughlin, Anion exchange membranes: Current status and moving forward, *J. Polym. Sci., Part B:Polym. Phys.*, 2013, **51**(24), 1727–1735.
19 E. Britt Erickson, 3M agrees to $10.3 billion PFAS settlement, *C&EN Global Enterprise*, 2023, **101**(21), 9–9, DOI: 10.1021/cen-10121-buscon1.
20 H. . Cheryl, 3M admits to unlawful release of PFAS, *Chem. Eng. News*, 2019, **97**(26), 16, DOI: 10.1021/CEN-09726-POLCON1.
21 A. Colles, K. De Brouwere, A. De Decker, I. Gabaret, E. Den Hond, H. Van De Maele, L. Van Rooy and B. Bautmans, PFAS in serum of residents living in the neighborhood of a major PFAS manufacturer plant in Belgium, *ISEE Conf. Abstr.*, 2022, **2022**(1), DOI: 10.1289/isee.2022.O-SY-019.
22 H. Cheryl, *Court dismisses industry suit on PFAS in drinking water*, 2023, **101**, 15, DOI: 10.1021/cen-10104-polcon3.
23 J. Jeff, Asahi Kasei, Michigan settle PFAS suit, *C&EN Glob. Enterp.*, 2023, **101**(5), 14, DOI: 10.1021/cen-10105-polcon1.
24 K. Kati, *Environmental risks caused by perfluorinated alkyl substances (PFAS) in Finland*, Finnish Environment Institute, 2005, http://hdl.handle.net/10138/38746.
25 Y. Chen, S. P. Dukes, A. Jeremiasse, W. Du, S. E. Hadjikyriacou and T. K. Mallmann, Pfas treatment scheme using separation and electrochemical elimination, *US Pat.*, US20220402794A1, 2022.
26 R. Sharma, P. Morgen, M. J. Larsen, M. C. Roda-Serrat, P. B. Lund, L. Grahl-Madsen and S. M. Andersen, Recovery, Regeneration, and Reapplication of PFSA Polymer from End-of-Life PEMFC MEAs, *ACS Appl. Mater. Interfaces*, 2023, **15**(41), 48705–48715.
27 Z. Wang, K. Chen, J. Han, X. Zhang, B. Wang, Q. Du and K. Jiao, Anion exchange membranes for fuel cells: equilibrium water content and conductivity characterization, *Adv. Funct. Mater.*, 2023, **33**(40), 2303857.
28 C. Chen, X. Zeng, Z. Peng and Z. Chen, Polyaromatic anion exchange membranes for alkaline fuel cells with high hydroxide conductivity and alkaline stability, *J. Appl. Polym. Sci.*, 2023, **140**(20), e53795.
29 X. Wu, N. Chen, C. Hu, H. A. Klok, Y. M. Lee and X. Hu, Fluorinated poly (aryl piperidinium) membranes for anion exchange membrane fuel cells, *Adv. Mater.*, 2023, **35**(26), 2210432.
30 K. Cao, J. Peng, C. Shan, Z. Liu, M. Liang, L. Wang, W. Hu and B. Liu, Beneficial use of hyperbranched polymer in cross-linked anion exchange membranes for fuel cells, *Int. J. Energy Res.*, 2022, **46**(15), 24395–24407.
31 Q. Wei, X. Cao, P. Veh, A. Konovalova, P. Mardle, P. Overton, S. Cassegrain, S. Vierrath, M. Breitwieser and S. Holdcroft, On the stability of anion exchange membrane fuel cells incorporating polyimidazolium ionene (Aemion+®) membranes and ionomers, *Sustain. Energy Fuels*, 2022, **6**(15), 3551–3564.
32 N. Chen, H. H. Wang, S. P. Kim, H. M. Kim, W. H. Lee, C. Hu, J. Y. Bae, E. S. Sim, Y. C. Chung, J. H. Jang and S. J. Yoo, Poly (fluorenyl aryl piperidinium) membranes and ionomers for anion exchange membrane fuel cells, *Nat. Commun.*, 2021, **12**(1), 2367.
33 J. H. Kim, M. Vinothkannan, A. R. Kim and D. J. Yoo, Anion exchange membranes obtained from poly (arylene ether sulfone) block copolymers comprising hydrophilic and hydrophobic segments, *Polymers*, 2020, **12**(2), 325.
34 X. Li, B. Zhang, J. Guo, Y. Chen, L. Dai, J. Zheng, S. Li and S. Zhang, High-strength, ultra-thin anion exchange membranes with a branched structure toward alkaline membrane fuel cells, *J. Mater. Chem. A*, 2023, **11**(20), 10738–10747.
35 Z. Wang, K. Chen, J. Han, X. Zhang, B. Wang, Q. Du and K. Jiao, Anion exchange membranes for fuel cells: equilibrium water content and conductivity characterization, *Adv. Funct. Mater.*, 2023, **33**(40), 2303857.
36 T. R. Maumau, N. W. Maxakato and P. F. Msomi, The Development of Anion Exchange Ionomer for Electrocatalysts in Application of Anion Exchange Membrane Fuel Cells, *ECS Meet. Abstr.*, 2022, **242**(43), 1613.
37 A. M. Samsudin, M. Bodner and V. Hacker, A brief review of poly (vinyl alcohol)-based anion exchange membranes for alkaline fuel cells, *Polymers*, 2022, **14**(17), 3565.
38 T. J. Omasta, L. Wang, X. Peng, C. A. Lewis, J. R. Varcoe and W. E. Mustain, Importance of balancing membrane and electrode water in anion exchange membrane fuel cells, *J. Power Sources*, 2018, **375**, 205–213.
39 C. Zheng, L. Wang, S. Zhang, X. Liu, J. Zhang, Y. Yin, K. Jiao, Q. Du, X. Li and M. D. Guiver, Microstructural orientation of anion exchange membrane through mechanical stretching for improved ion transport, *Front. Membr. Sci. Technol.*, 2023, **2**, 1193355.
40 Z. Wang, K. Chen, J. Han, X. Zhang, B. Wang, Q. Du and K. Jiao, Anion exchange membranes for fuel cells: equilibrium water content and conductivity characterization, *Adv. Funct. Mater.*, 2023, **33**(40), 2303857.
41 Q. G. Chen and M. T. Lee, Anion Exchange Membranes for Fuel Cells Based on Quaternized Polystyrene-b-poly (ethylene-co-butylene)-b-polystyrene Triblock Copolymers with Spacer-Sidechain Design, *Polymers*, 2022, **14**(14), 2860.
42 V. Vijayakumar and S. Y. Nam, Recent Advances in Anion Exchange Membranes for Fuel Cell Applications, *Progress in Polymer Research for Biomedical, Energy and Specialty Applications*, 2022, vol. 3, pp. 229–250.
43 C. Chen, X. Zeng, Z. Peng and Z. Chen, Polyaromatic anion exchange membranes for alkaline fuel cells with high hydroxide conductivity and alkaline stability, *J. Appl. Polym. Sci.*, 2023, **140**(20), e53795.

44 Z. Zhao, Z. Yang, M. Zhang, W. Du, W. Lan, X. Zhang and M. Fan, Tripartite cationic interpenetrating polymer network anion exchange membranes for fuel cells, *ACS Appl. Energy Mater.*, 2023, **6**(3), 1488–1500.

45 A. M. Samsudin, M. Roschger, S. Wolf and V. Hacker, Preparation and characterization of QPVA/PDDA electrospun nanofiber anion exchange membranes for alkaline fuel cells, *Nanomaterials*, 2022, **12**(22), 3965.

46 C. N. Ouma, K. O. Obodo and D. Bessarabov, Computational approaches to alkaline anion-exchange membranes for fuel cell applications, *Membranes*, 2022, **12**(11), 1051.

47 M. E. Thomas, Computational Approaches to Alkaline Anion Exchange Membranes, *Alkaline Anion Exchange Membranes for Fuel Cells: From Tailored Materials to Novel Applications*, 2024, vol. 4, pp. 285–308.

48 N. Ul Hassan, M. J. Zachman, M. Mandal, H. Adabi Firouzjaie, P. A. Kohl, D. A. Cullen and W. E. Mustain, Understanding recoverable vs unrecoverable voltage losses and long-term degradation mechanisms in anion exchange membrane fuel cells, *ACS Catal.*, 2022, **12**(13), 8116–8126.

49 K. N. Grew and W. K. Chiu, A dusty fluid model for predicting hydroxyl anion conductivity in alkaline anion exchange membranes, *J. Electrochem. Soc.*, 2010, **157**(3), B327.

50 M. E. Tuckerman, D. Marx and M. Parrinello, The nature and transport mechanism of hydrated hydroxide ions in aqueous solution, *Nature*, 2002, **417**(6892), 925–929.

51 G. Merle, M. Wessling and K. Nijmeijer, Anion exchange membranes for alkaline fuel cells: A review, *J. Membr. Sci.*, 2011, **377**(1–2), 1–35.

52 K. Kordesh and M. Weissenbacher, Rechargeable alkaline manganese dioxide/zinc batteries, *J. Power Sources*, 1994, **51**(1–2), 61–78.

53 R. M. Ormerod, Solid oxide fuel cells, *Chem. Soc. Rev.*, 2003, **32**(1), 17–28.

54 T. J. Omasta, A. M. Park, J. M. LaManna, Y. Zhang, X. Peng, L. Wang, D. L. Jacobson, J. R. Varcoe, D. S. Hussey, B. S. Pivovar and W. E. Mustain, Beyond catalysis and membranes: visualizing and solving the challenge of electrode water accumulation and flooding in AEMFCs, *Energy Environ. Sci.*, 2018, **11**(3), 551–558.

55 S. Willdorf-Cohen, A. Zhegur-Khais, J. Ponce-Gonzalez, S. Bsoul-Haj, J. R. Varcoe, C. E. Diesendruck and D. R. Dekel, Alkaline stability of anion-exchange membranes, *ACS Appl. Energy Mater.*, 2023, **6**(2), 1085–1092.

56 J. Hyun, S. H. Yang, G. Doo, S. Choi, D. H. Lee, D. W. Lee, J. Kwen, W. Jo, S. H. Shin, J. Y. Lee and H. T. Kim, Degradation study for the membrane electrode assembly of anion exchange membrane fuel cells at a single-cell level, *J. Mater. Chem. A*, 2021, **9**(34), 18546–18556.

57 J. Hyun, W. Jo, S. H. Yang, S. H. Shin, G. Doo, S. Choi, D. H. Lee, D. W. Lee, E. Oh, J. Y. Lee and H. T. Kim, Tuning of water distribution in the membrane electrode assembly of anion exchange membrane fuel cells using functionalized carbon additives, *J. Power Sources*, 2022, **543**, 231835.

58 M. Chatenet, S. Berthon-Fabry, Y. Ahmad, K. Guérin, M. Colin, H. Farhat, L. Frezet, G. Zhang and M. Dubois, Fluorination and its Effects on Electrocatalysts for Low-Temperature Fuel Cells, *Adv. Energy Mater.*, 2023, **13**(15), 2204304.

59 K. Yassin, I. G. Rasin, S. Willdorf-Cohen, C. E. Diesendruck, S. Brandon and D. R. Dekel, A surprising relation between operating temperature and stability of anion exchange membrane fuel cells, *J. Power Sources Adv.*, 2021, **11**, 100066.

60 C. Hu, J. H. Park, N. Y. Kang, X. Zhang, Y. J. Lee, S. W. Jeong and Y. M. Lee, Effects of hydrophobic side chains in poly (fluorenyl-co-aryl piperidinium) ionomers for durable anion exchange membrane fuel cells, *J. Mater. Chem. A*, 2023, **11**(4), 2031–2041.

61 J. Lilloja, E. Kibena-Põldsepp, A. Sarapuu, M. Käärik, J. Kozlova, P. Paiste, A. Kikas, A. Treshchalov, J. Leis, A. Tamm and V. Kisand, Transition metal and nitrogen-doped mesoporous carbons as cathode catalysts for anion-exchange membrane fuel cells, *Appl. Catal. B Environ.*, 2022, **306**, 121113.

62 A. M. Herring, N. C. Buggy, I. Wu, M. C. Kuo, M. Ezell, K. Beiler, A. Johnson and K. Dunn, Controlling Charge Transfer and Ion Transport in Electrodes for the Oxygen Evolution Reaction, *ECS Meet. Abstr.*, 2022, **242**(57), 2170.

63 J. Lilloja, M. Mooste, E. Kibena-Põldsepp, A. Sarapuu, A. Kikas, V. Kisand, M. Käärik, J. Kozlova, A. Treshchalov, P. Paiste, J. Aruväli, J. Leis, A. Tamm, S. Holdcroft and K. Tammeveski, Cobalt-, iron-and nitrogen-containing ordered mesoporous carbon-based catalysts for anion-exchange membrane fuel cell cathode, *Electrochimica Acta*, 2023, **439**, 141676, DOI: 10.1016/j.electacta.2022.141676.

64 M. Shao, Q. Chang, J. P. Dodelet and R. Chenitz, Recent advances in electrocatalysts for oxygen reduction reaction, *Chem. Rev.*, 2016, **116**(6), 3594–3657.

65 R. Liu, D. Wu, X. Feng and K. Müllen, Nitrogen-doped ordered mesoporous graphitic arrays with high electrocatalytic activity for oxygen reduction, *Angew. Chem.*, 2010, **122**(14), 2619–2623.

66 J. Lilloja, M. Mooste, E. Kibena-Põldsepp, A. Sarapuu, B. Zulevi, A. Kikas, H. M. Piirsoo, A. Tamm, V. Kisand, S. Holdcroft and A. Serov, Mesoporous iron-nitrogen co-doped carbon material as cathode catalyst for the anion exchange membrane fuel cell, *J. Power Sources Adv.*, 2021, **8**, 100052.

67 C. Venkateswara Rao and Y. Ishikawa, Activity, selectivity, and anion-exchange membrane fuel cell performance of virtually metal-free nitrogen-doped carbon nanotube electrodes for oxygen reduction reaction, *J. Phys. Chem. C*, 2012, **116**(6), 4340–4346.

68 Y. J. Sa, C. Park, H. Y. Jeong, S. H. Park, Z. Lee, K. T. Kim, G. G. Park and S. H. Joo, Carbon nanotubes/heteroatom-doped carbon core–sheath nanostructures as highly active, metal-free oxygen reduction electrocatalysts for alkaline fuel cells, *Angew. Chem.*, 2014, **126**(16), 4186–4190.

69 V. M. Truong, T. Q. Le, T. N. Le, N. B. Duong and T. M. Tang, Development of Non-Platinum Metal Catalysts for Anion Exchange Membrane Fuel Cells, *Mater. Sci. Forum*, 2022, **1064**, 139–147.

70 P. Gayen, S. Saha, X. Liu, K. Sharma and V. K. Ramani, High-performance AEM unitized regenerative fuel cell using Pt-pyrochlore as bifunctional oxygen electrocatalyst, *Proc. Natl. Acad. Sci. U. S. A.*, 2021, **118**(40), e2107205118.

71 S. Minelli, M. Civelli, S. Rondinini, A. Minguzzi and A. Vertova, Aemfc exploiting a pd/ceo2-based anode compared to classic pemfc via lca analysis, *Hydrogen*, 2021, **2**(3), 246–261.

72 H. Adabi Firouzjaie, A. Shakouri, C. Williams, J. R. Regalbuto and W. E. Mustain, Highly Efficient Multi-Atom Pt and PtRu Catalysts for Anion Exchange Membrane Fuel Cells, *ECS Meeting Abstr.*, 2022, **241**(45), 1895.

73 E. Daş, S. A. Gürsel and A. B. Yurtcan, Pt-alloy decorated graphene as an efficient electrocatalyst for PEM fuel cell reactions, *J. Supercrit. Fluids*, 2020, **165**, 104962.

74 H. Xin, H. Wang, W. Zhang, Y. Chen, Q. Ji, G. Zhang, H. Liu, A. D. Taylor and J. Qu, In operando visualization and dynamic manipulation of electrochemical processes at the electrode–solution interface, *Angew. Chem., Int. Ed.*, 2022, **61**(36), e202206236.

75 S. Pei, C. Shen, C. Zhang, N. Ren and S. You, Characterization of the interfacial joule heating effect in the electrochemical advanced oxidation process, *Environ. Sci. Technol.*, 2019, **53**(8), 4406–4415.

76 I. Gunasekara, I. Kendrick and S. Mukerjee, Interfacial Kinetics of HOR/MOR at the AEM/Pt Microelectrode Interface: Investigation of the Influence of CO32− on the Reaction Kinetics and the Mass Transport through Membrane, *J. Electrochem. Soc.*, 2019, **166**(13), F889.

77 V. Gurau and J. A. Mann, Effect of interfacial phenomena at the gas diffusion layer-channel interface on the water evolution in a PEMFC, *J. Electrochem. Soc.*, 2010, **157**(4), B512.

78 P. R. Scheller, Some aspects of electrochemistry of interfaces, *Treatise Process Metall.*, 2014, 79–93.

79 Z. K. Goldsmith, M. F. Andrade and A. Selloni, Effects of applied voltage on water at a gold electrode interface from ab initio molecular dynamics, *Chem. Sci.*, 2021, **12**(16), 5865–5873.

80 A. Shandilya, K. Schwarz and R. Sundararaman, Interfacial water asymmetry at ideal electrochemical interfaces, *J. Chem. Phys.*, 2022, **156**(1), 014705.

81 J. K. Choi, H. B. Kang, J. W. Lee, S. B. Jung and C. W. Yang, A study on interfacial reaction between electroless plated Ni-P/Au UBM and Sn-Bi eutectic solder using AEM, *Mater. Sci. Forum*, 2004, **449**, 405–408.

82 J. M. Ahlfield, L. Liu and P. A. Kohl, PEM/AEM junction design for bipolar membrane fuel cells, *J. Electrochem. Soc.*, 2017, **164**(12), F1165.

83 A. J. Bard, H. D. Abruna, C. E. Chidsey, L. R. Faulkner, S. W. Feldberg, K. Itaya, M. Majda, O. Melroy and R. W. Murray, The electrode/electrolyte interface-a status report, *J. Phys. Chem.*, 1993, **97**(28), 7147–7173.

84 Y. Huang, W. Dong, C. Zhu and L. Xiao, Electromechanical Design of Self-Similar Inspired Surface Electrodes for Human-Machine Interaction, *Complexity*, 2018, **2018**(1), 3016343.

85 M. V. Pagliaro, C. Wen, B. Sa, B. Liu, M. Bellini, F. Bartoli, S. Sahoo, R. K. Singh, S. P. Alpay, H. A. Miller and D. R. Dekel, Improving alkaline hydrogen oxidation activity of palladium through interactions with transition-metal oxides, *ACS Catal.*, 2022, **12**(17), 10894–10904.

86 L. Su, C. Cui, S. Zhou, H. Wu, S. Zhang and H. Pang, Alkaline hydrogen oxidation reaction on ruthenium-based catalysts: From mechanism insights to catalyst advances, *Nano Energy*, 2025, **24**, 111051.

87 J. Guo, J. Zhou, D. Chu and R. Chen, Tuning the electrochemical interface of Ag/C electrodes in alkaline media with metallophthalocyanine molecules, *J. Phys. Chem. C*, 2013, **117**(8), 4006–4017.

88 H. Mousa, L. Xing and P. K. Das, Investigation of gradient platinum loading and porosity distribution for anion exchange membrane fuel cells, *J. Electrochem. Energy Convers. Storage*, 2023, **20**(4), 041001.

89 B. Eriksson, P. G. Santori, N. Bibent, F. Lecoeur, M. Dupont and F. Jaouen, Shedding Light on Water Management during Operation of AEMFC with Humidity Sensors, *ECS Meet. Abstr.*, 2022, **241**(35), 1462.

90 S. Willdorf-Cohen, S. Li, S. Srebnik, C. E. Diesendruck and D. R. Dekel, Effect of Carbonate Anions on the Stability of Quaternary Ammonium Groups for Aemfcs, *ECS Meet. Abstr.*, 2022, **242**(43), 1609.

91 Z. Yao, Y. Lum, A. Johnston, L. M. Mejia-Mendoza, X. Zhou, Y. Wen, A. Aspuru-Guzik, E. H. Sargent and Z. W. Seh, Machine learning for a sustainable energy future, *Nat. Rev. Mater.*, 2023, **8**(3), 202–215.

92 P. Berg, K. Promislow, J. S. Pierre, J. Stumper and B. Wetton, Water management in PEM fuel cells, *J. Electrochem. Soc.*, 2004, **151**(3), A341.

93 X. Xu, K. Li, Z. Liao, J. Cao and R. Wang, A closed-loop water management methodology for PEM fuel cell system based on impedance information feedback, *Energies*, 2022, **15**(20), 7561.

94 T. J. Omasta, X. Peng, C. A. Lewis, J. Varcoe and W. E. Mustain, Improving performance in alkaline membrane fuel cells through enhanced water management, *ECS Trans.*, 2016, **75**(14), 949.

95 H. S. Shiau, I. V. Zenyuk and A. Z. Weber, Water management in an alkaline-exchange-membrane fuel cell, *ECS Trans.*, 2015, **69**(17), 985.

96 T. J. Omasta and W. E. Mustain, Water and ion transport in anion exchange membrane fuel cells, in *Anion Exchange Membrane Fuel Cells: Principles, Materials and Systems*, Springer International Publishing, Cham, 2018, pp. 1–31.

97 A. Saco, P. S. Sundari and A. Paul, An optimized data analysis on a real-time application of PEM fuel cell design by using machine learning algorithms, *Algorithms*, 2022, **15**(10), 346.

98 J. Lu, Y. Gao, L. Zhang, K. Li and C. Yin, PEMFC water management fault diagnosis method based on principal

component analysis and support vector data description, in *IECON 2021–47th Annual Conference of the IEEE Industrial Electronics Society*, IEEE, 2021, pp. 1–8.

99 H. Ungan and A. B. Yurtcan, Water management improvement in PEM fuel cells via addition of PDMS or APTESpolymers to the catalyst layer, *Turk. J. Chem.*, 2020, **44**(5), 1227–1243.

100 A. Wirth, Cyberinsights: Artificial Intelligence: Friend and Foe, *Biomed. Instrum. Technol.*, 2019, **53**(5), 378–383.

101 A. Früh and D. Haux, *Foundations of Artificial Intelligence and Machine Learning*, 2022, DOI: 10.34669/WI.WS/29.

102 L. Vichard, F. Harel, A. Ravey, P. Venet and D. Hissel, Degradation prediction of PEM fuel cell based on artificial intelligence, *Int. J. Hydrogen Energy*, 2020, **45**(29), 14953–14963.

103 P. Sinha, D. Roshini, V. Daoo, B. M. Abraham and J. K. Singh, Integrating machine learning and molecular simulation for material design and discovery, *Trans. Indian Natl. Acad. Eng.*, 2023, **8**(3), 325–340.

104 T. Wang, Brief Introduction of the Machine Learning Method, in *Artificial Intelligence for Materials Science*, Springer International Publishing, Cham, 2021, pp. 1–20.

105 A. B. Dorothy, N. Kamalraj, S. Pundir, S. Verma and G. Jakka, Real-Time Intelligent Information Protection Using AI and Machine Learning Model, in *2023 Eighth International Conference on Science Technology Engineering and Mathematics (ICONSTEM)*, IEEE, 2023, pp. 1–5.

106 S. Edwards, B. Dorn, and D. Sanders, Problem solving algorithms sofia, 2012, http://sofia.cs.vt.edu/cs1114-ebooklet/chapter4.html.

107 Z. Ghahramani, Unsupervised learning, in *Summer School on Machine Learning*, Springer Berlin Heidelberg, Berlin, Heidelberg, 2003, pp. 72–112.

108 X. Zou, J. Pan, Z. Sun, B. Wang, Z. Jin, G. Xu and F. Yan, Machine learning analysis and prediction models of alkaline anion exchange membranes for fuel cells, *Energy Environ. Sci.*, 2021, **14**(7), 3965–3975.

109 P. Fragiacomo, E. Astorino, G. Chippari, G. De Lorenzo, W. T. Czarnetzki and W. Schneider, Anion exchange membrane fuel cell modelling, *Int. J. Sustain. Energy*, 2018, **37**(4), 340–353.

110 D. R. Dekel, K. Yassin, I. G. Rasin and S. Brandon, Modeling direct ammonia anion-exchange membrane fuel cells, *J. Power Sources*, 2023, **558**, 232616.

111 X. Zou, G. Xu, P. Fang, W. Li, Z. Jin, S. Guo, Y. Hu, M. Li, J. Pan, Z. Sun and F. Yan, Unsupervised Learning-Guided Accelerated Discovery of Alkaline Anion Exchange Membranes for Fuel Cells, *Angew. Chem., Int. Ed.*, 2023, **62**(19), e202300388.

112 T. Wilberforce, M. Biswas and A. Omran, Power and voltage modelling of a proton-exchange membrane fuel cell using artificial neural networks, *Energies*, 2022, **15**(15), 5587.

113 G. E. Hinton and R. R. Salakhutdinov, Reducing the dimensionality of data with neural networks, *Science*, 2006, **313**(5786), 504–507.

114 B. Soni, P. Mathur and A. Bora, In depth analysis, applications and future issues of artificial neural network, *Enabling AI Applications in Data Science*, 2021, pp. 149–183.

115 K. Lachhwani, Application of Neural Network Models for Mathematical Programming Problems: A State of Art Review, *Arch. Comput. Methods Eng.*, 2020, **27**(1), 171.

116 G. Di Franco and M. Santurro, Machine learning, artificial neural networks and social research, *Qual. Quantity*, 2021, **55**(3), 1007–1025.

117 Q. Yang, G. Xiao, T. Liu, B. Gao and S. Chen, Efficient Prediction of Fuel Cell Performance Using Global Modeling Method, *Energies*, 2022, **15**(22), 8549.

118 A. Goshtasbi, J. Chen, J. R. Waldecker, S. Hirano and T. Ersal, Effective parameterization of PEM fuel cell models—part II: robust parameter subset selection, robust optimal experimental design, and multi-step parameter identification algorithm, *J. Electrochem. Soc.*, 2020, **167**(4), 044505.

119 M. Kandidayeni, A. Macias, L. Boulon and J. P. Trovão, Online modeling of a fuel cell system for an energy management strategy design, *Energies*, 2020, **13**(14), 3713.

120 M. Shao, H. Wei and S. Xu, *Parameter Identification for One-Dimension Fuel Cell Model Using GA-PSO Algorithm (No. 2019-01-5041). SAE Technical Paper*, 2019.

121 T. Wilberforce, M. Biswas and A. Omran, Power and voltage modelling of a proton-exchange membrane fuel cell using artificial neural networks, *Energies*, 2022, **15**(15), 5587.

122 K. Yassin, I. G. Rasin, S. Brandon and D. R. Dekel, Which Properties Should Anion-Exchange Membranes Have to Achieve a Longer Fuel Cell Lifetime?, *ECS Meet. Abstr.*, 2022, **242**(43), 1607.

123 A. Goshtasbi, J. Chen, J. Waldecker, S. Hirano and T. Ersal, Optimal Experimental Design for Parameter Identification of PEM Fuel Cell Models, *ECS Meet. Abstr.*, 2019, **236**(32), 1384.

124 J. Zhao, X. Li, C. Shum and J. McPhee, A computationally efficient and high-fidelity 1D steady-state performance model for PEM fuel cells, *J. Phys.: Energy*, 2023, **5**(1), 015003.

125 A. G. Vidales, N. C. Millan and C. Bock, Modeling of anion exchange membrane water electrolyzers: The influence of operating parameters, *Chem. Eng. Res. Des.*, 2023, **194**, 636–648.

126 R. Ding, R. Wang, Y. Ding, W. Yin, Y. Liu, J. Li and J. Liu, Designing AI-aided analysis and prediction models for nonprecious metal electrocatalyst-based proton-exchange membrane fuel cells, *Angew. Chem.*, 2020, **132**(43), 19337–19345.

127 P. Fragiacomo, E. Astorino, G. Chippari, G. De Lorenzo, W. T. Czarnetzki and W. Schneider, Anion exchange membrane fuel cell modelling, *Int. J. Sustain. Energy*, 2018, **37**(4), 340–353.

128 M. K. Singla, J. Gupta, B. Singh, P. Nijhawan, A. Y. Abdelaziz and A. El-Shahat, Parameter estimation of fuel cells using a hybrid optimization algorithm, *Sustainability*, 2023, **15**(8), 6676.

129 M. Buscema, A brief overview and introduction to artificial neural networks, *Subst. Use Misuse*, 2002, **37**(8–10), 1093–1148.

130 A. Abraham, Artificial neural networks, *Handbook of Measuring System Design*, 2005.

131 J. Zou, Y. Han and S. S. So, Overview of Artificial Neural Networks, in *Artificial Neural Networks, Methods in Molecular Biology™*, ed. Livingstone, D. J., Humana Press, 2008, vol. 458, DOI: 10.1007/978-1-60327-101-1_2.

132 T. Rabczuk and K. J. Bathe, *Machine Learning in Modeling and Simulation: Methods and Applications*, Springer International Publishing AG, 2023.

133 C. Hu, H. H. Wang, J. H. Park, H. M. Kim, N. Chen and Y. M. Lee, Strategies for Improving Anion Exchange Membrane Fuel Cell Performance by Optimizing Electrode Conditions, *J. Electrochem. Soc.*, 2022, **169**(1), 014515.

134 F. Li, S. H. Chan and Z. Tu, Recent development of anion exchange membrane fuel cells and performance optimization strategies: a review, *Chem. Rec.*, 2024, **24**(1), e202300067.

135 J. Zhang, W. Zhu, T. Huang, C. Zheng, Y. Pei, G. Shen, Z. Nie, D. Xiao, Y. Yin and M. D. Guiver, Recent insights on catalyst layers for anion exchange membrane fuel cells, *Adv. Sci.*, 2021, **8**(15), 2100284.

136 C. Hu, H. H. Wang, J. H. Park, H. M. Kim, N. Chen and Y. M. Lee, Strategies for Improving Anion Exchange Membrane Fuel Cell Performance by Optimizing Electrode Conditions, *J. Electrochem. Soc.*, 2022, **169**(1), 014515.

137 Z. Wang, K. Chen, J. Han, X. Zhang, B. Wang, Q. Du and K. Jiao, Anion exchange membranes for fuel cells: equilibrium water content and conductivity characterization, *Adv. Funct. Mater.*, 2023, **33**(40), 2303857.

138 H. Yuan, D. Tan, X. Wei and H. Dai, Fault diagnosis of fuel cells by a hybrid deep learning network fusing characteristic impedance, *IEEE Trans. Transp. Electrification*, 2023, **10**(1), 1482–1493.

139 S. Barhate, R. Mudhalwadkar and S. Madhe, Fault Detection Methods Suitable for Automotive Applications in Proton Exchange Fuel Cells, *Eng. Technol. Appl. Sci. Res.*, 2022, **12**(6), 9607–9613.

140 J. Lv, J. Kuang, Z. Yu, G. Sun, J. Liu and J. I. Leon, Diagnosis of PEM fuel cell system based on electrochemical impedance spectroscopy and deep learning method, *IEEE Trans. Ind. Electron.*, 2023, **71**(1), 657–666.

141 Y. Zhang, C. Du and T. Pan, A method for automotive fuel cell fault diagnosis based on PCA-APSO-SVM, in *International Conference on Cloud Computing, Performance Computing, and Deep Learning (CCPCDL 2023)*, SPIE, 2023, vol. 12712, pp. 244–256.

142 Y. Xing, B. Wang, Z. Gong, Z. Hou, F. Xi, G. Mou, Q. Du, F. Gao and K. Jiao, Data-driven fault diagnosis for PEM fuel cell system using sensor pre-selection method and artificial neural network model, *IEEE Trans. Energy Convers.*, 2022, **37**(3), 1589–1599.

143 W. He and Y. Shi, PEMFC fault diagnosis based on SAE, in *2023 IEEE 6th International Electrical and Energy Conference (CIEEC)*, IEEE, 2023, pp. 1653–1657.

144 M. Jung, O. Niculita and Z. Skaf, Comparison of different classification algorithms for fault detection and fault isolation in complex systems, *Procedia Manuf.*, 2018, **19**, 111–118.

145 S. Fujii, Y. Shimizu, J. Hyodo, A. Kuwabara and Y. Yamazaki, Discovery of Unconventional Proton-Conducting Inorganic Solids via Defect-Chemistry-Trained, *Interpretable Machine Learning*, 2023, **13**(39), 2301892.

146 M. J. Eslamibidgoli, K. Malek and M. Eikerling, Autonomous Image Analysis to Accelerate the Discovery and Integration of Energy Materials, *ECS Meet. Abstr.*, 2022, **241**, 1908.

147 A. Colliard-Granero, M. Batool, J. Jankovic, J. Jitsev, M. H. Eikerling, K. Malek and M. J. Eslamibidgoli, Deep learning for the automation of particle analysis in catalyst layers for polymer electrolyte fuel cells, *Nanoscale*, 2022, **14**(1), 10–18.

148 Z. Wang, Y. Han, J. Cai, A. Chen and J. Li, An end-to-end artificial intelligence platform enables real-time assessment of superionic conductors, *SmartMat*, 2023, **4**(6), e1183.

149 X. Hu, B. Yang, S. Ke, Y. Liu, M. Fang, Z. Huang and X. Min, Review and perspectives of carbon-supported platinum-based catalysts for proton exchange membrane fuel cells, *Energy Fuels*, 2023, **37**(16), 11532–11566.

150 F. Cai, S. Cai, S. Li and Z. Tu, Performance Enhancement in Proton Exchange Membrane Fuel Cells with the Grooved Gas Diffusion Layer, *Energy Fuels*, 2024, **38**(19), 19011–19028.

151 W. Wang, J. Guo, T. Gu, R. Shi, X. Wei, Q. Zhang, H. Wang and R. Yang, Gradient Hydrophobic Microporous Layer for High-Performance Proton-Exchange Membrane Fuel Cells, *Energy Fuels*, 2024, **38**(3), 2368–2376.

152 J. M. Sonawane, D. Pant, P. C. Ghosh and S. B. Adeloju, Polyaniline–copper composite: A non-precious metal cathode catalyst for low-temperature fuel cells, *Energy Fuels*, 2021, **35**(4), 3385–3395.

153 D. Hou, N. Wu, X. Tian, Y. Liu, S. Zhang, R. Yang, Y. Qi and L. Wang, Coaly Graphite as an Eco-Friendly Material in the Microporous Layer of Proton Exchange Membrane Fuel Cells, *Energy Fuels*, 2023, **37**(12), 8592–8599.

154 H. Xu, Z. Xia, M. Sun, Z. Zhang, J. Huang, H. Li, F. Jing, D. Feng, S. Wang and G. Sun, Non-uniform Anode Design for High-Temperature Polymer Electrolyte Membrane Fuel Cells with Mitigated Hydrogen Starvation, *Energy Fuels*, 2023, **37**(9), 6733–6739.

155 J. Wang, H. He, Y. Wu, C. Yang, H. Zhang, Q. Zhang, J. Li, H. Cheng and W. Cai, Review on electric resistance in proton exchange membrane fuel cells: advances and outlook, *Energy Fuels*, 2024, **38**(4), 2759–2776.

156 A. Kraytsberg and Y. Ein-Eli, Review of advanced materials for proton exchange membrane fuel cells, *Energy Fuels*, 2014, **28**(12), 7303–7330.

157 B. M. Abraham, M. V. Jyothirmai, P. Sinha, F. Viñes, J. K. Singh and F. Illas, Catalysis in the digital age: Unlocking the power of data with machine learning, *Wiley Interdiscip. Rev. Comput. Mol. Sci.*, 2024, **14**(5), e1730, DOI: 10.1002/wcms.1730.

158 C. Charalambous, E. Moubarak, J. Schilling, E. Sanchez Fernandez, J. Y. Wang, L. Herraiz, F. Mcilwaine, S. B. Peh, M. Garvin, K. M. Jablonka and S. M. Moosavi, A holistic platform for accelerating sorbent-based carbon capture, *Nature*, 2024, 1–6.

159 A. Aspuru-Guzik, and K. Persson, Materials Acceleration Platform: Accelerating Advanced Energy Materials Discovery by Integrating High-Throughput Methods and Artificial Intelligence, *Mission Innovation: Innovation Challenge 6*, 2018, http://nrs.harvard.edu/urn-3:HUL.InstRepos:35164974.

160 P. S. Gromski, A. B. Henson, J. M. Granda, *et al.*, How to explore chemical space using algorithms and automation, *Nat. Rev. Chem.*, 2019, **3**, 119–128, DOI: 10.1038/s41570-018-0066-y.

161 R. S. Ali, J. Meng, M. E. Khan and X. Jiang, Machine learning advancements in organic synthesis: A focused exploration of artificial intelligence applications in chemistry, *Artif. Intell. Chem.*, 2024, **2**(1), 100049.

162 P. Reiser, M. Neubert, A. Eberhard, L. Torresi, C. Zhou, C. Shao, H. Metni, C. van Hoesel, H. Schopmans, T. Sommer and P. Friederich, Graph neural networks for materials science and chemistry, *Commun. Mater.*, 2022, **3**(1), 93.

163 O. Queen, G. A. McCarver, S. Thatigotla, B. P. Abolins, C. L. Brown, V. Maroulas and K. D. Vogiatzis, Polymer graph neural networks for multitask property learning, *npj Comput. Mater.*, 2023, **9**(1), 90.

164 Y. Wang, B. Seo, B. Wang, N. Zamel, K. Jiao and X. C. Adroher, Fundamentals, materials, and machine learning of polymer electrolyte membrane fuel cell technology, *Energy AI*, 2020, **1**, 100014.

165 P. Tian, X. Liu, K. Luo, H. Li and Y. Wang, Deep learning from three-dimensional multiphysics simulation in operational optimization and control of polymer electrolyte membrane fuel cell for maximum power, *Appl. Energy*, 2021, **288**, 116632.

166 Z. Niu, W. Zhao, H. Deng, L. Tian, V. J. Pinfield, P. Ming and Y. Wang, Generative artificial intelligence for designing multi-scale hydrogen fuel cell catalyst layer nanostructures, *ACS Nano*, 2024, **18**(31), 20504–20517.

167 S. Stocker, G. Csányi, K. Reuter and J. T. Margraf, Machine learning in chemical reaction space, *Nat. Commun.*, 2020, **11**(1), 5505.

168 M. Hübel, N. Nirmala, M. Deligant and L. Li, Hybrid physical-AI based system modeling and simulation approach demonstrated on an automotive fuel cell, in *Modelica Conferences*, 2022, vol. 22, pp. 157–163.

169 M. M. Peksen, Artificial intelligence-based machine learning toward the solution of climate-friendly hydrogen fuel cell electric vehicles, *Vehicles*, 2022, **4**(3), 663–680.

170 A. Zhegur-Khais, F. Kubannek, U. Krewer and D. R. Dekel, Measuring the true hydroxide conductivity of anion exchange membranes, *J. Membr. Sci.*, 2020, **612**, 118461.

171 W. Ni, T. Wang, F. Héroguel, A. Krammer, S. Lee, L. Yao, A. Schüler, J. S. Luterbacher, Y. Yan and X. Hu, An efficient nickel hydrogen oxidation catalyst for hydroxide exchange membrane fuel cells, *Nat. Mater.*, 2022, **21**(7), 804–810.

172 K. Yassin, I. G. Rasin, S. Brandon and D. R. Dekel, How can we design anion-exchange membranes to achieve longer fuel cell lifetime?, *J. Membr. Sci.*, 2024, **690**, 122164.

173 D. R. Dekel, I. G. Rasin and S. Brandon, Predicting performance stability of anion exchange membrane fuel cells, *J. Power Sources*, 2019, **420**, 118–123.

174 K. Yassin, I. G. Rasin, S. Brandon and D. R. Dekel, Quantifying the critical effect of water diffusivity in anion exchange membranes for fuel cell applications, *J. Membr. Sci.*, 2020, **608**, 118206.

175 J. Xue, J. C. Douglin, K. Yassin, T. Huang, H. Jiang, J. Zhang, Y. Yin, D. R. Dekel and M. D. Guiver, High-temperature anion-exchange membrane fuel cells with balanced water management and enhanced stability, *Joule*, 2024, **8**(5), 1457–1477.

176 K. Yassin, I. G. Rasin, S. Brandon and D. R. Dekel, Quantifying the critical effect of water diffusivity in anion exchange membranes for fuel cell applications, *J. Membr. Sci.*, 2020, **608**, 118206.

177 J. C. Douglin, J. R. Varcoe and D. R. Dekel, A high-temperature anion-exchange membrane fuel cell, *J. Power Sources Adv.*, 2020, **5**, 100023.

178 L. Chen, G. Pilania, R. Batra, T. D. Huan, C. Kim, C. Kuenneth and R. Ramprasad, Polymer informatics: Current status and critical next steps, *Mater. Sci. Eng. R Rep.*, 2021, **144**, 100595.

179 H. Tran, R. Gurnani, C. Kim, G. Pilania, H. K. Kwon, R. P. Lively and R. Ramprasad, Design of functional and sustainable polymers assisted by artificial intelligence, *Nat. Rev. Mater.*, 2024, **9**(12), 866–886.

180 W. Ge, R. De Silva, Y. Fan, S. A. Sisson and M. H. Stenzel, Machine learning in polymer research, *Adv. Mater.*, 2025, **37**(11), 2413695.

181 J. F. Rodrigues Jr, L. Florea, M. C. De Oliveira, D. Diamond and O. N. Oliveira Jr, Big data and machine learning for materials science, *Discov. Mater.*, 2021, **1**(1), 12.

182 C. Suh, C. Fare, J. A. Warren and E. O. Pyzer-Knapp, Evolving the materials genome: How machine learning is fueling the next generation of materials discovery, *Annu. Rev. Mater. Res.*, 2020, **50**(1), 1–25.

183 A. Y. Wang, R. J. Murdock, S. K. Kauwe, A. O. Oliynyk, A. Gurlo, J. Brgoch, K. A. Persson and T. D. Sparks, Machine learning for materials scientists: an introductory guide toward best practices, *Chem. Mater.*, 2020, **32**(12), 4954–4965.

184 S. Meraghni, L. S. Terrissa, M. Yue, J. Ma, S. Jemei and N. Zerhouni, A data-driven digital-twin prognostics method for proton exchange membrane fuel cell

remaining useful life prediction, *Int. J. Hydrogen Energy*, 2021, **46**(2), 2555–2564.

185 A. U. Rehman, S. W. Ryu, H. Park and J. W. Jung, A critical review of recent industrial developments, trends, and future perspectives of power electronic systems: Fuel cell electric vehicles, *IEEE Trans. Ind. Inf.*, 2024, **20**(4), 6060–6074.

186 Z. Gong, B. Wang, M. Benbouzid, B. Li, Y. Xu, K. Yang, Z. Bao, Y. Amirat, F. Gao and K. Jiao, Cross-domain diagnosis for polymer electrolyte membrane fuel cell based on digital twins and transfer learning network, *Energy AI*, 2024, **17**, 100412.

187 D. Latoń, J. Grela and A. Ożadowicz, Applications of Deep Reinforcement Learning for Home Energy Management Systems: A Review, *Energies*, 2024, **17**(24), 6420.

188 J. Li, J. Liu, Q. Yang, T. Wang, H. He, H. Wang and F. Sun, Reinforcement learning based energy management for fuel cell hybrid electric vehicles: A comprehensive review on decision process reformulation and strategy implementation, *Renew. Sustain. Energy Rev.*, 2025, **213**, 115450.

189 X. Niu, Y. Chen, M. Sun, S. Nagao, Y. Aoki, Z. Niu and L. Zhang, Bayesian learning-assisted catalyst discovery for efficient iridium utilization in electrochemical water splitting, *Sci. Adv.*, 2025, **11**(34), eadw0894.

190 D. Su, J. Zheng, J. Ma, Z. Dong, Z. Chen and Y. Qin, Application of machine learning in fuel cell research, *Energies*, 2023, **16**(11), 4390.

191 R. Ma, T. Yang, E. Breaz, Z. Li, P. Briois and F. Gao, Data-driven proton exchange membrane fuel cell degradation predication through deep learning method, *Appl. Energy*, 2018, **231**, 102–115.

192 J. Zhou, X. Shu, J. Zhang, F. Yi, C. Jia, C. Zhang, X. Kong, J. Zhang and G. Wu, A deep learning method based on CNN-BiGRU and attention mechanism for proton exchange membrane fuel cell performance degradation prediction, *Int. J. Hydrogen Energy*, 2024, **94**, 394–405.

193 X. Sun, M. Xie, J. Fu, F. Zhou and J. Liu, An improved neural network model for predicting the remaining useful life of proton exchange membrane fuel cells, *Int. J. Hydrogen Energy*, 2023, **48**(65), 25499–25511.

194 K. Chen, S. Laghrouche and A. Djerdir, Degradation prediction of proton exchange membrane fuel cell based on grey neural network model and particle swarm optimization, *Energy Convers. Manage.*, 2019, **195**, 810–818.

195 B. Zuo, J. Cheng and Z. Zhang, Degradation prediction model for proton exchange membrane fuel cells based on long short-term memory neural network and Savitzky-Golay filter, *Int. J. Hydrogen Energy*, 2021, **46**(29), 15928–15937.

196 J. Bao, C. Wang, Z. Xu and B. J. Koeppel, *Physics-Informed Machine Learning with Application to Solid Oxide Fuel Cell System Modeling and Optimization (No. PNNL-29124)*, Pacific Northwest National Laboratory (PNNL), Richland, WA (United States), 2019.

197 W. Schertzer, M. A. Otmi, J. Sampath, R. P. Lively and R. Ramprasad, AI-Assisted Physics-Informed Predictions of Degradation Behavior of Polymeric Anion Exchange Membranes, *arXiv*, 2025, preprint, arXiv:2510.12655, DOI: 10.48550/arXiv.2510.12655.

198 Y. Hu, Z. Xiao, D. Xia, B. Pang, X. Yan, X. Wu, W. Chen and G. He, An Attention-Enhanced Deep Learning Framework for Designing Alkaline Anion Exchange Membranes, *J. Membr. Sci.*, 2025, **27**, 124273.

199 Y. K. Phua, T. Fujigaya and K. Kato, Predicting the anion conductivities and alkaline stabilities of anion conducting membrane polymeric materials: development of explainable machine learning models, *Sci. Technol. Adv. Mater.*, 2023, **24**(1), 2261833.

200 X. Zhang, R. Pöschl, A. Ennemoser and A. A. Franco, Nanostructure-Informed Multiscale Modeling of Degradation Effects on Proton Conductivity in Nafion Membranes, *ACS Appl. Mater. Interfaces*, 2025, **17**(27), 39155–39172.

201 P. W. Faught, M. Shojaei, A. S. Joyce and P. L. Ferguson, Colloidal Side-Chain Fluorinated Polymer Nanoparticles Are a Significant Source of Polyfluoroalkyl Substance Contamination in Textile Wastewater, *Environ. Sci. Technol. Lett.*, 2025, **12**(12), 1669–1674.

202 R. Hardian, Z. Liang, X. Zhang and G. Szekely, Artificial intelligence: The silver bullet for sustainable materials development, *Green Chem.*, 2020, **22**(21), 7521–7528.

203 Y. Jia, X. Hou, Z. Wang and X. Hu, Machine learning boosts the design and discovery of nanomaterials, *ACS Sustain. Chem. Eng.*, 2021, **9**(18), 6130–6147.

204 S. M. Moosavi, K. M. Jablonka and B. Smit, The role of machine learning in the understanding and design of materials, *J. Am. Chem. Soc.*, 2020, **142**(48), 20273–20287.

205 H. Wang, Y. Ji and Y. Li, Simulation and design of energy materials accelerated by machine learning, *Wiley Interdiscip. Rev.: Comput. Mol. Sci.*, 2020, **10**(1), e1421.

206 H. Xin, T. Mou, H. S. Pillai, S. H. Wang and Y. Huang, Interpretable machine learning for catalytic materials design toward sustainability, *Acc. Mater. Res.*, 2023, **5**(1), 22–34.

207 K. C. Leonard, F. Hasan, H. F. Sneddon and F. You, Can artificial intelligence and machine learning be used to accelerate sustainable chemistry and engineering?, *ACS Sustain. Chem. Eng.*, 2021, **9**(18), 6126–6129.

208 I. Iqbal, G. A. Odesanmi, J. Wang and L. Liu, Comparative investigation of learning algorithms for image classification with small dataset, *Appl. Artif. Intell.*, 2021, **35**(10), 697–716.

209 M. S. Naveed, M. F. Hanif, M. Metwaly, I. Iqbal, E. Lodhi, X. Liu and J. Mi, Leveraging advanced AI algorithms with transformer-infused recurrent neural networks to optimize solar irradiance forecasting, *Front. Energy Res.*, 2024, **12**, 1485690.

210 J. Hyun and H. T. Kim, Powering the hydrogen future: current status and challenges of anion exchange membrane fuel cells, *Energy Environ. Sci.*, 2023, **16**(12), 5633–5662.

211 S. Ratso, A. Zitolo, M. Käärik, M. Merisalu, A. Kikas, V. Kisand, M. Rähn, P. Paiste, J. Leis, V. Sammelselg and

S. Holdcroft, Non-precious metal cathodes for anion exchange membrane fuel cells from ball-milled iron and nitrogen doped carbide-derived carbons, *Renewable Energy*, 2021, **167**, 800–810.

212 Y. Yang, P. Li, X. Zheng, W. Sun, S. X. Dou, T. Ma and H. Pan, Anion-exchange membrane water electrolyzers and fuel cells, *Chem. Soc. Rev.*, 2022, **51**(23), 9620–9693.

213 R. Ding, S. Zhang, Y. Chen, Z. Rui, K. Hua, Y. Wu, X. Li, X. Duan, X. Wang, J. Li and J. Liu, Application of machine learning in optimizing proton exchange membrane fuel cells: A review, *Energy AI*, 2022, **9**, 100170.

214 Y. Yuan, P. Fang, H. Yuan, X. Zou, Z. Sun and F. Yan, Machine Learning for Prediction and Synthesis of Anion Exchange Membranes, *Acc. Mater. Res.*, 2025, **6**(3), 352–365.

215 A. Legala, J. Zhao and X. Li, Machine learning modeling for proton exchange membrane fuel cell performance, *Energy AI*, 2022, **10**, 100183.

216 C. Chen, Y. Zuo, W. Ye, X. Li, Z. Deng and S. P. Ong, A critical review of machine learning of energy materials, *Adv. Energy Mater.*, 2020, **10**(8), 1903242.

217 K. M. Jablonka, D. Ongari, S. M. Moosavi and B. Smit, Big-data science in porous materials: materials genomics and machine learning, *Chem. Rev.*, 2020, **120**(16), 8066–8129.

218 E. Schulz, M. Speekenbrink and A. Krause, A tutorial on Gaussian process regression: Modelling, exploring, and exploiting functions, *J. Math. Psychol.*, 2018, **85**, 1–6.

219 B. Dou, Z. Zhu, E. Merkurjev, L. Ke, L. Chen, J. Jiang, Y. Zhu, J. Liu, B. Zhang and G. W. Wei, Machine learning methods for small data challenges in molecular science, *Chem. Rev.*, 2023, **123**(13), 8736–8780.

220 H. Mai, T. C. Le, D. Chen, D. A. Winkler and R. A. Caruso, Machine learning for electrocatalyst and photocatalyst design and discovery, *Chem. Rev.*, 2022, **122**(16), 13478–13515.

221 T. Le, V. C. Epa, F. R. Burden and D. A. Winkler, Quantitative structure–property relationship modeling of diverse materials properties, *Chem. Rev.*, 2012, **112**(5), 2889–2919.

222 B. Huang and O. A. Von Lilienfeld, Ab initio machine learning in chemical compound space, *Chem. Rev.*, 2021, **121**(16), 10001–10036.

223 X. Jia, A. Lynch, Y. Huang, M. Danielson, I. Lang'at, A. Milder, A. E. Ruby, H. Wang, S. A. Friedler, A. J. Norquist and J. Schrier, Anthropogenic biases in chemical reaction data hinder exploratory inorganic synthesis, *Nature*, 2019, **573**(7773), 251–255.

224 S. R. Kalidindi and M. De Graef, Materials data science: current status and future outlook, *Annu. Rev. Mater. Res.*, 2015, **45**(1), 171–193.

225 H. Mai, T. C. Le, D. Chen, D. A. Winkler and R. A. Caruso, Machine learning for electrocatalyst and photocatalyst design and discovery, *Chem. Rev.*, 2022, **122**(16), 13478–13515.

226 Y. LeCun, L. Bottou, Y. Bengio and P. Haffner, Gradient-based learning applied to document recognition, *Proc. IEEE*, 2002, **86**(11), 2278–2324.

227 S. Kajita, N. Ohba, R. Jinnouchi and R. Asahi, A universal 3D voxel descriptor for solid-state material informatics with deep convolutional neural networks, *Sci. Rep.*, 2017, **7**(1), 16991.

228 J. Hoffmann, L. Maestrati, Y. Sawada, J. Tang, J. M. Sellier and Y. Bengio, Data-driven approach to encoding and decoding 3-d crystal structures, *arXiv*, 2019, preprint, arXiv:1909.00949, DOI: 10.48550/arXiv.1909.00949.

229 C. Chen, Y. Zuo, W. Ye, X. Li, Z. Deng and S. P. Ong, A critical review of machine learning of energy materials, *Adv. Energy Mater.*, 2020, **10**(8), 1903242.

230 K. T. Schütt, F. Arbabzadah, S. Chmiela, K. R. Müller and A. Tkatchenko, Quantum-chemical insights from deep tensor neural networks, *Nat. Commun.*, 2017, **8**(1), 13890.

231 C. Chen, W. Ye, Y. Zuo, C. Zheng and S. P. Ong, Graph networks as a universal machine learning framework for molecules and crystals, *Chem. Mater.*, 2019, **31**(9), 3564–3572.

232 Z. Wu, B. Ramsundar, E. N. Feinberg, J. Gomes, C. Geniesse, A. S. Pappu, K. Leswing and V. Pande, MoleculeNet: a benchmark for molecular machine learning, *Chem. Sci.*, 2018, **9**(2), 513–530.

233 X. Zou, J. Pan, Z. Sun, B. Wang, Z. Jin, G. Xu and F. Yan, Machine learning analysis and prediction models of alkaline anion exchange membranes for fuel cells, *Energy Environ. Sci.*, 2021, **14**(7), 3965–3975.

234 J. Schmidt, M. R. Marques, S. Botti and M. A. Marques, Recent advances and applications of machine learning in solid-state materials science, *npj Comput. Mater.*, 2019, **5**(1), 83.

235 T. Xie and J. C. Grossman, Crystal graph convolutional neural networks for an accurate and interpretable prediction of material properties, *Phys. Rev. Lett.*, 2018, **120**(14), 145301.

236 R. Ding, J. Chen, Y. Chen, J. Liu, Y. Bando and X. Wang, Unlocking the potential: machine learning applications in electrocatalyst design for electrochemical hydrogen energy transformation, *Chem. Soc. Rev.*, 2024, **53**, 11390–11461.

237 A. H. Wani and A. Sharma, Optimizing the Electrocatalytic Discovery with Machine Learning as a Novel Paradigm, in *Electrocatalytic Materials*, ed. Patra, S., Shukla, S. K. and Sillanpää, M., Springer, Cham, 2024, DOI: 10.1007/978-3-031-65902-7_7.

238 H. Ooka, J. Huang and K. S. Exner, The sabatier principle in electrocatalysis: Basics, limitations, and extensions, *Front. Energy Res.*, 2021, **9**, 654460.

239 R. Brandiele, A. Guadagnini, L. Girardi, G. Dražić, M. C. Dalconi, G. A. Rizzi, V. Amendola and C. Durante, Climbing the oxygen reduction reaction volcano plot with laser ablation synthesis of Pt x Y nanoalloys, *Catal. Sci. Technol.*, 2020, **10**(14), 4503–4508.

240 S. M. Stratton, S. Zhang and M. M. Montemore, Addressing complexity in catalyst design: From volcanos and scaling to more sophisticated design strategies, *Surf. Sci. Rep.*, 2023, **78**(3), 100597.

241 C. Z. Loyola, S. Ureta-Zañartu, J. H. Zagal and F. Tasca, Activity volcano plots for the oxygen reduction reaction using FeN4 complexes: From reported experimental data to the electrochemical meaning, *Curr. Opin. Electrochem.*, 2022, **32**, 100923.

242 J. Liu and M. Secanell, Exploring the impact of ionomer content and distribution on inkjet printed cathodes for anion exchange membrane fuel cells, *Electrochim. Acta*, 2025, **509**, 145293.

243 C. Xiao, H. Huang, Z. Zhang, Y. Jiang, G. Wang, H. Liu, Y. Liu, L. Xing and L. Zeng, Optimizing catalyst layer structure design for improved water management of anion exchange membrane fuel cells, *J. Power Sources*, 2024, **606**, 234509.

244 M. Elshamy, L. Metzler, J. Disch, S. Vierrath and S. Koch, Influence of nickel hydroxide catalyst ink formulation on direct bar coating of anion exchange membranes, *RSC Adv.*, 2024, **14**(52), 38996–39003.

245 C. Lei, F. Yang, N. Macauley, M. Spinetta, G. Purdy, J. Jankovic, D. A. Cullen, K. L. More, Y. S. Kim and H. Xu, Impact of catalyst ink dispersing solvent on PEM fuel cell performance and durability, *J. Electrochem. Soc.*, 2021, **168**(4), 044517.

246 D. Yang, Y. Guo, H. Tang, D. Yang, P. Ming, C. Zhang, B. Li and S. Zhu, Effect of rheological properties of catalyst slurry on the structure of catalyst layer in PEMFC, *Int. J. Hydrogen Energy*, 2022, **47**(14), 8956–8964.

247 H. Tao, G. Chen, C. Lian, H. Liu and M. O. Coppens, Multiscale modeling of ion transport in porous electrodes, *AIChE J.*, 2022, **68**(4), e17571.

248 R. A. Rica, D. Brogioli, R. Ziano, D. Salerno and F. Mantegazza, Ions transport and adsorption mechanisms in porous electrodes during capacitive-mixing double layer expansion (CDLE), *J. Phys. Chem. C*, 2012, **116**(32), 16934–16938.

249 M. Duquesnoy, T. Lombardo, F. Caro, F. Haudiquez, A. C. Ngandjong, J. Xu, H. Oularbi and A. A. Franco, Functional data-driven framework for fast forecasting of electrode slurry rheology simulated by molecular dynamics, *npj Comput. Mater.*, 2022, **8**(1), 161.

250 R. L. Omongos, D. E. Galvez-Aranda, F. M. Zanotto, A. Vernes and A. A. Franco, Machine learning-driven optimization of gas diffusion layer microstructure for PEM fuel cells, *J. Power Sources*, 2025, **625**, 235583.

251 E. S. Davydova, S. Mukerjee, F. Jaouen and D. R. Dekel, Electrocatalysts for hydrogen oxidation reaction in alkaline electrolytes, *ACS Catal.*, 2018, **8**(7), 6665–6690.

252 T. Tang, L. Ding, Z. C. Yao, H. R. Pan, J. S. Hu and L. J. Wan, Synergistic electrocatalysts for alkaline hydrogen oxidation and evolution reactions, *Adv. Funct. Mater.*, 2022, **32**(2), 2107479.

253 B. Meredig, E. Antono, C. Church, M. Hutchinson, J. Ling, S. Paradiso, B. Blaiszik, I. Foster, B. Gibbons, J. Hattrick-Simpers and A. Mehta, Can machine learning identify the next high-temperature superconductor? Examining extrapolation performance for materials discovery, *Mol. Syst. Des. Eng.*, 2018, **3**(5), 819–825.

254 Y. Zhang and C. Ling, A strategy to apply machine learning to small datasets in materials science, *npj Comput. Mater.*, 2018, **4**(1), 25.

255 L. Ward and C. Wolverton, Atomistic calculations and materials informatics: A review, *Curr. Opin. Solid State Mater. Sci.*, 2017, **21**(3), 167–176.

256 K. T. Butler, J. M. Frost, J. M. Skelton, K. L. Svane and A. Walsh, Computational materials design of crystalline solids, *Chem. Soc. Rev.*, 2016, **45**(22), 6138–6146.

257 A. Ziletti, D. Kumar, M. Scheffler and L. M. Ghiringhelli, Insightful classification of crystal structures using deep learning, *Nat. Commun.*, 2018, **9**(1), 2775.

258 J. Schmidhuber, Deep learning in neural networks: An overview, *Neural Netw.*, 2015, **61**, 85–117.

259 F. Burden and D. Winkler, Bayesian regularization of neural networks, *Artificial Neural Networks: Methods and Applications*, 2008, pp. 23–42.

260 F. R. Burden and D. A. Winkler, Robust QSAR models using Bayesian regularized neural networks, *J. Med. Chem.*, 1999, **42**(16), 3183–3187.

261 Y. LeCun, Y. Bengio and G. Hinton, Deep learning, *Nature*, 2015, **521**(7553), 436–444.

262 Y. Men, D. Wu, Y. Hu, L. Li, P. Li, S. Jia, J. Wang, G. Cheng, S. Chen and W. Luo, Understanding alkaline hydrogen oxidation reaction on PdNiRuIrRh high-entropy-alloy by machine learning potential, *Angew. Chem., Int. Ed.*, 2023, **62**(27), e202217976.

263 J. L. Hitt, D. Yoon, J. R. Shallenberger, D. A. Muller and T. E. Mallouk, High-throughput fluorescent screening and machine learning for feature selection of electrocatalysts for the alkaline hydrogen oxidation reaction, *ACS Sustain. Chem. Eng.*, 2022, **10**(49), 16299–16312.

264 R. Ding, W. Yin, G. Cheng, Y. Chen, J. Wang, X. Wang, M. Han, T. Zhang, Y. Cao, H. Zhao and S. Wang, Effectively increasing Pt utilization efficiency of the membrane electrode assembly in proton exchange membrane fuel cells through multiparameter optimization guided by machine learning, *ACS Appl. Mater. Interfaces*, 2022, **14**(6), 8010–8024.

265 A. M. Herring, S. Ponnada and M. C. Kuo, Controlling Flooding and Parameter Sensitivity in an Anion Exchange Membrane Fuel Cell Using a Triblock Copolymer Membrane and Matched Ionomers, *ECS Meet. Abstr.*, 2024, (43), 2937.